Library Copy
K.A. a 21 S 171

C2

CONFIDENTIAL

Copy 45
RM SL54F28

NACA RM SL54F28

CLASSIFICATION CHANGED
UNCLASSIFIED
NASA CON #79 8-17-66
9-14-66

RESEARCH MEMORANDUM

for the

U. S. Air Force

INVESTIGATION OF A 1/4-SCALE MODEL OF THE REPUBLIC F-105 AIRPLANE IN THE LANGLEY 19-FOOT PRESSURE TUNNEL

LONGITUDINAL STABILITY AND CONTROL OF THE MODEL EQUIPPED WITH A SUPERSONIC-TYPE ELLIPTICAL WING-ROOT INLET

By H. Neale Kelly and Patrick A. Cancro

Langley Aeronautical Laboratory
Langley Field, Va.

JUL 26 1954

CLASSIFIED DOCUMENT

This material contains information affecting the National Defense of the United States within the meaning of the espionage laws, Title 18, U.S.C., Secs. 793 and 794, the transmission or revelation of which in any manner to an unauthorized person is prohibited by law.

NATIONAL ADVISORY COMMITTEE FOR AERONAUTICS

WASHINGTON

JUL 21 1954

CONFIDENTIAL

3 1176 00506 6130

NATIONAL ADVISORY COMMITTEE FOR AERONAUTICS

RESEARCH MEMORANDUM

for the

U. S. Air Force

NASA CCN # 74

INVESTIGATION OF A 1/4-SCALE MODEL OF THE REPUBLIC F-105 AIRPLANE IN THE LANGLEY 19-FOOT PRESSURE TUNNEL

LONGITUDINAL STABILITY AND CONTROL OF THE MODEL EQUIPPED WITH A SUPERSONIC-TYPE ELLIPTICAL WING-ROOT INLET

By H. Neale Kelly and Patrick A. Cancro

8-17-66

9-14-66

SUMMARY

Development tests on a 1/4-scale model of the Republic F-105 airplane are being conducted in the Langley 19-foot pressure tunnel.

The initial tests, the results of which are presented herein, were made at a Reynolds number of 9.0×10^6 and a corresponding Mach number of 0.20 on the model equipped with a supersonic-type elliptical wing-root inlet. Included in the present paper are the results of the following:

(1) Longitudinal stability and control tests of the basic design provided by the contractor

(2) Tests of various modifications designed to improve the stability characteristics of the model with the trailing-edge flaps deflected

(3) Brief exploratory lateral-control and rudder-effectiveness tests

(4) Stall studies and duct air-flow measurements

In order to expedite the issuance of the data for this airplane, no analysis of the results has been made.

INTRODUCTION

The F-105 airplane is a 45° sweptback, midwing, low-tail, supersonic fighter-bomber being developed by the Republic Aviation Corporation for the United States Air Force. At the request of the Air Force, development tests on a 1/4-scale model of the F-105 are being conducted in the Langley 19-foot pressure tunnel to determine the low-speed aerodynamic characteristics of the basic design and, if necessary, to develop modifications which will provide the model with satisfactory low-speed stability and control characteristics.

The initial tests, the results of which are presented herein, were primarily concerned with the low-speed longitudinal stability and control of the model equipped with a supersonic-type elliptical wing-root inlet with and without various high lift and stall-control devices. In addition to the longitudinal stability and control investigation, brief exploratory lateral-control and rudder-effectiveness tests were made and the results are included. The tests were carried out at a Reynolds number of 9.0×10^6 and a corresponding Mach number of 0.20 through an angle-of-attack range from -4° to 29°.

In order to expedite the issuance of the data for this airplane, no analysis has been made.

COEFFICIENTS AND SYMBOLS

C_L lift coefficient, $\frac{\text{Lift}}{qS}$

C_D drag coefficient, $\frac{\text{Drag}}{qS}$

C_m pitching-moment coefficient (an additional subscript denotes moment center), $\frac{\text{Pitching moment}}{qS\bar{c}}$

C_n yawing-moment coefficient (an additional subscript denotes moment center), $\frac{\text{Yawing moment}}{qS\bar{c}}$

C_y side-force coefficient, $\frac{\text{Side force}}{qS}$

A	capture area of both inlets, sq ft
b	wing span, ft
c	local streamwise chord, ft
$\bar{c}$	mean aerodynamic chord, $\frac{2}{S}\int_0^{b/2} c^2 dy$, ft
H	total pressure, lb/sq ft
P	static pressure, lb/sq ft
q	free-stream dynamic pressure, lb/sq ft
Q	volume rate of flow at jet exit, cu ft/sec
V	velocity, ft/sec
y	spanwise distance from the plane of symmetry, ft
z	vertical distance from the mean-aerodynamic-chord extended, ft
α	angle of attack, deg
δ	control deflection in a plane perpendicular to the control hinge line, deg
i_t	tail incidence relative to the wing chord plane, deg
$\frac{H_e - P_o}{q}$	total-pressure recovery at jet exit
$\frac{V_i}{V_o}$	inlet velocity ratio, $\frac{Q}{AV_o}$

Subscripts:

i	inlet
e	exit
o	free stream
max	maximum

MODEL

Model Description

The model was primarily of steel-reinforced wood construction; however, the inlets, trailing-edge flaps, leading-edge flaps, and lateral-control spoilers were aluminum. The model and the geometric characteristics presented herein were supplied by Republic and have not been checked for accuracy.

Basic model.- The basic model for the longitudinal stability and control tests was a 1/4-scale replica of the F-105 airplane wing, fuselage, and vertical tail equipped with a supersonic-type elliptical wing-root inlet. Principal dimensions and design features of the model and a photograph of the model installed in the Langley 19-foot pressure tunnel can be found in figures 1 to 4 and table I.

Horizontal tail.- The original horizontal tail (see fig. 1 and table I) could be set at tail incidences of 0° and -3° (relative to the fuselage center line) at tail heights of $0.057b/2$ and $0.090b/2$ below the mean-aerodynamic-chord plane extended. At a tail height of $-0.123b/2$, tail incidences of 7°, 3.5°, 0°, -3.5°, -7°, -14°, -20°, and -25° were available. A tail having the same plan form as the original tail, but incorporating modified NACA 1-series airfoil sections (see table II) was tested at tail incidences of 0°, -3.5°, -7°, and -14° at the $-0.123b/2$ position.

Trailing-edge flaps.- The wing was equipped with a single slotted trailing-edge flap which extended spanwise from the fuselage to 80 percent of the wing semispan (see fig. 5(a) and table I). Flap deflection angles of 0°, 35°, and 46° in a plane perpendicular to the flap hinge line were obtained through the use of interchangeable steel positioning brackets. For some of the tests the flap span was reduced from 80 to 60 percent of the wing semispan.

Stall-control devices.- An inversely tapered drooped leading-edge flap with interchangeable deflection brackets of 0°, 20°, and 30° in a plane perpendicular to the hinge line was originally provided to serve as a stall-control device. For some of the tests this flap was cut and the outboard and inboard halves were deflected differentially. Chord-extensions of various spans having leading-edge radii of $0.0091\bar{c}$ and extensions of 15 percent of the local streamwise chord, and wing fences having heights of 2.54 and 5.12 percent of the mean aerodynamic wing chord were also tested as stall-control devices. Details of the various devices can be found in figure 6 and table I.

Speed brakes.- Speed-brake panels were provided at the rear end of the fuselage (see fig. 7(b) and table I). These panels could be attached at 30° and 45° deflection in the vertical plane and 26.7° and 40° in the horizontal plane.

External stores.- For some of the tests, external stores representative of 450-gallon pylon-mounted wing tanks were attached at the 0.606b/2 station. Details of the stores with and without stability fins can be found in figure 7(a) and table I.

Lateral-control spoiler.- A flap-type lateral-control spoiler was attached to the upper surface of the left wing. This spoiler extended spanwise from the fuselage to 70 percent of the wing semispan and could be deflected 61° in a plane perpendicular to its hinge line. Because of the abrupt change in wing contour at the 0.382b/2 station, a small gap was provided to permit deflection of the spoiler. Additional details of the spoiler can be found in figure 5(b) and table I.

Model Nomenclature

Listed below are the designations given to the various component parts of the model. Details of the various components may be found in figures 1 to 7 and tables I and II. The complete model configurations are obtained by combining the appropriate model components with the basic model.

A basic model (wing plus fuselage)

B speed brakes
- first subscript: vertical deflection, deg
- second subscript: horizontal deflection, deg

C chord-extension
- suffix: span (fraction of wing semispan)

E external stores
- prefix: Δ indicates 41.16 sq in. half-delta fin added to outboard side of each store
  - 15Δ indicates leading edge of fin is deflected 15° relative to the store center line
- subscript: 0 indicates outboard location (0.606b/2)
- suffix: 450 indicates 450-gallon fuel tank

F single slotted trailing-edge flap
- prefix: flap span (fraction of wing semispan)
- superscript: 1 indicates flap inflector door open
- subscript: deflection, deg

I wing-root inlet
  subscript: SE indicates supersonic-type elliptical inlet

N inversely tapered droop leading-edge flap
  subscript: deflection, deg
  suffix (used when only a portion of the flap is deflected):
    span (fraction of wing semispan)

R deflected rudder
  subscript: deflection, trailing edge right for positive deflection, deg

S flap-type lateral-control spoiler (left wing only)
  subscript: deflection, deg

T horizontal tail
  (primed T indicates modified airfoil section - see table II)
  prefix: vertical position (fraction of wing semispan)
  subscript: incidence, trailing edge down for positive deflection, deg
  suffix: (end plate) - plate with height of 4 times maximum thickness of horizontal tail, attached at juncture of horizontal tail and fuselage

V vertical tail

W wing fence
  prefix:

    1 indicates height equals 2.54 percent of mean aerodynamic chord

    2 indicates height equals 5.12 percent of mean aerodynamic chord

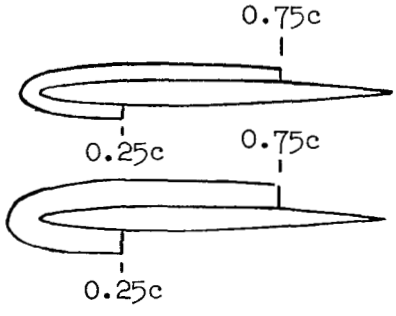

  subscript: spanwise position (fraction of wing semispan)

TESTS

All tests reported herein were conducted in the Langley 19-foot pressure tunnel at a tunnel pressure of approximately $2\frac{1}{3}$ atmospheres. A Reynolds number, based on the mean aerodynamic chord, of 9.0×10^6 and a corresponding Mach number of 0.20 were maintained throughout the

investigation. The model was mounted on the normal three-support system at 0° angle of yaw and was tested through an angle-of-attack range of -4° to 29°, except when limited by physical interference between the extended speed brakes and the support system.

Longitudinal characteristics of the model with and without various horizontal-tail arrangements, high-lift and stall-control devices, external stores, and speed brakes were obtained. Lateral-control characteristics of the flap-type spoiler aileron were investigated at only one spoiler deflection with and without drooped leading-edge and trailing-edge flaps. In addition, the effectiveness of the rudder was measured at one rudder deflection.

CORRECTIONS

Jet-boundary corrections determined by the method of reference 1 have been applied to all force and moment data. Rolling-moment, side-force, and yawing-moment coefficients have been corrected for model and air-stream asymmetry. Corrections for support tare and interference effects and for air-flow misalinement have not been applied. Internal drag of the inlets and duct system is included in the drag data presented herein.

PRESENTATION OF DATA

The results of the longitudinal stability and control investigation of the 1/4-scale model of the Republic F-105 airplane are summarized in table III. Details of the test results may be found in figures 8 to 20 for the basic design and figures 21 to 33 for the model equipped with various modifications intended to improve the flap-down stability of the basic design.

The results of the brief exploratory lateral-control and rudder-effectiveness tests are contained in figures 34, 35, and 36.

Stall studies, duct air-flow effects on the longitudinal stability characteristics, and duct air-flow measurements are presented in figures 37 to 40.

Langley Aeronautical Laboratory,
National Advisory Committee for Aeronautics,
Langley Field, Va., June 11, 1954.

H. Neale Kelly
H. Neale Kelly
Aeronautical Research Scientist

Patrick A. Cancro
Patrick A. Cancro
Mechanical Engineer

Approved: Mark R. Nichols
for Eugene C. Draley
Chief of Full-Scale Research Division

cg

REFERENCE

1. Sivells, James C., and Salmi, Rachel M.: Jet-Boundary Corrections for Complete and Semispan Swept Wings in Closed Circular Wind Tunnels. NACA TN 2454, 1951.

TABLE I

DESIGN CHARACTERISTICS OF THE REPUBLIC F-105 AIRPLANE AND THE

1/4-SCALE MODEL OF THE F-105 AIRPLANE

	Full-scale	1/4-scale
Wing Assembly		
Basic data:		
Root airfoil, measured parallel to airplane center line at 0.38b/2	NACA 65A005.5	NACA 65A005.5
Tip airfoil, measured parallel to airplane center line	NACA 65A003.7	NACA 65A003.7
Angle of incidence, deg	0	0
Geometric twist, deg	0	0
Sweep of quarter-chord line (true), deg	45	45
Taper ratio	0.467	0.467
Aspect ratio (excluding inlet area)	3.182	3.182
Dihedral, deg	-3.5	-3.5
Dimensions:		
Root chord (theoretical), parallel to airplane center line, ft	15.000	3.750
Tip chord (theoretical), parallel to airplane center line, ft	7.000	1.750
Mean aerodynamic chord, parallel to airplane center line, ft	11.485	2.871
Location of mean aerodynamic chord, spanwise (projected), ft	7.690	1.933
Span, measured normal to airplane center line, ft	34.934	8.734
Area:		
Wing area (excluding inlet area), sq ft	385.0	24.062
Horizontal-Tail Assembly		
Basic data:		
Root airfoil, streamwise	NACA 65A006	NACA 65A006
Tip airfoil, streamwise	NACA 65A004	NACA 65A004
Modified airfoil section	----------	See table II
Angle of incidence at -		
Position 1, deg	+7 to -25	+7 to -25
Position 2, deg	----------	0, -3
Position 3, deg	----------	0, -3
Dihedral, deg	0	0
Taper ratio	0.456	0.456
Aspect ratio	3.06	3.06
Dimensions:		
Root chord (theoretical), ft	7.50	1.875
Tip chord (theoretical), ft	3.42	0.855
Mean aerodynamic chord (theoretical), ft	5.71	1.428
Span, ft	16.67	4.168
0.25$\bar{c}$ of wing to 0.25$\bar{c}$ of horizontal tail (theoretical), ft	20.68	5.232
Vertical location below fuselage center line:		
Position 1, in.	-18.00	-4.50
Position 2, in.	----------	-2.75
Position 3, in.	----------	-1.00
Area:		
Horizontal tail area (theoretical), sq ft	90.97	5.685
Horizontal tail area (exposed), sq ft	60.77	3.798
Vertical-Tail Assembly		
Basic data:		
Root airfoil, measured parallel to airplane center line at 0.167b/2	NACA 65A006	NACA 65A006
Tip airfoil, measured parallel to airplane center line	NACA 65A004	NACA 65A004
Sweepback of quarter-chord line, deg	45	45
Aspect ratio (theoretical)	1.593	1.593
Taper ratio (theoretical)	0.365	0.365
Sweepback of rudder hinge line, deg	29.358	29.358
Rudder deflections, measured in a plane normal to the hinge line, deg	+32 to -32	0, 12, 24, 35

TABLE I - Continued

DESIGN CHARACTERISTICS OF THE REPUBLIC F-105 AIRPLANE AND THE

1/4-SCALE MODEL OF THE F-105 AIRPLANE

	Full-scale	1/4-scale
Dimensions:		
Root chord (theoretical), ft	10.03	2.508
Tip chord (theoretical), ft	3.67	0.9175
Mean aerodynamic chord (theoretical), ft	7.34	1.835
0.25$\bar{c}$ of wing to 0.25$\bar{c}$ of vertical tail (theoretical), ft	17.40	4.412
Vertical tail height, measured from fuselage center line, ft	10.92	2.729
Rudder chord (average), ft	1.86	0.458
Rudder span, measured normal to fuselage center line, ft	6.83	1.708
Areas:		
Vertical tail area (theoretical), sq ft	74.8	4.670
Vertical tail area (exposed), sq ft	48.0	3.000
Rudder area (including overhang), sq ft	11.39	0.712
Fuselage		
Length, ft	62.0	15.049
Maximum width, ft	4.375	1.094
Maximum height (excluding canopy), ft	6.50	1.625
Volume (including canopy), cu ft	1142	17.87
Location of station 0 (measured upstream from nose of airplane), ft	39.672	9.918
Side area (excluding vertical tail), sq ft	346	21.6
Frontal area (including canopy), sq ft	24.7	1.542
Trailing-Edge Flaps		
Basic data:		
Type	Single slotted	Single slotted
Deflection, measured in a plane normal to 0.82c, deg	0 to 46.2	0, 30, 35, 40, 46
Dimensions:		
Average chord, measured parallel to airplane center line	0.25c	0.25c
Span (one flap), measured normal to airplane center line, ft	11.7	2.925
Location of outboard edge, measured normal to airplane center line, in.	168.0	42
Location of inboard edge, measured normal to airplane center line, in.	27.85	6.963
Area:		
Area of both trailing-edge flaps, sq ft	69.6	4.35
Leading-Edge Flaps		
Basic data:		
Type	Drooped nose	Drooped nose
Deflection, measured in a plane normal to hinge line, deg	0 to 20	0, 15, 20, 25, 30
Location of inboard edge, measured normal to airplane center line, in.	82.149	20.537
Location of outboard edge, measured normal to airplane center line, in.	199.78	49.945
Dimensions:		
Average leading-edge flap chord (streamwise)	0.12c	0.12c
Span (one flap), measured normal to airplane center line, ft	9.8	2.45
Area:		
Area of both leading-edge flaps, sq ft	22.7	1.419

TABLE I - Concluded

DESIGN CHARACTERISTICS OF THE REPUBLIC F-105 AIRPLANE AND THE

1/4-SCALE MODEL OF THE F-105 AIRPLANE

	Full-Scale	1/4-scale
Spoiler Ailerons		
Basic data:		
Type	Flap	Flap
Angular travel, measured normal to hinge line, deg	0 to 61	0, 18, 36, 61, 74, 90
Location of inboard edge, measured normal to airplane center line, in.	38.0	9.50
Location of outboard edge, measured normal to airplane center line, in.	147.0	36.75
Dimensions:		
Average chord (streamwise)	0.12c	0.12c
Location of hinge center line	0.70c	0.70c
Span, measured normal to airplane center line, ft	9.1	2.275
Areas:		
Area of both spoilers, sq ft -		
Including gaps	24.2	0.756
Excluding gaps	23.1	0.722
External Tanks (450-gallon capacity for inboard wing pylon)		
Length, in.	227.55	56.89
Diameter (max.), in.	29.0	7.25
Angle of incidence, relative to fuselage center line, deg	-3.0	-3.0
Spanwise location, measured from fuselage center line, in.	129.0	31.75
Vertical location of nose of tank, measured below fuselage center line, in.	-40.04	-10.01
Longitudinal location, measured from fuselage station 0, in.	496.0	124.0
Speed Brakes		
Location, measured from fuselage station 0		
Top and bottom, in.	728.0	181.75
Sides, in.	739.5	184.75
Area		
Top and bottom, sq ft	17.5	1.090
Sides, sq ft	11.0	0.690
Deflection		
Top and bottom, measured normal to hinge line, deg	0 to 45	0, 30, 45
Sides, measured normal to hinge line, deg	0 to 40	0, 26.7, 40

TABLE II

ORDINATES FOR MODIFIED HORIZONTAL TAIL

Station 0.264b/2		Station 1.00b/2	
x, percent c	±y, percent c	x, percent c	±y, percent c
0	0	0	0
.468	1.239	.501	.937
1.879	2.326	2.008	1.769
4.261	3.188	4.541	2.413
7.648	3.746	8.114	2.818
12.049	4.000	12.717	2.983
15	3.992	18.292	2.962
20	3.940	24.727	2.810
25	3.852	31.828	2.561
30	3.713	35	2.442
35	3.546	40	2.254
40	3.348	45	2.066
45	3.123	50	1.952
50	2.876	55	1.867
55	2.611	60	1.742
60	2.602	65	1.584
65	2.364	70	1.400
70	2.087	75	1.193
75	1.775	80	.966
80	1.437	85	.728
85	1.083	90	.490
90	.727	95	.249
95	.370	100	.009
100	.013		
L.E. rad. = 1.7 percent c		L.E. rad. = 0.805 percent c	

TABLE III

SUMMARY OF THE LONGITUDINAL STABILITY CHARACTERISTICS OF A

1/4-SCALE MODEL OF THE F-105 AIRPLANE

Wing, aspect ratio 3.18	Fuselage . . . . . basic
Tail, aspect ratio 3.06	Inlet . . . supersonic elliptical

Wing configuration		Speed-brake deflection		Store	Tail configuration			C_L at $\alpha=12^\circ$	$C_{L_{max}}$	α at $C_{L_{max}}$	C_m characteristics about $0.25\bar{c}$	Fig.
T.E. device	Stall-control device	Horizontal, deg	Vertical, deg		Height $2z/b$	NACA airfoil section	i_t, deg					
None	None	0	0	None	--	--	Off	0.635	0.960	26.0	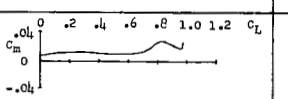	8
					-0.057	65A series	0.1	0.705	1.155	28.8[a]	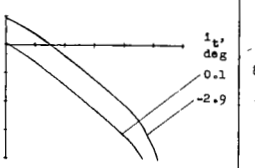	8
							-2.9	0.675	1.160	28.8[a]		
					-0.090	65A series	0.1	0.705	1.160	28.8[a]	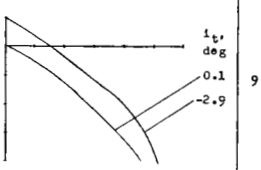	9
							-2.9	0.685	1.150	28.0		
					-0.123	65A series	7.0	0.775	1.145	22.0	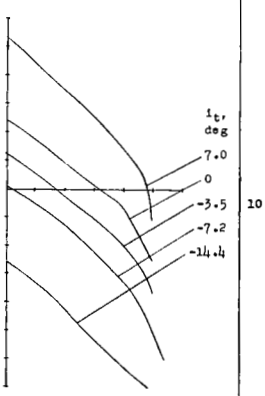	10
							0	0.708	1.150	26.0		
							-3.5	0.690	1.145	28.0		
							-7.2	0.645	1.122	28.0		
							-14.4	0.597	1.060	28.0		
		26.7	30	None	-0.123	65A series	Off	0.645	0.945	23.7	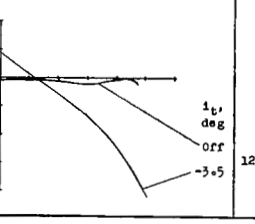	12
							-3.5	0.690	1.115	23.8[a]		

[a]Highest angle of test.

TABLE III.- Continued

SUMMARY OF THE LONGITUDINAL STABILITY CHARACTERISTICS OF A 1/4-SCALE MODEL OF THE F-105 AIRPLANE

Wing configuration		Speed-brake deflection		Store	Tail configuration			C_L at $\alpha=12^\circ$	$C_{L_{max}}$	α at $C_{L_{max}}$	C_m characteristics about 0.25c	Fig.
T.E. device	Stall-control device	Horizontal, deg	Vertical, deg		Height 2z/b	NACA airfoil section	i_t, deg					
None	None	40	45	None	-0.123	65A series	Off	0.640	0.950	23.7°	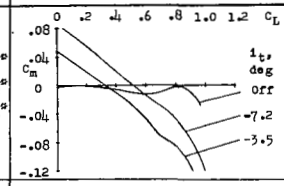	11
							-3.5	0.681	1.100	23.8°		
							-7.2	0.662	1.065	23.8°		
		0	0	450 gal No fin	-0.123	65A series	Off	0.628	0.935	20.7	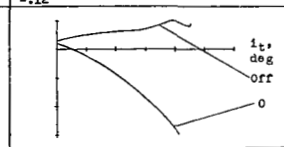	13
							0	0.700	1.130	26.5		
Single-slotted flap 0.133b/2 to 0.800b/2 δ = 46°	None	0	0	None	-0.123	65A series	Off	1.107	1.182	18.4	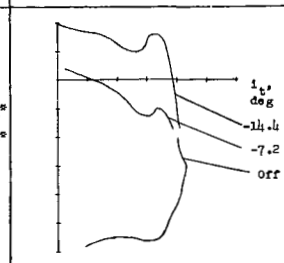	14
							-7.2	1.048	1.277	28.9°		
							-14.4	0.980	1.205	28.9°		
Single-slotted flap 0.133b/2 to 0.600b/2 δ = 46°	None	0	0	None	-0.123	Modified 1 series	-7.2	0.984	1.190	28.8°	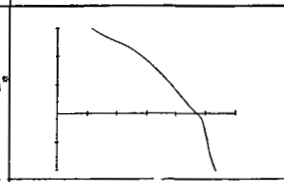	—
				450 gal finned store δ = 0°	-0.123	65A series	-7.2	0.995	1.230	28.8°	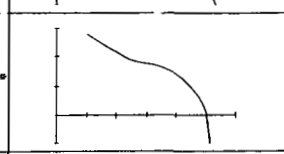	32
				450 gal finned store δ = 15°	-0.123	65A series	-7.2	0.960	1.190	28.8°	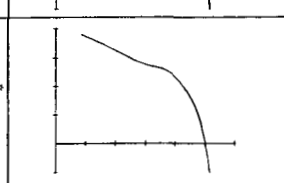	32
Single-slotted flap 0.133b/2 to 0.800b/2 δ = 46°	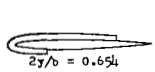 2y/b = 0.654	0	0	None	-0.123	Modified 1 series	-7.2	1.122	1.265	28.9°	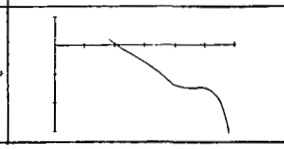	26

°Highest angle of test.

TABLE III.- Continued

SUMMARY OF THE LONGITUDINAL STABILITY CHARACTERISTICS OF A

1/4-SCALE MODEL OF THE F-105 AIRPLANE

Wing configuration		Speed-brake deflection		Store	Tail configuration			C_L at $\alpha=12^\circ$	$C_{L_{max}}$	α at $C_{L_{max}}$	C_m characteristics about $0.25\bar{c}$	Fig.
T.E. device	Stall-control device	Horizontal, deg	Vertical, deg		Height $2z/b$	NACA airfoil section	i_t, deg					
Single-slotted flap 0.133b/2 to 0.800b/2 $\delta = 46^\circ$	2y/b = 0.654 height = 0.0512$\bar{c}$	0	0	None	-0.123	Modified 1 series	-7.2	1.100	1.267	28.9*	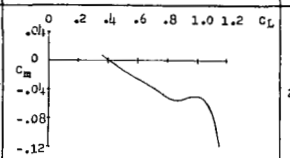	26
	2y/b = 0.654 height = 0.0512$\bar{c}$; 2y/b = 0.800 height = 0.0254$\bar{c}$	0	0	None	-0.123	Modified 1 series	-7.2	1.080	1.275	28.9*	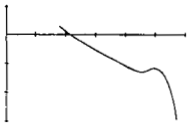	26
	2y/b = 0.704 height = 0.0512$\bar{c}$; 2y/b = 0.480 height = 0.0254$\bar{c}$	0	0	None	-0.123	Modified 1 series	-7.2	1.045	1.261	28.9*	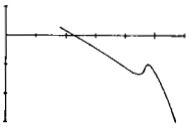	26
	2y/b = 0.480 height = 0.0512$\bar{c}$; 2y/b = 0.720 height = 0.0254$\bar{c}$	0	0	None	-0.123	Modified 1 series	-7.2	1.090	1.275	28.9*	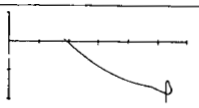	26
	L.E. flap 0.382b/2 to 0.950b/2 $\delta = 20^\circ$	0	0	None	—	—	Off	1.175	1.240	20.8	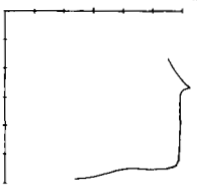	15
					-0.123	65A series	-7.2 -14.4 -20.3 -25.1	1.114 1.045 1.032 1.010	1.300 1.230 1.170 1.140	20.9 28.9* 20.8 28.8*	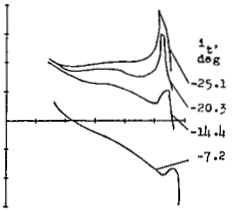	15
		40	0	None	-0.123	65A series	Off -14.4	1.180 1.050	1.230 1.240	20.8 28.9*	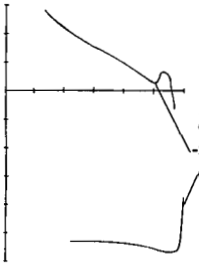	18

*Highest angle of test.

TABLE III.- Continued

SUMMARY OF THE LONGITUDINAL STABILITY CHARACTERISTICS OF A

1/4-SCALE MODEL OF THE F-105 AIRPLANE

Wing configuration		Speed-brake deflection		Store	Tail configuration			C_L at $\alpha=12^\circ$	$C_{L_{max}}$	α at $C_{L_{max}}$	C_m characteristics about 0.25$\bar{c}$	Fig.
T.E. device	Stall-control device	Horizontal, deg	Vertical, deg		Height $2z/b$	NACA airfoil section	i_t, deg					
Single-slotted flap 0.133b/2 to 0.800b/2 $\delta = 46^\circ$	L.E. flap 0.382b/2 to 0.950b/2 $\delta = 20^\circ$	40	45	None	-0.123	65A series	Off	1.120	1.230	20.8	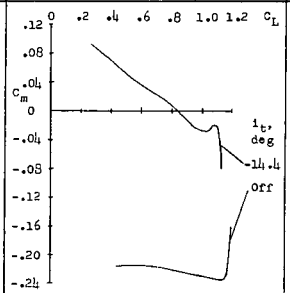	18
							-14.4	1.060	1.268	20.8		
		0	0	450 gal No fin	-0.123	65A series	Off	1.185	1.280	18.9	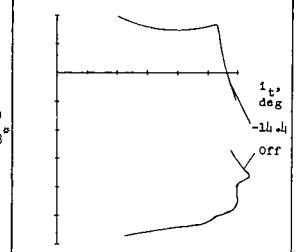	19
							-14.4	1.055	1.237	28.8[a]		
Single-slotted flap 0.133b/2 to 0.600b/2 $\delta = 46^\circ$	L.E. flap 0.382b/2 to 0.950b/2 $\delta = 20^\circ$	0	0	None	—	—	Off	1.095	1.160	21.1	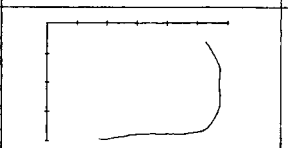	30
					-0.123	65A series	0.1	1.087	1.340	20.8	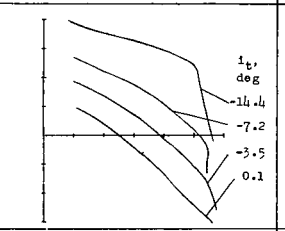	30
							-3.5	1.049	1.280	21.5		
							-7.2	1.013	1.230	21.4		
							-14.4	0.950	1.175	21.2		
						Modified series	0	1.075	1.292	26.4	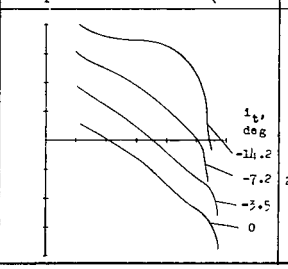	28
							-3.5	1.042	1.281	21.3		
							-7.2	1.020	1.230	28.9		
							-14.2	0.915	1.170	21.3		

[a]Highest angle of test.

TABLE III.- Continued

SUMMARY OF THE LONGITUDINAL STABILITY CHARACTERISTICS OF A 1/4-SCALE MODEL OF THE F-105 AIRPLANE

Wing configuration		Speed-brake deflection		Store	Tail configuration			C_L at $\alpha=12^\circ$	$C_{L_{max}}$	α at $C_{L_{max}}$	C_m characteristics about $0.25\bar{c}$	Fig.
T.E. device	Stall-control device	Horizontal, deg	Vertical, deg		Height z_t/b	NACA airfoil section	i_t, deg					
Single-slotted flap 0.133b/2 to 0.500b/2 $\delta = 46^\circ$	L.E. flap 0.382b/2 to 0.950b/2 $\delta = 20^\circ$	0	0	450 gal No fin	—	—	off	1.074	1.160	18.6	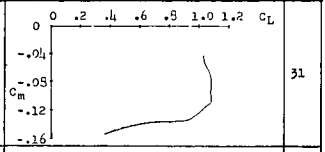	31
				450 gal No fin	-0.123	65A series	3.4 0.1 -3.5 -7.2 -14.4	1.087 1.044 1.018 0.985 0.938	1.270 1.260 1.250 1.200 1.160	19.6 20.0 26.9 19.2 28.9[a]	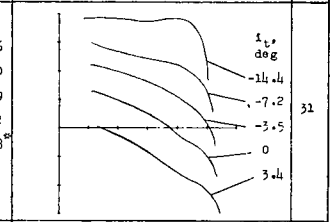	31
				450 gal finned store $\delta = 0^\circ$	-0.123	65A series	-7.2	1.006	1.242	26.9[a]	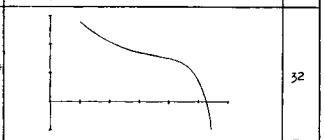	32
				450 gal finned store $\delta = 15^\circ$	-0.123	65A series	-7.2	0.980	1.218	28.9	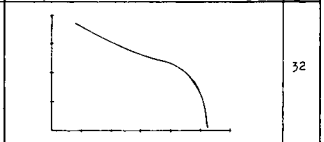	32
		40	0	450 gal No fin	-0.123	65A series	off 3.4 0.1	1.065 1.060 1.025	1.150 1.291 1.260	18.8 19.8 28.9[a]	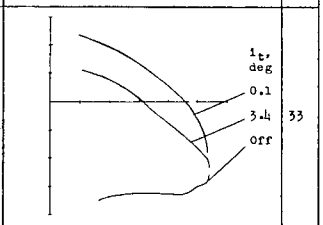	33
Single-slotted flap 0.133b/2 to 0.500b/2 $\delta = 46^\circ$	L.E. flap 0.382b/2 to 0.950b/2 $\delta = 30^\circ$	0	0	None	—	—	off	1.175	1.280	22.8	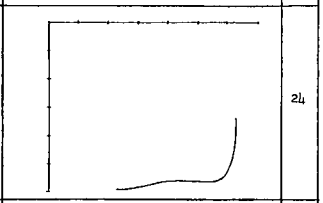	24
					-0.123	65A series	-7.2 -14.4 -20.3 -25.1	1.100 1.035 1.033 1.019	1.340 1.262 1.205 1.152	23.0 22.8 22.8 22.3	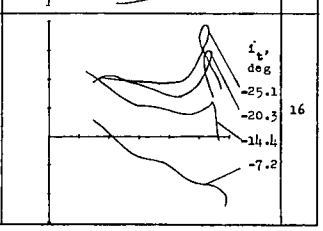	16

[a]Highest angle of test.

TABLE III.- Continued

SUMMARY OF THE LONGITUDINAL STABILITY CHARACTERISTICS OF A 1/4-SCALE MODEL OF THE F-105 AIRPLANE

Wing configuration		Speed-brake deflection		Store	Tail configuration			C_L at $\alpha=12^\circ$	$C_{L_{max}}$	α at $C_{L_{max}}$	C_m characteristics about $0.25\bar{c}$	Fig.
T.E. device	Stall-control device	Horizontal, deg	Vertical, deg		Height $2z/b$	NACA airfoil section	i_t, deg					
Single-slotted flap 0.133b/2 to 0.800b/2 $\delta = 46^\circ$	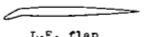	0	0	450 gal No fin	-0.123	65A series	off -14.4	1.178 1.055	1.382 1.260	21.0 18.9°	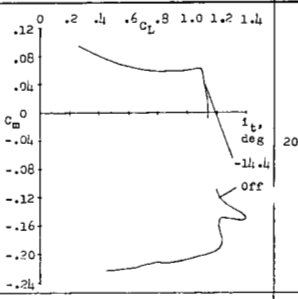	20
	L.E. flap 0.382b/2 to 0.950b/2 $\delta = 30^\circ$	40	0	None	-0.123	65A series	off -7.2 -14.4	1.200 1.140 1.064	1.263 1.298 1.277	21.8 22.6 22.8	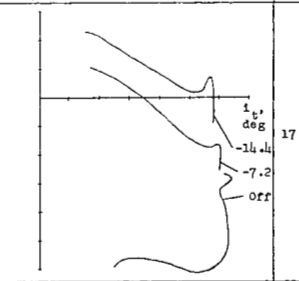	17
	L.E. flap 0.654b/2 to 0.950b/2 $\delta = 30^\circ$	0	0	None	-0.123	65A series	-14.2	1.040	1.291	19.4	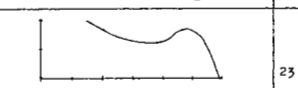	23
	L.E. flap 0.382b/2 to 0.950b/2 $\delta = 30^\circ$	0	0	None	-0.123	Modified 1 series	-7.2 -14.2	1.130 1.065	1.350 1.282	23.0 22.0	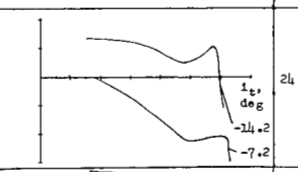	24
	L.E. flap 0.382b/2 to 0.654b/2 $\delta = 30^\circ$	0	0	None	-0.123	Modified 1 series	-7.2 -14.2	1.127 1.060	1.320 1.240	28.9° 28.9°	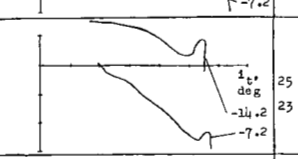	25 23
	L.E. flap 0.382b/2 to 0.950b/2 $\delta = 30^\circ$ 2z/b = 0.654 height = $0.0254\bar{c}$	0	0	None	-0.123	Modified 1 series	-7.2	1.110	1.338	22.0		25

*Highest angle of test.

TABLE III.- Continued

SUMMARY OF THE LONGITUDINAL STABILITY CHARACTERISTICS OF A

1/4-SCALE MODEL OF THE F-105 AIRPLANE

Wing configuration		Speed-brake deflection		Store	Tail configuration			C_L at $\alpha=12^\circ$	$C_{L_{max}}$	α at $C_{L_{max}}$	C_m characteristics about 0.25$\bar{c}$	Fig.
T.E. device	Stall-control device	Horizontal, deg	Vertical, deg		Height 2z/b	NACA airfoil section	i_t, deg					
Single-slotted flap 0.133b/2 to 0.800b/2 $\delta = 46^\circ$	L.E. flap 0.654b/2 to 0.950b/2 $\delta = 30^\circ$ 2y/b = 0.654 height = 0.0254$\bar{c}$	0	0	None	-0.123	Modified 1 series	-7.2	1.088	1.300	28.9°	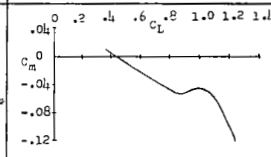	25
	L.E. flap 0.382b/2 to 0.654b/2 $\delta = 30^\circ$ 2y/b = 0.654 height = 0.0254$\bar{c}$	0	0	None	-0.123	Modified 1 series	-7.2	1.120	1.320	28.9°	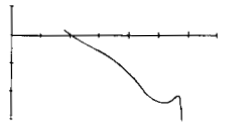	25
Single-slotted T.E. flap 0.133b/2 to 0.800b/2 $\delta = 35^\circ$	L.E. flap 0.382b/2 to 0.950b/2 $\delta = 30^\circ$	0	0	None	-0.123	Modified 1 series	Off -7.2 -14.2	1.045 1.030 0.970	1.148 1.338 1.268	20.6 24.2 24.9	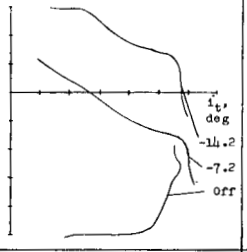	27
Single-slotted T.E. flap 0.133b/2 to 0.600b/2 $\delta = 46^\circ$	L.E. flap 0.382b/2 to 0.950b/2 $\delta = 30^\circ$	0	0	None	—	—	Off	1.085	1.260	20.9	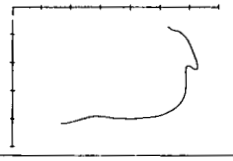	29
					-0.123	Modified 1 series	0 -3.5 -7.2	1.065 1.040 1.028	1.360 1.332 1.310	21.0 22.2 21.4	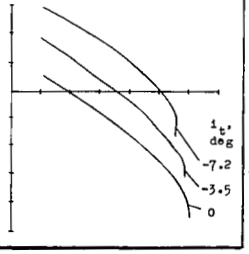	29

*Highest angle of test.

TABLE III.- Concluded

SUMMARY OF THE LONGITUDINAL STABILITY CHARACTERISTICS OF A

1/4-SCALE MODEL OF THE F-105 AIRPLANE

Wing configuration		Speed-brake deflection		Store	Tail configuration			C_L at $\alpha=12^\circ$	$C_{L_{max}}$	α at $C_{L_{max}}$	C_m characteristics about 0.25c	Fig.
T.E. device	Stall-control device	Horizontal, deg	Vertical, deg		Height $2z/b$	NACA airfoil section	i_t, deg					
Single-slotted T.E. flap 0.133b/2 to 0.800b/2 $\delta = 46^\circ$	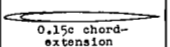 0.15c chord-extension 0.550b/2 to 0.950b/2	0	0	None	-0.123	65A series	-14.4	1.117	1.280	28.9°	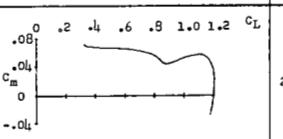	21
	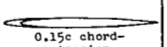 0.15c chord-extension 0.600b/2 to 0.950b/2	0	0	None	-0.123	65A series	-14.4	1.110	1.260	28.9°		21
	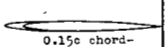 0.15c chord-extension 0.650b/2 to 0.950b/2	0	0	None	-0.123	65A series	-7.2 -14.4	1.165 1.108	1.323 1.263	28.9° 28.9*	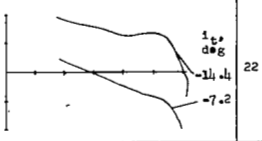	22
	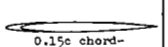 0.15c chord-extension 0.700b/2 to 0.950b/2	0	0	None	-0.123	65A series	-14.4	1.075	1.245	28.9*	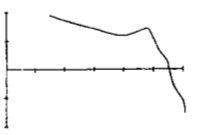	21
	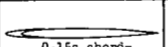 0.15c chord-extension 0.750b/2 to 0.950b/2	0	0	None	-0.123	65A series	-14.4	1.045	1.248	28.9*	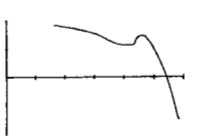	21

*Highest angle of test.

[redacted]

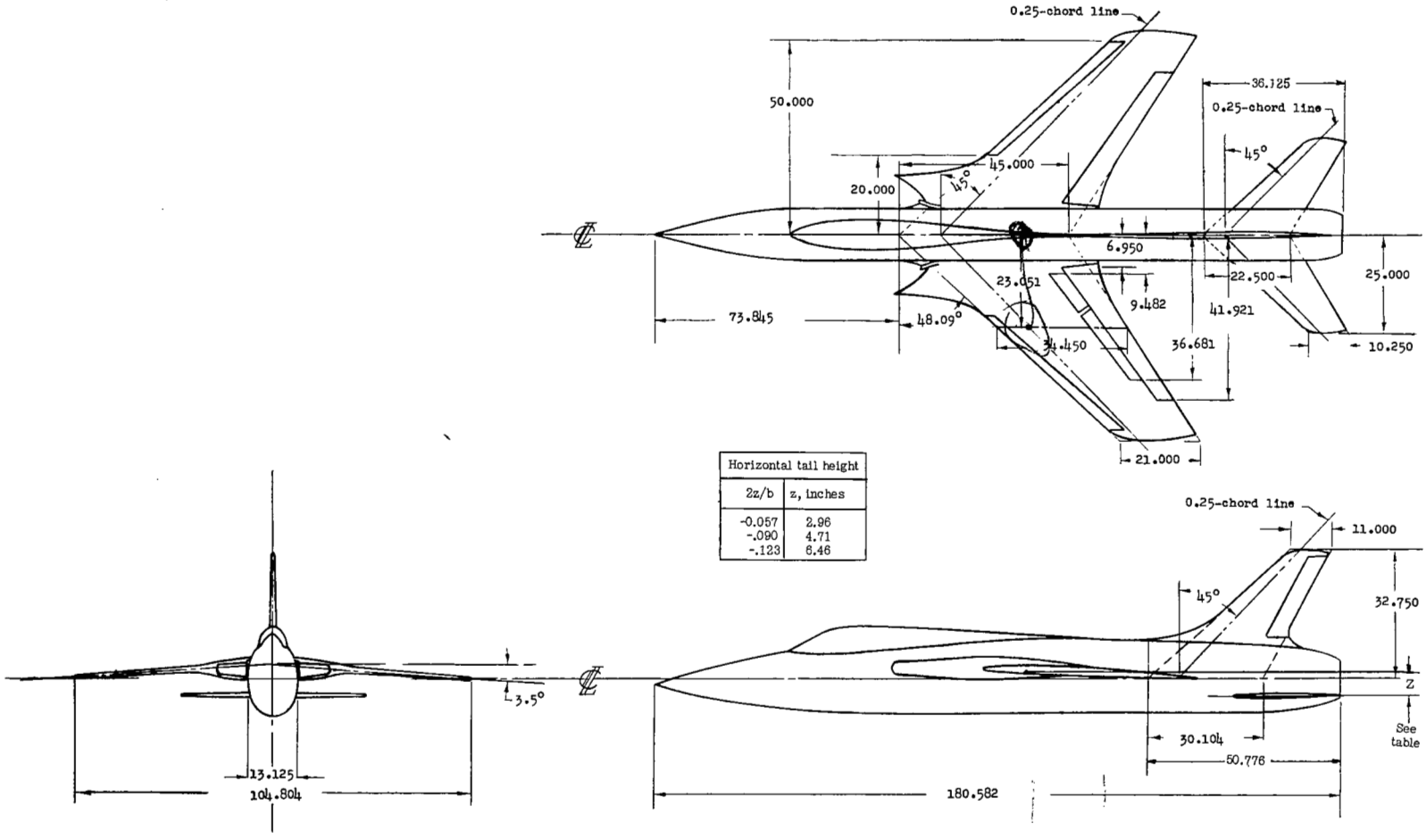

Horizontal tail height	
2z/b	z, inches
-0.057	2.96
-.090	4.71
-.123	6.46

Figure 1.- Three-view drawing of a 1/4-scale model of the Republic F-105 airplane. (Dimensions in inches unless otherwise noted.)

[redacted]

L-84117

Figure 2.- The 1/4-scale model of the F-105 airplane mounted on the normal three-support system of the Langley 19-foot pressure tunnel.

[redacted]

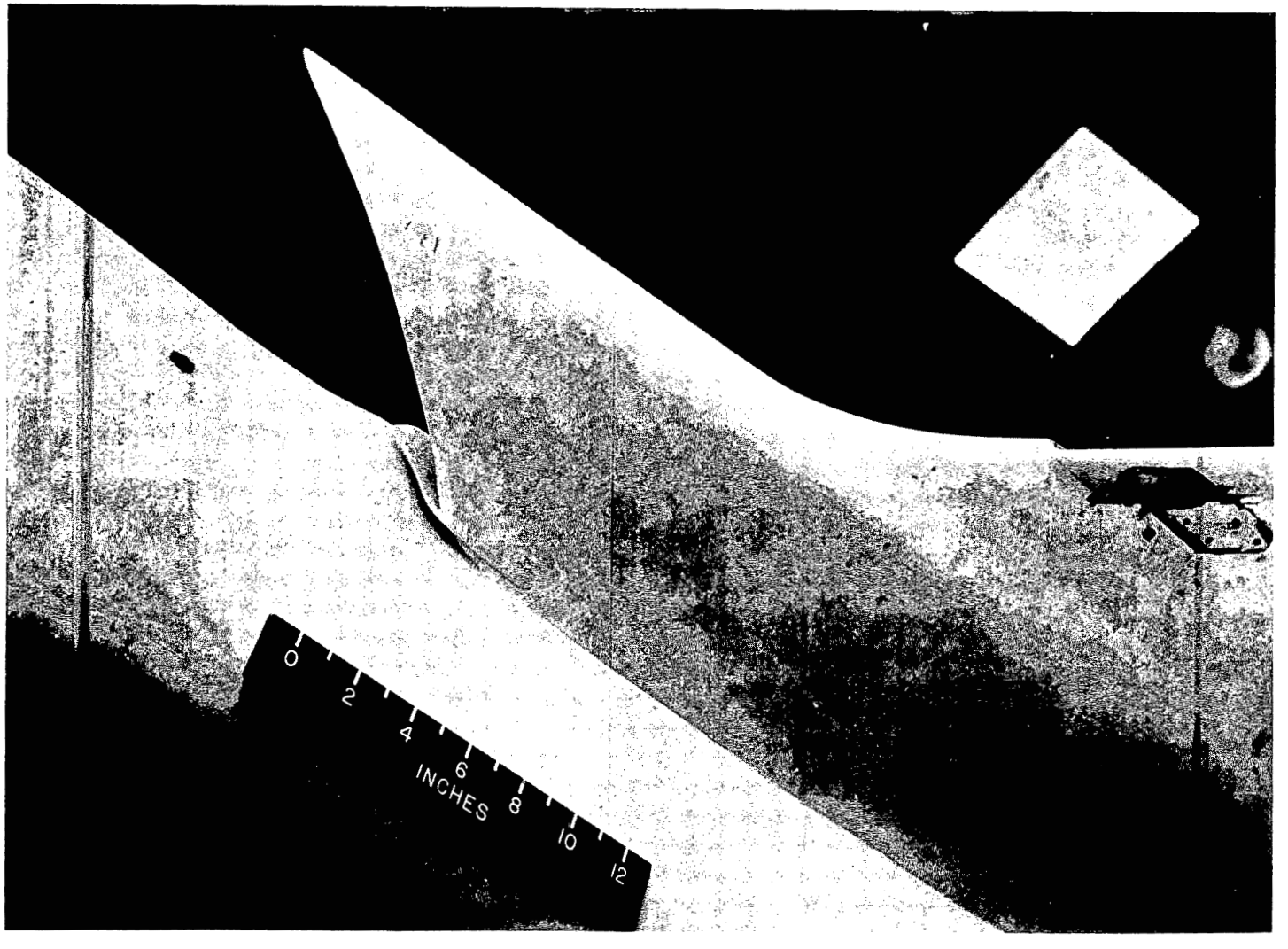

L-84118

Figure 3.- The 1/4-scale F-105 supersonic-type elliptical wing-root inlet as viewed from below.

[redacted]

[redacted]

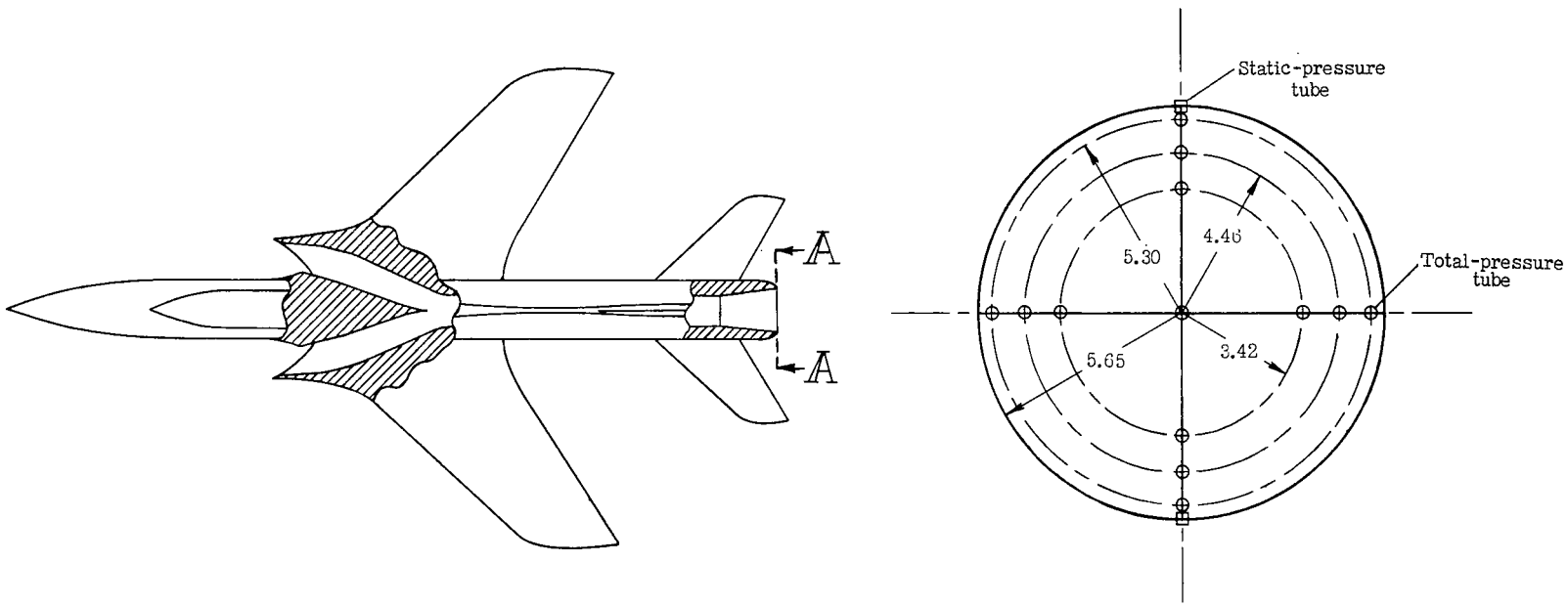

View A-A
(enlarged)

Figure 4.- Details of the duct lines and the pressure-rake installation. (All dimensions in inches.)

[redacted]

[redacted]

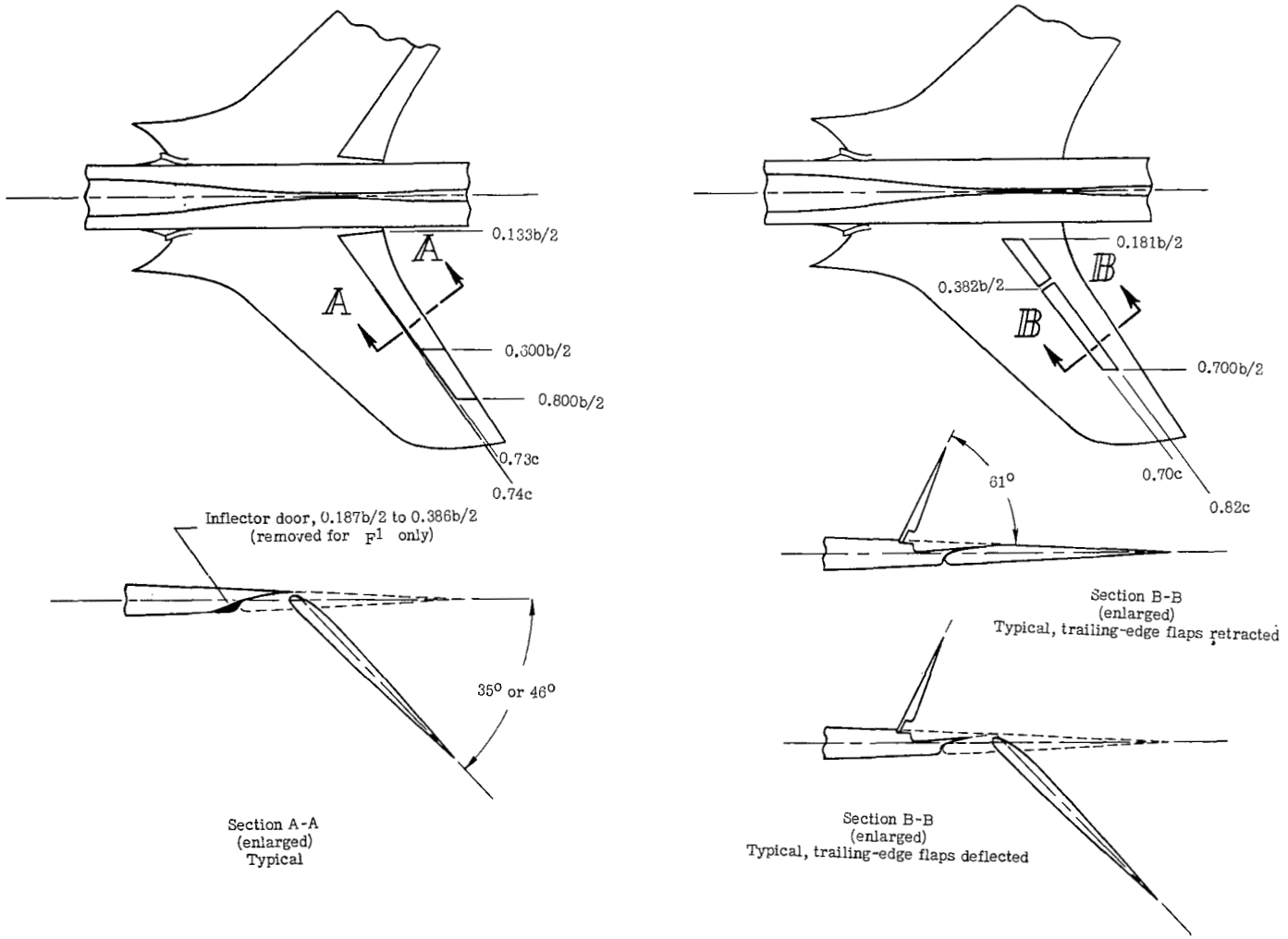

(a) Trailing-edge flap F. (b) Lateral-control spoiler S.

Figure 5.- Details of the trailing-edge flaps and the lateral-control spoiler.

[redacted]

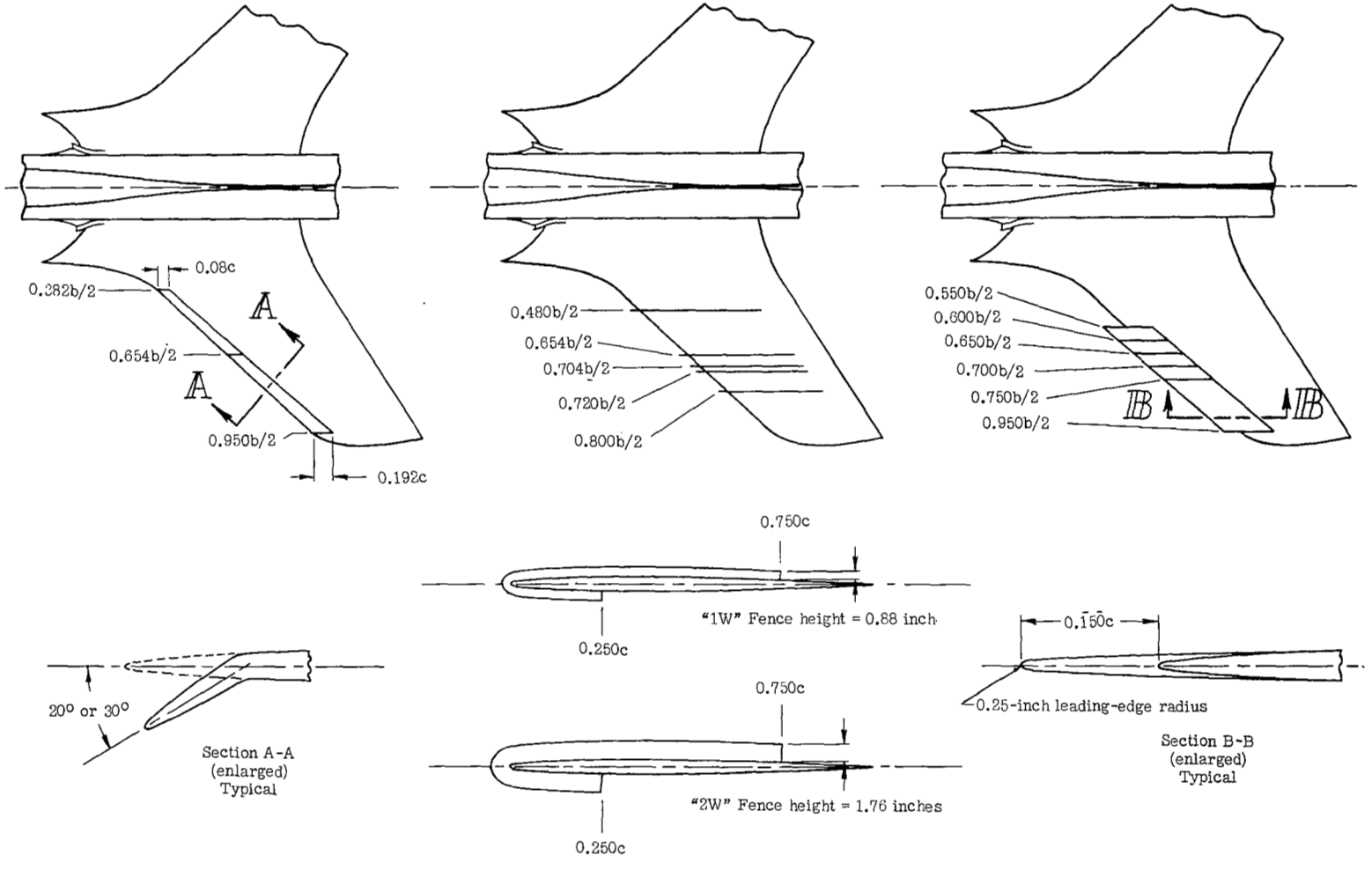

(a) Leading-edge droop N. (b) Wing fences W. (c) Chord-extension C.

Figure 6.- Details of the stall-control devices.

[redacted]

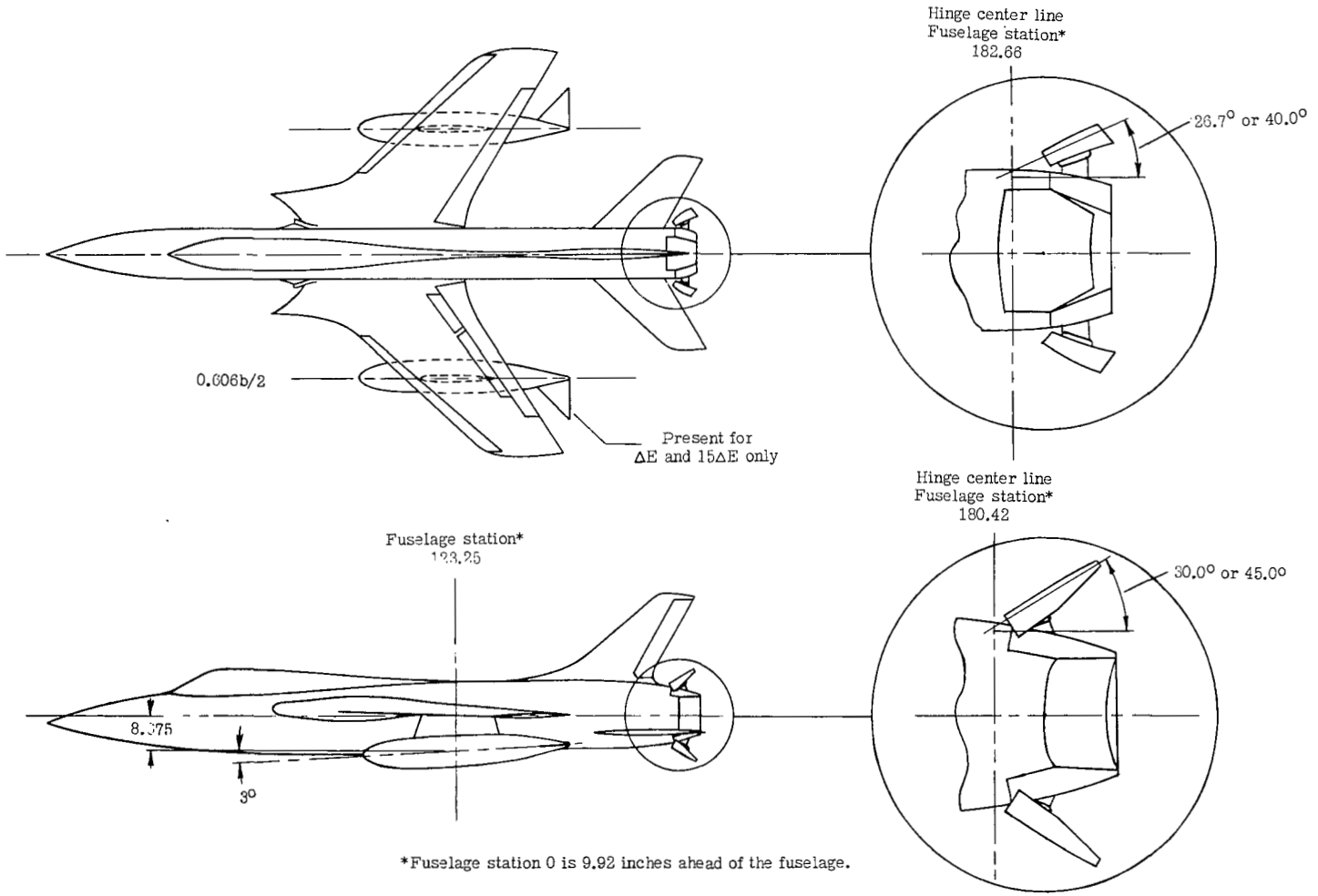

(a) External stores E. (b) Speed brakes B.

Figure 7.- Details of the external stores and the fuselage speed brakes. (Dimensions in inches except as noted.)

[redacted]

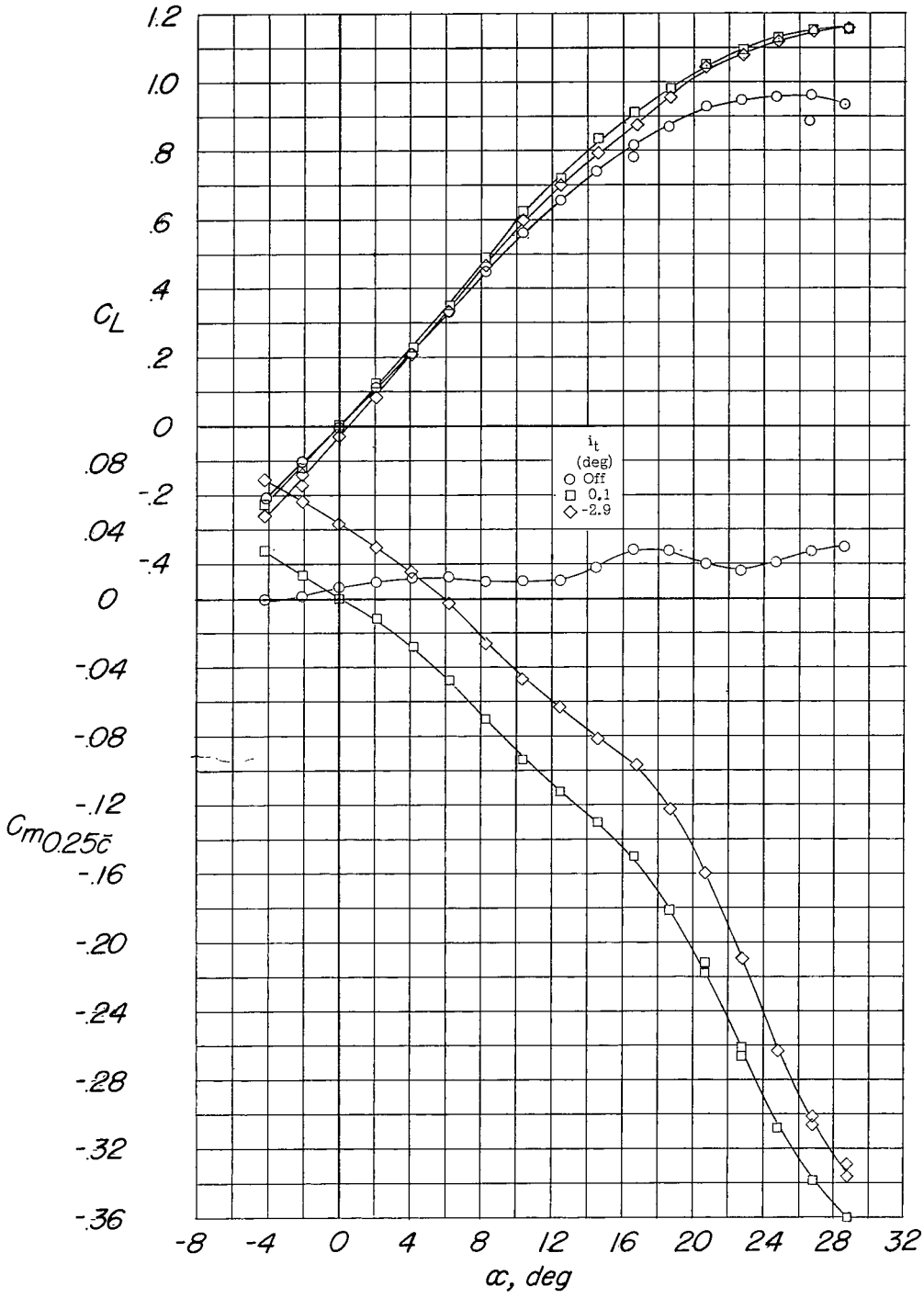

(a) C_L and C_m against α.

Figure 8.- Longitudinal characteristics of the model equipped with a horizontal tail located 0.057b/2 below the wing mean-aerodynamic-chord plane. Configuration A + V + I_{SE} + (-0.057)T.

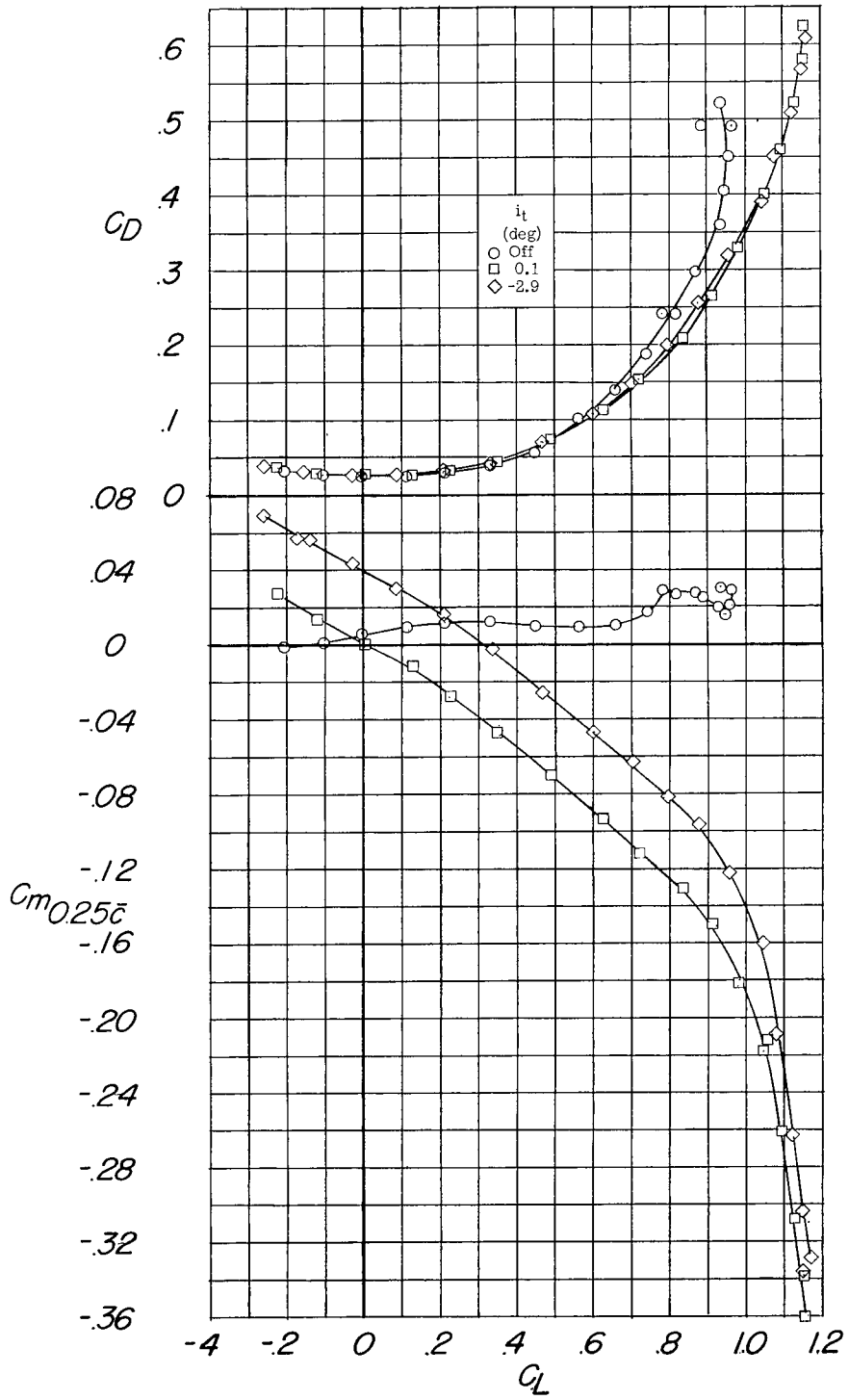

(b) C_D and C_m against C_L.

Figure 8.- Concluded.

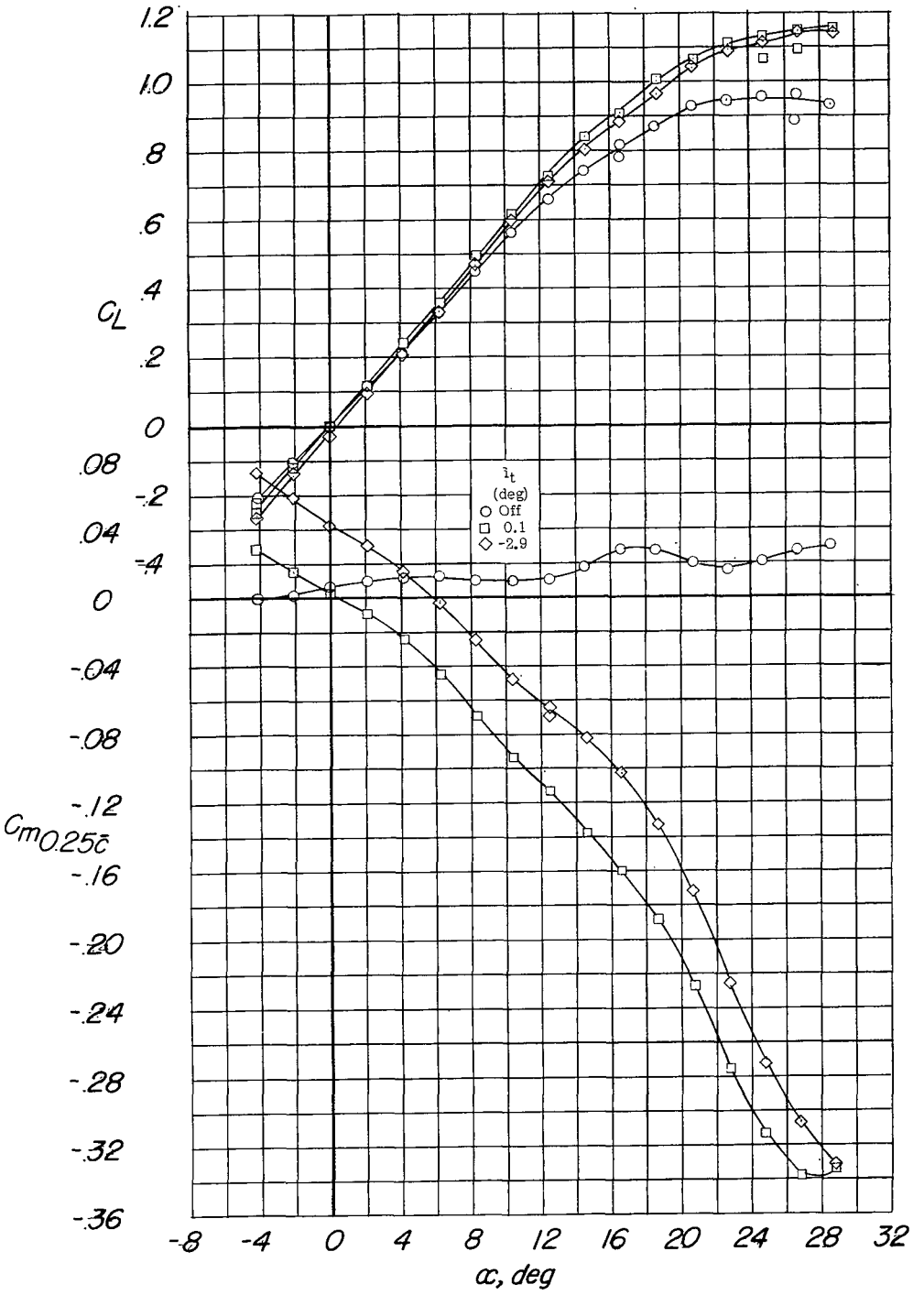

(a) C_L and C_m against α.

Figure 9.- Longitudinal characteristics of the model equipped with a horizontal tail located 0.090b/2 below the wing mean-aerodynamic-chord plane. Configuration A + V + I_{SE} + (-0.090)T.

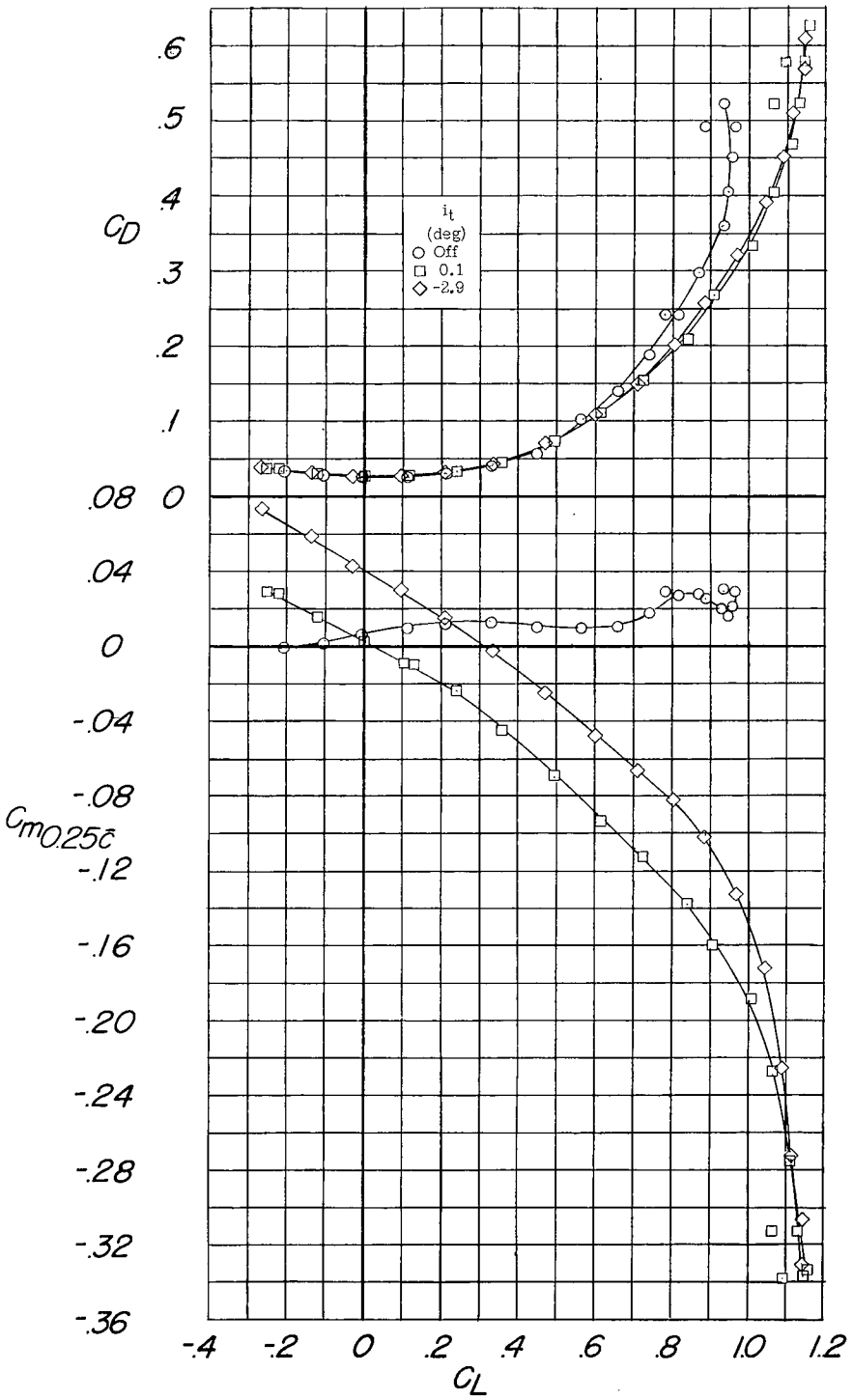

(b) C_D and C_m against C_L.

Figure 9.- Concluded.

[redacted]

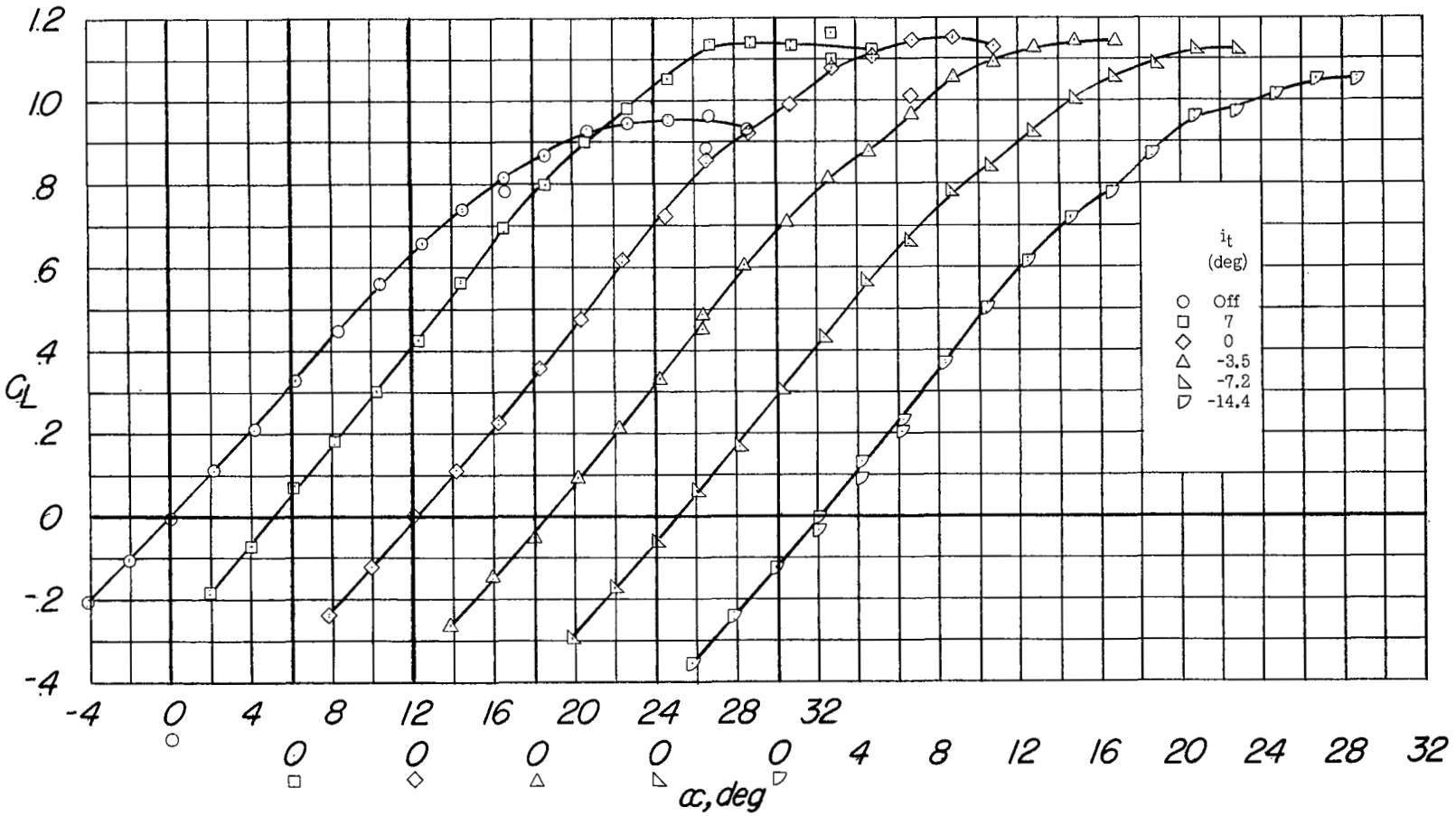

(a) C_L against α.

Figure 10.- Longitudinal characteristics of the model equipped with a horizontal tail located 0.123b/2 below the wing mean-aerodynamic-chord plane. Configuration A + V + I_{SE} + (-0.123)T.

[redacted]

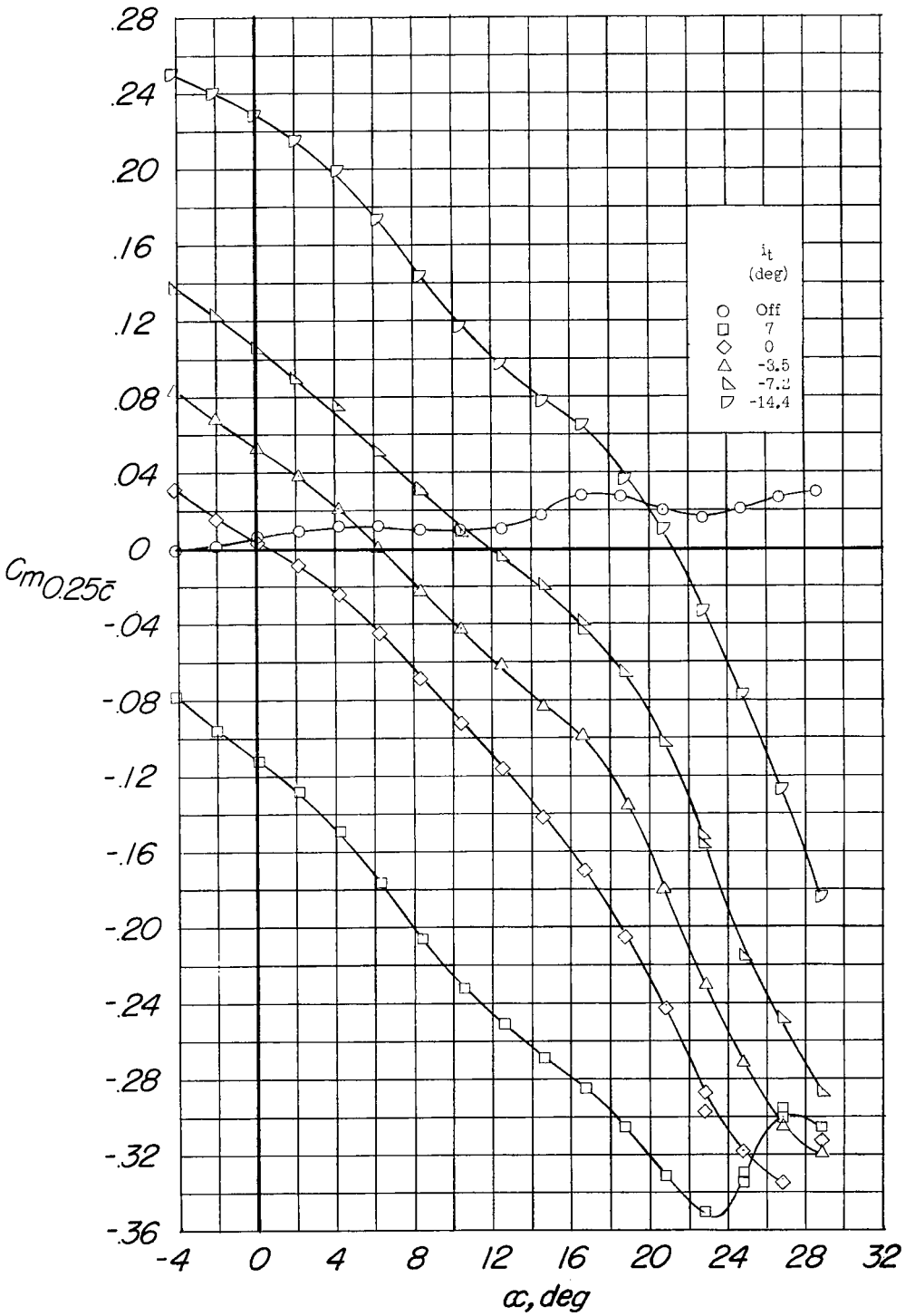

(b) C_m against α.

Figure 10.- Continued.

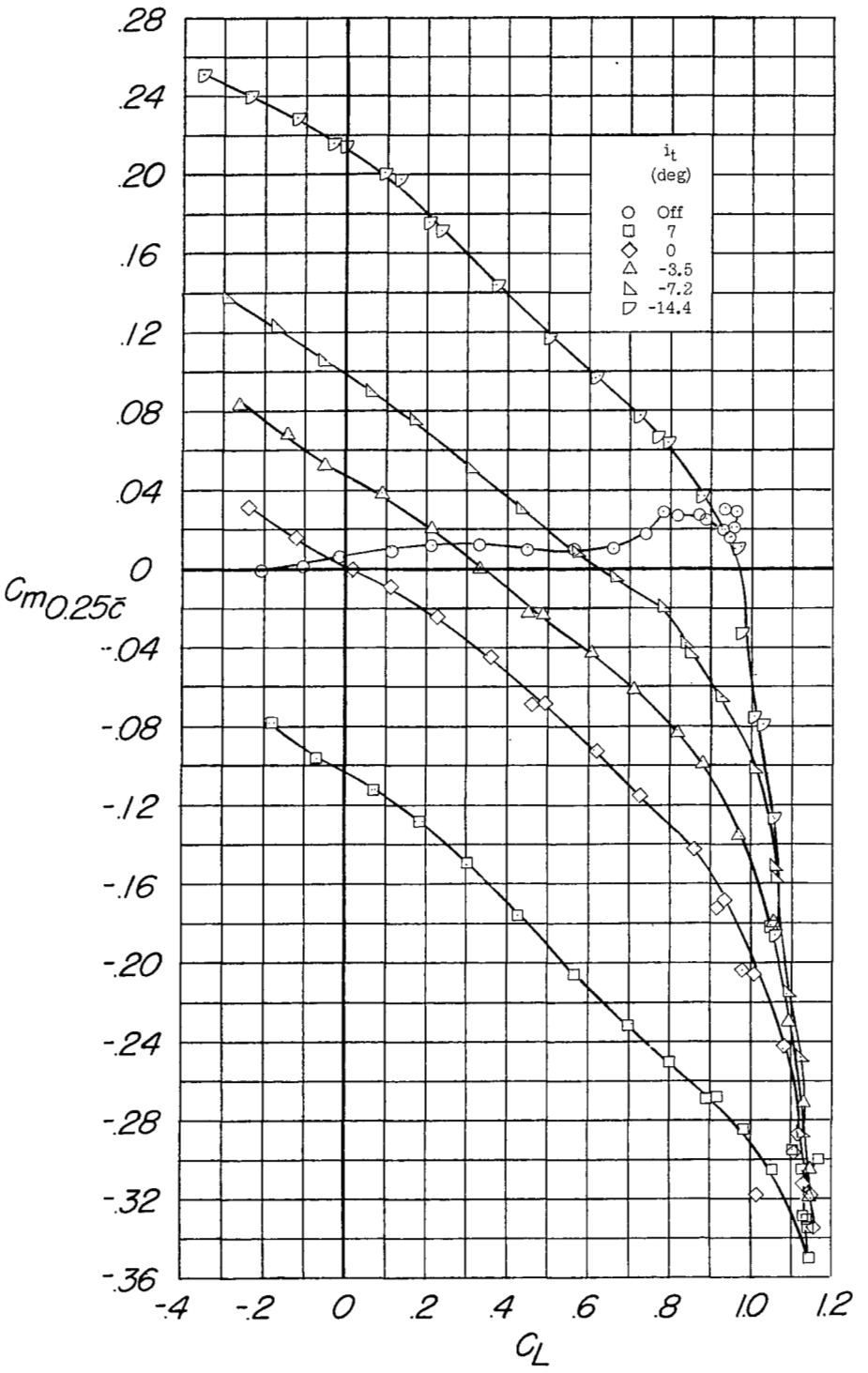

(c) C_m against C_L.

Figure 10.- Continued.

[redacted]

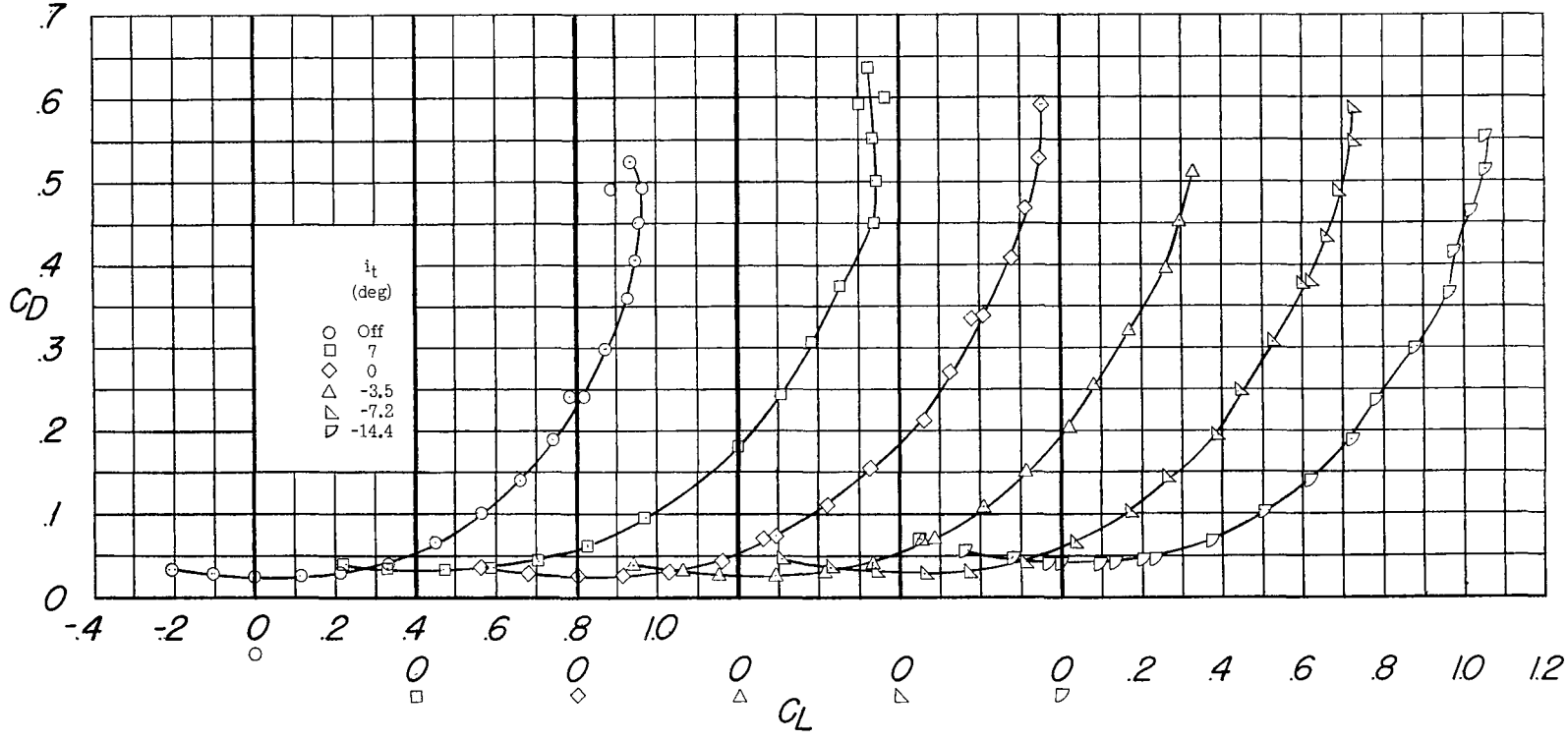

(d) C_D against C_L.

Figure 10.- Concluded.

[redacted]

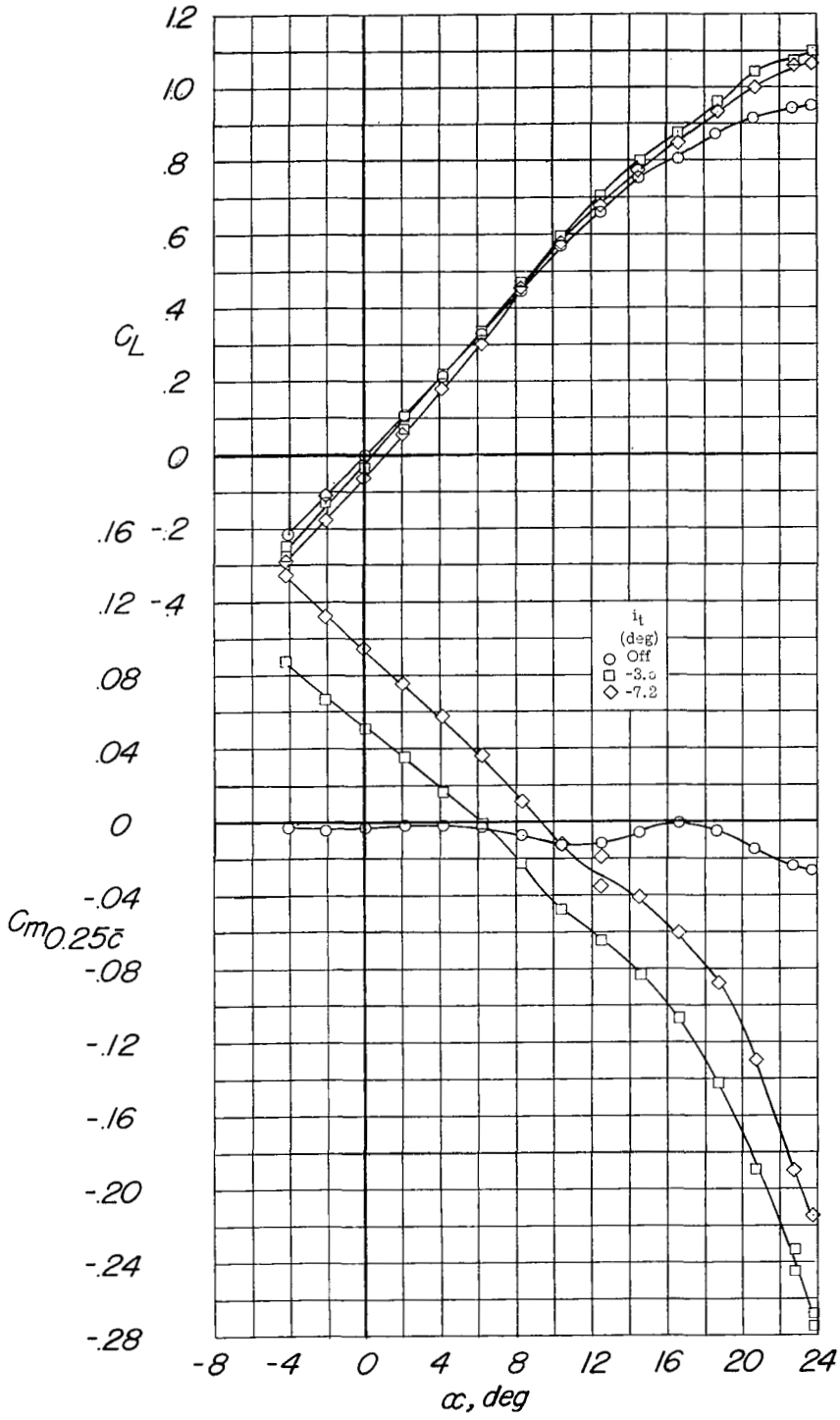

(a) C_L and C_m against α.

Figure 11.- Longitudinal characteristics of the model with the speed brakes deflected. Configuration A + V + I_{SE} + (-0.123)T + $B_{45,40}$.

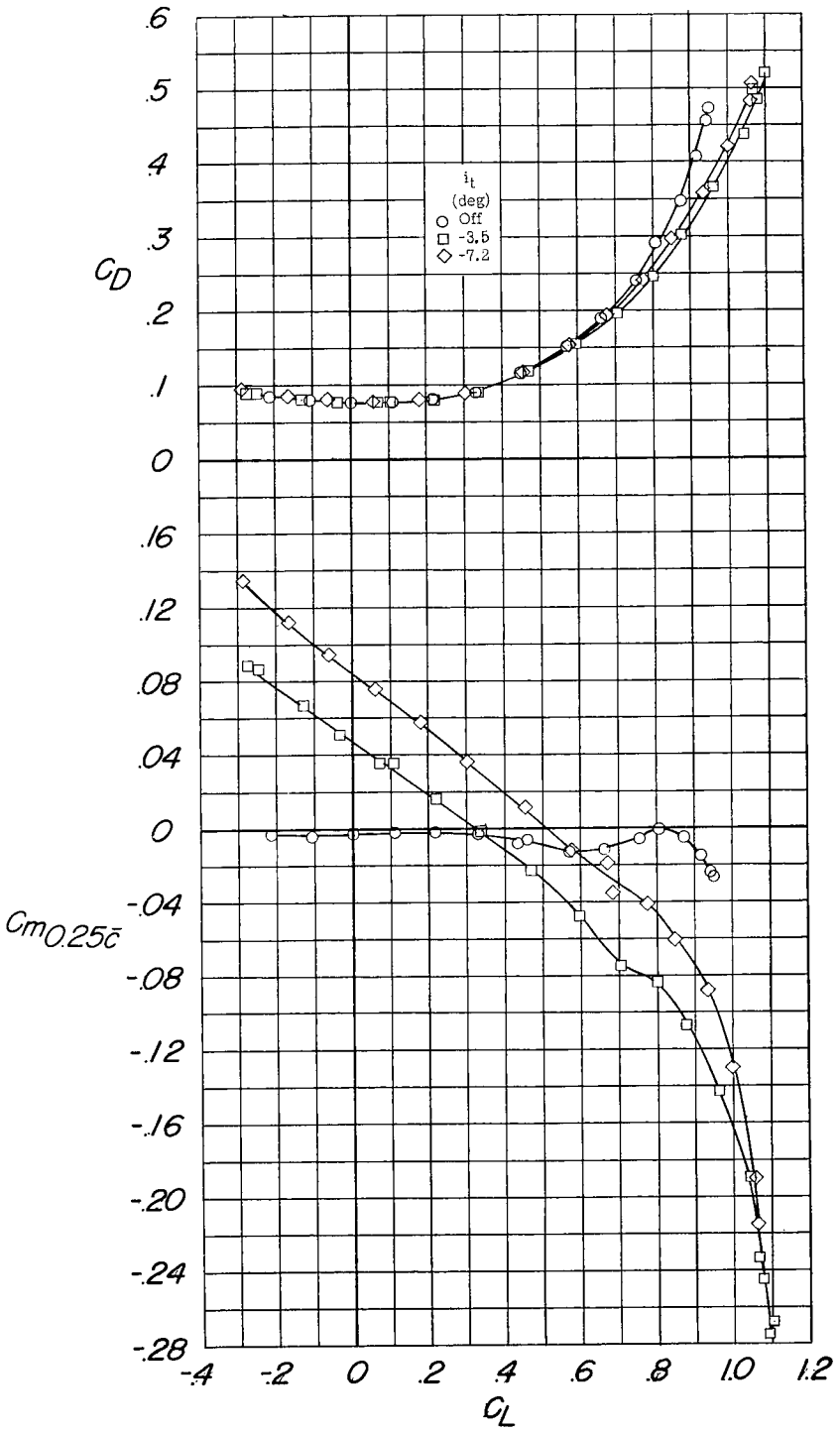

(b) C_D and C_m against C_L.

Figure 11.- Concluded.

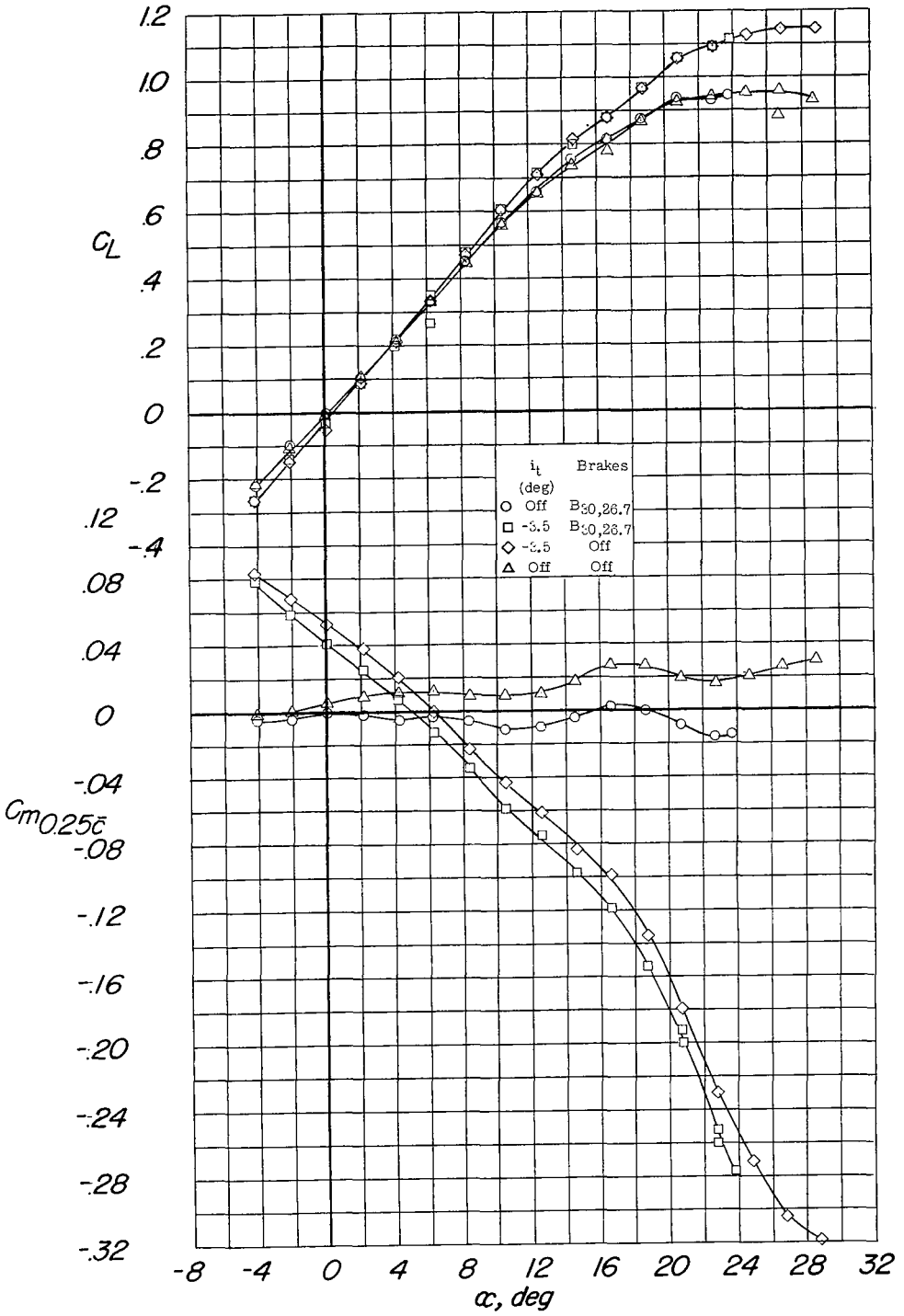

(a) C_L and C_m against α.

Figure 12.- Longitudinal characteristics of the model with the speed brakes deflected. Configuration A + V + I_{SE} + (-0.123)T + $B_{30,26.7}$.

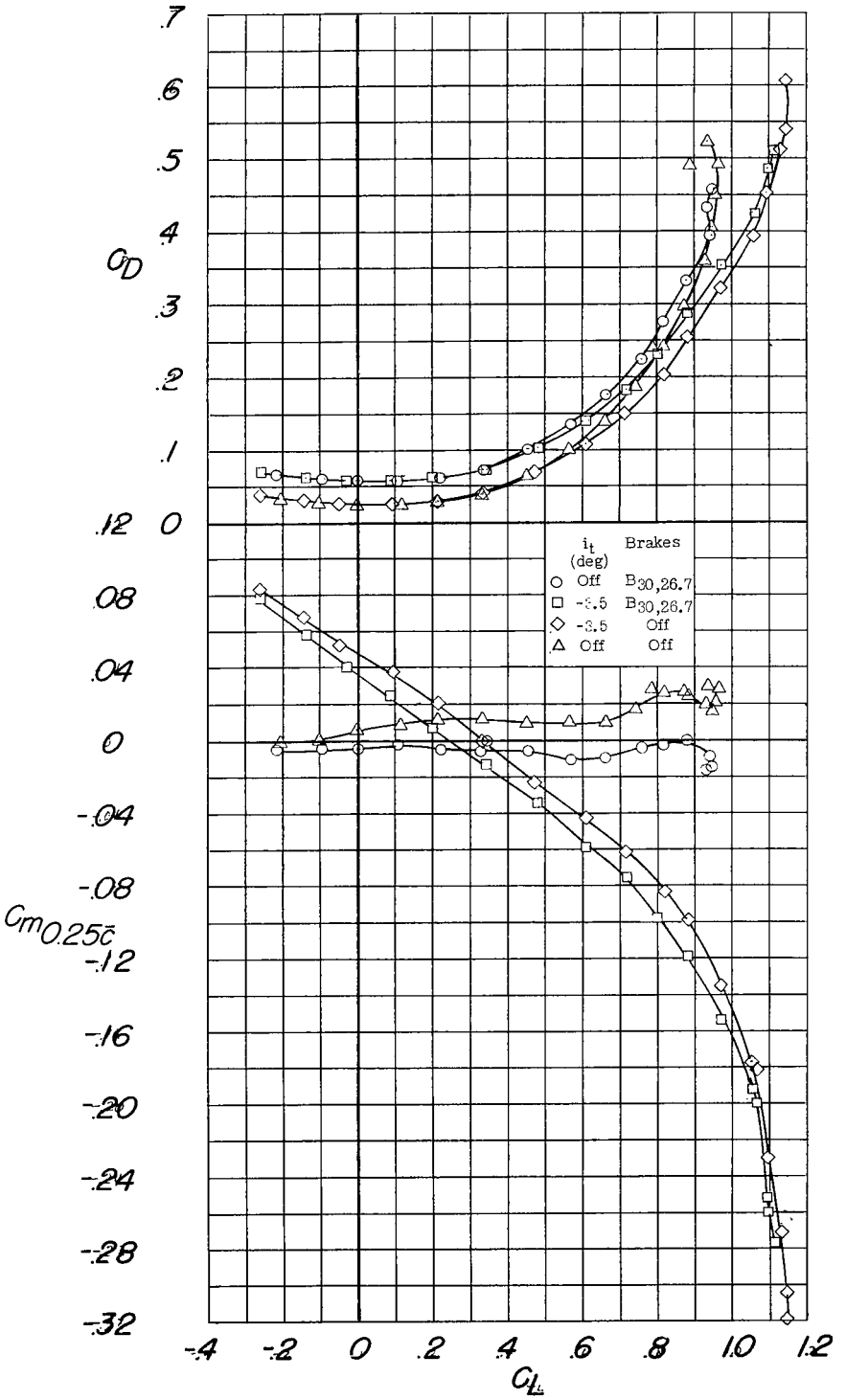

(b) C_D and C_m against C_L.

Figure 12.- Concluded.

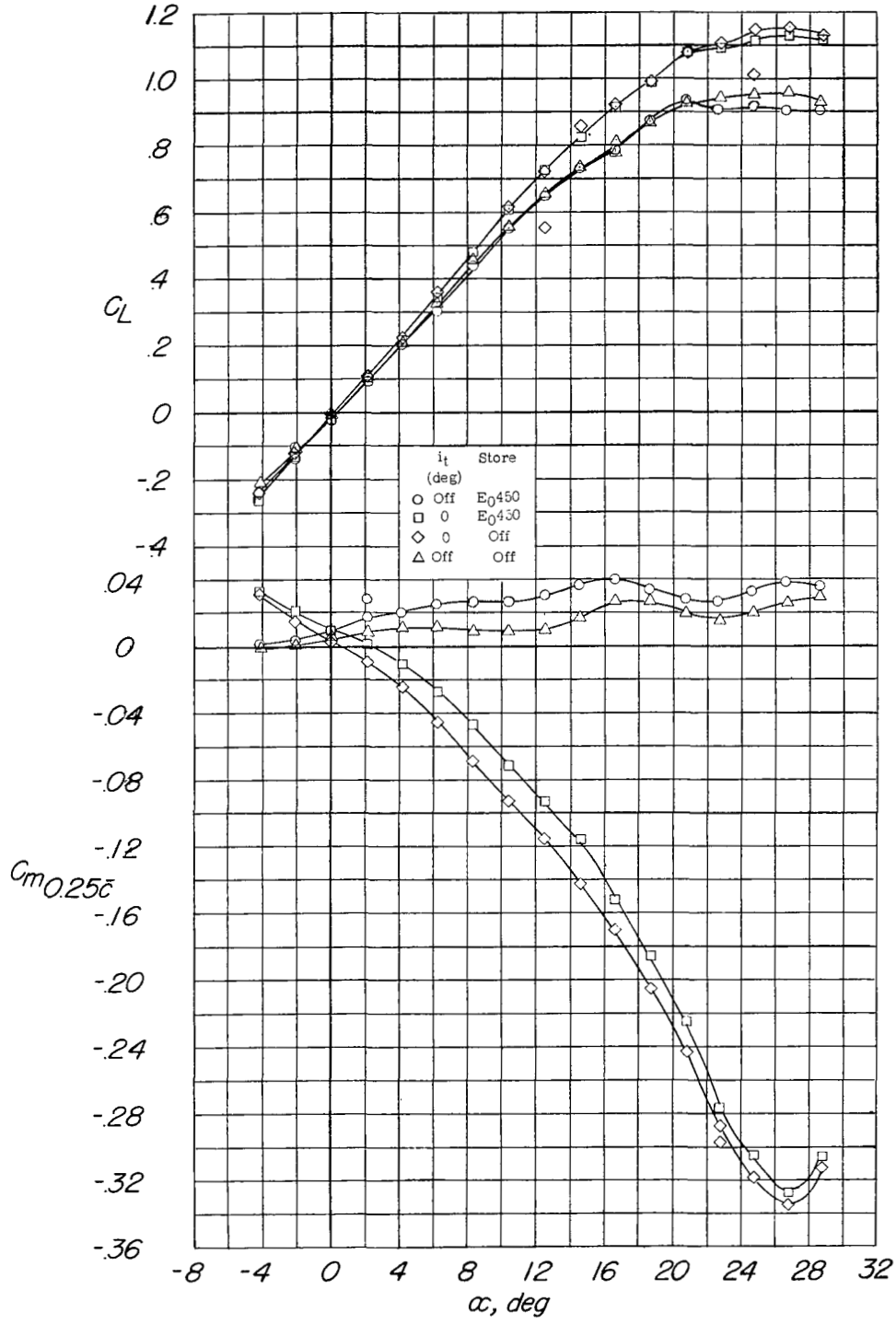

(a) C_L and C_m against α.

Figure 13.- Longitudinal characteristics of the model equipped with pylon-mounted external stores. Configuration A + V + I_{SE} + (-0.123)T + E_0450.

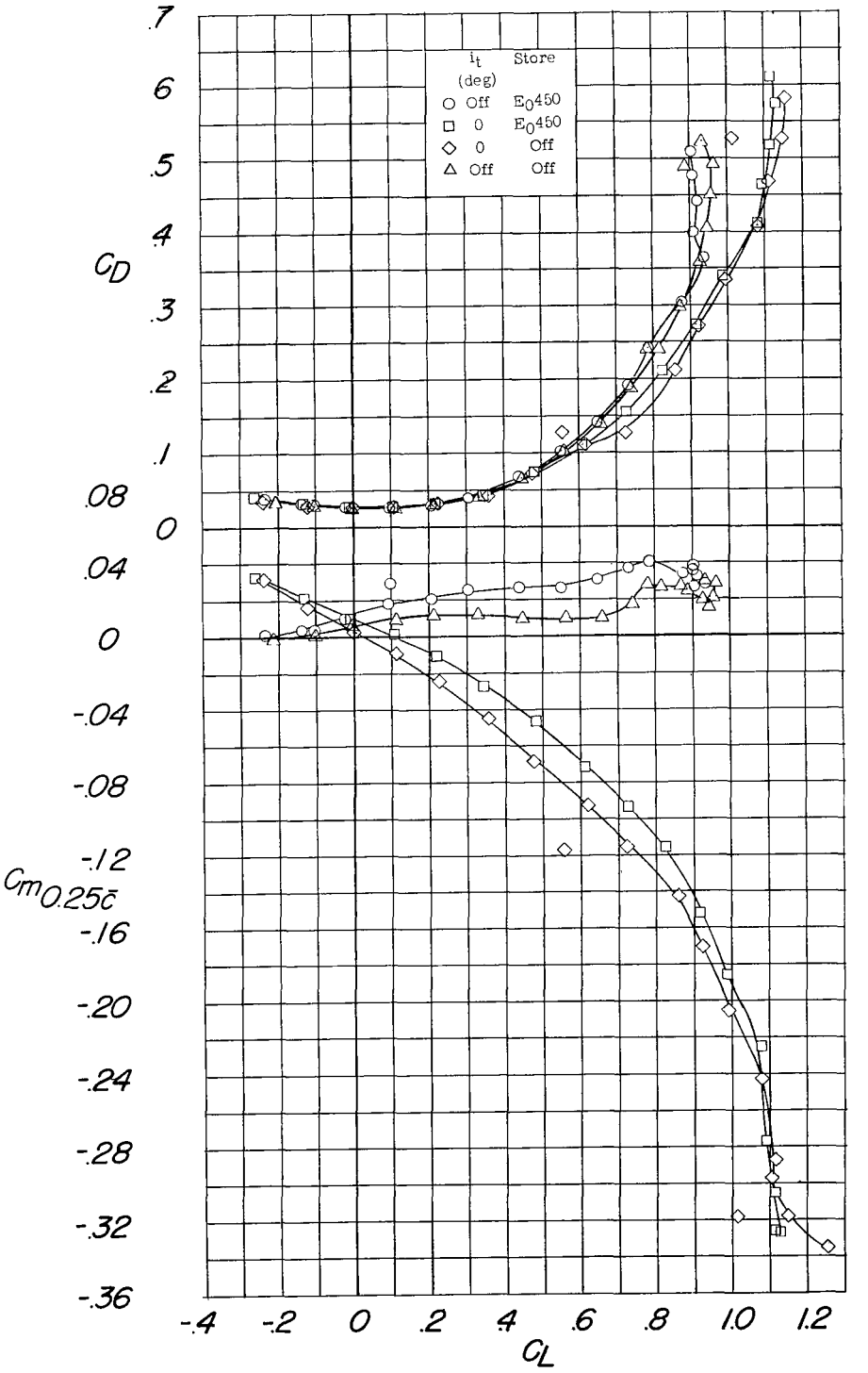

(b) C_D and C_m against C_L.

Figure 13.- Concluded.

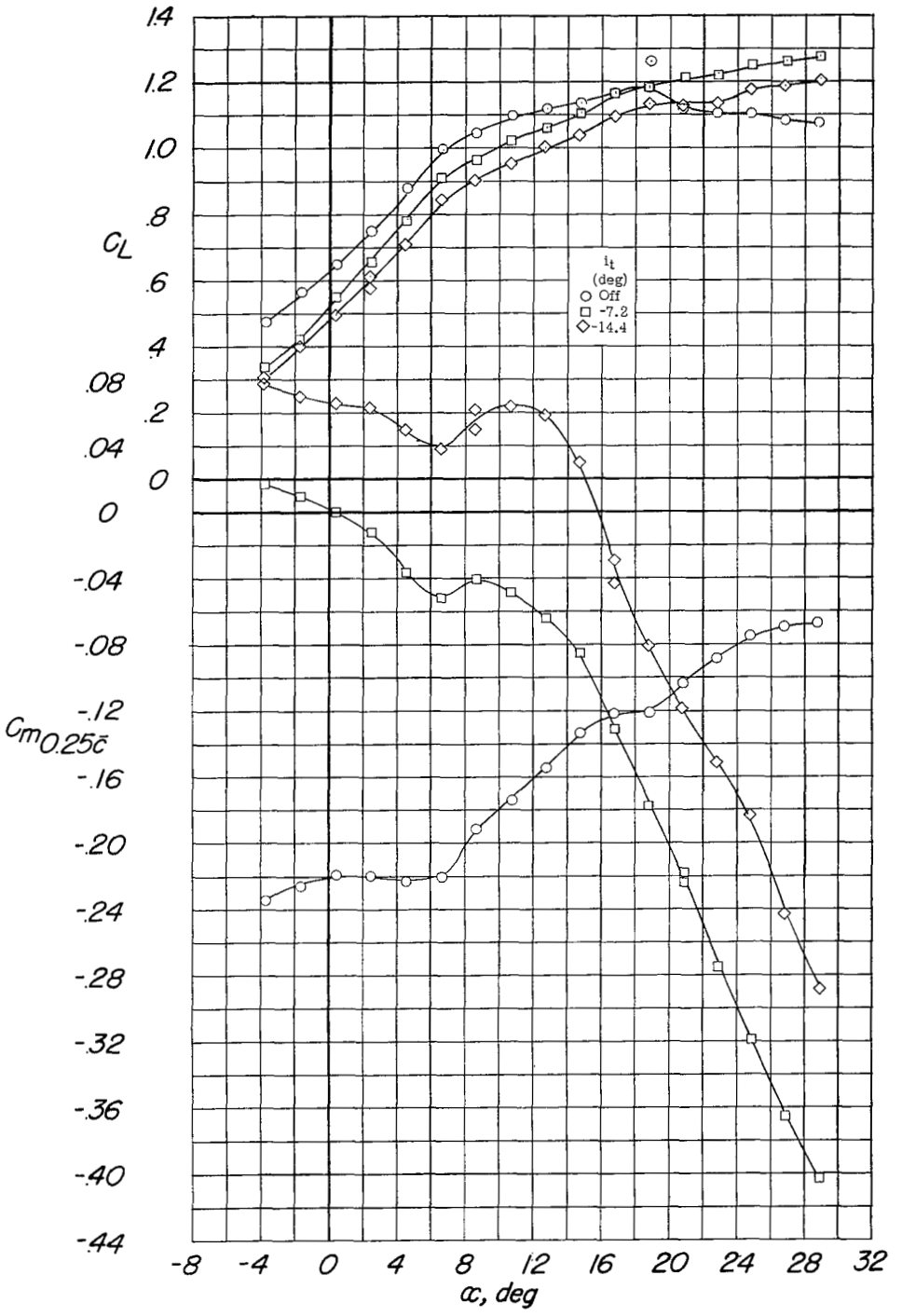

(a) C_L and C_m against α.

Figure 14.- Longitudinal characteristics of the model with 80-percent-span trailing-edge flap deflected. Configuration A + V + I_{SE} + (-0.123)T + 0.80F46.

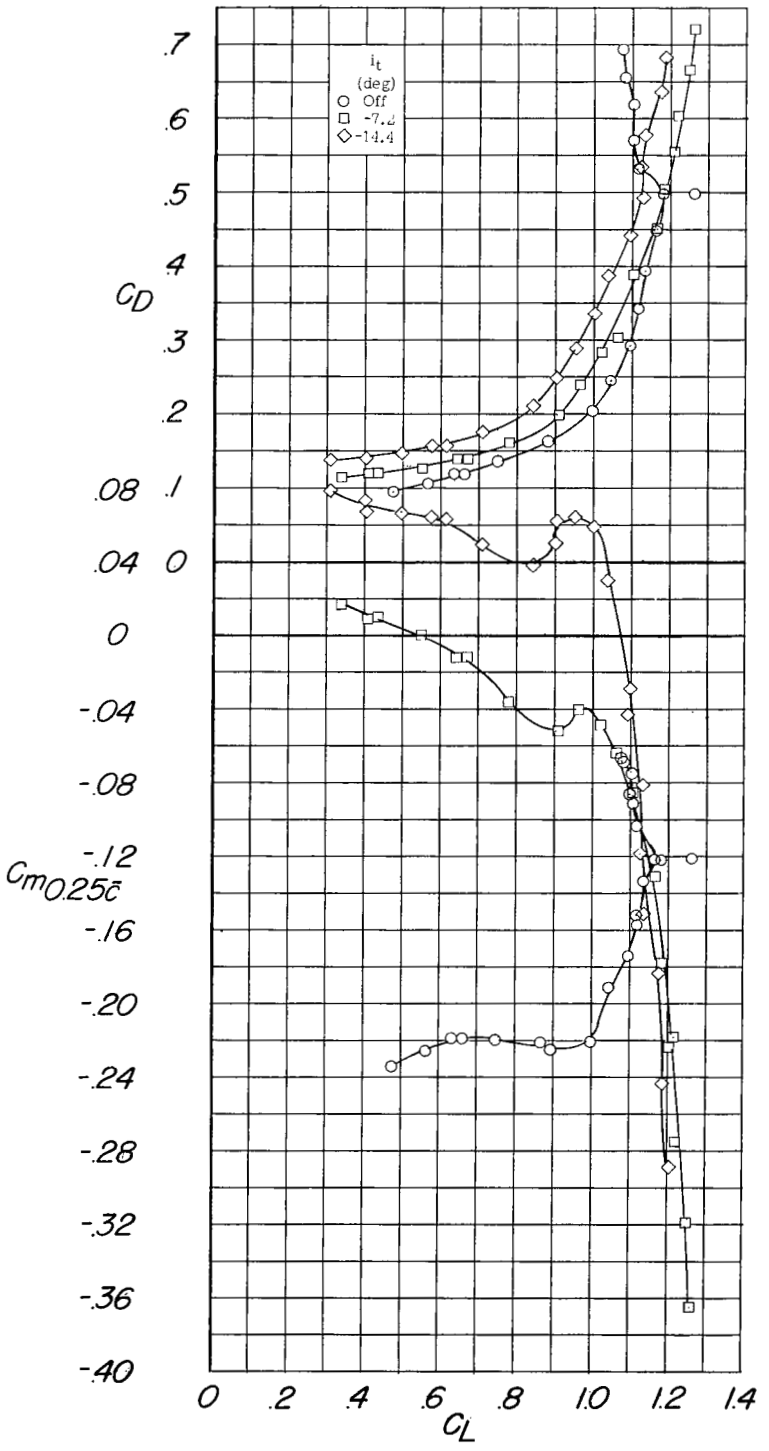

(b) C_D and C_m against C_L.

Figure 14.- Concluded.

[redacted]

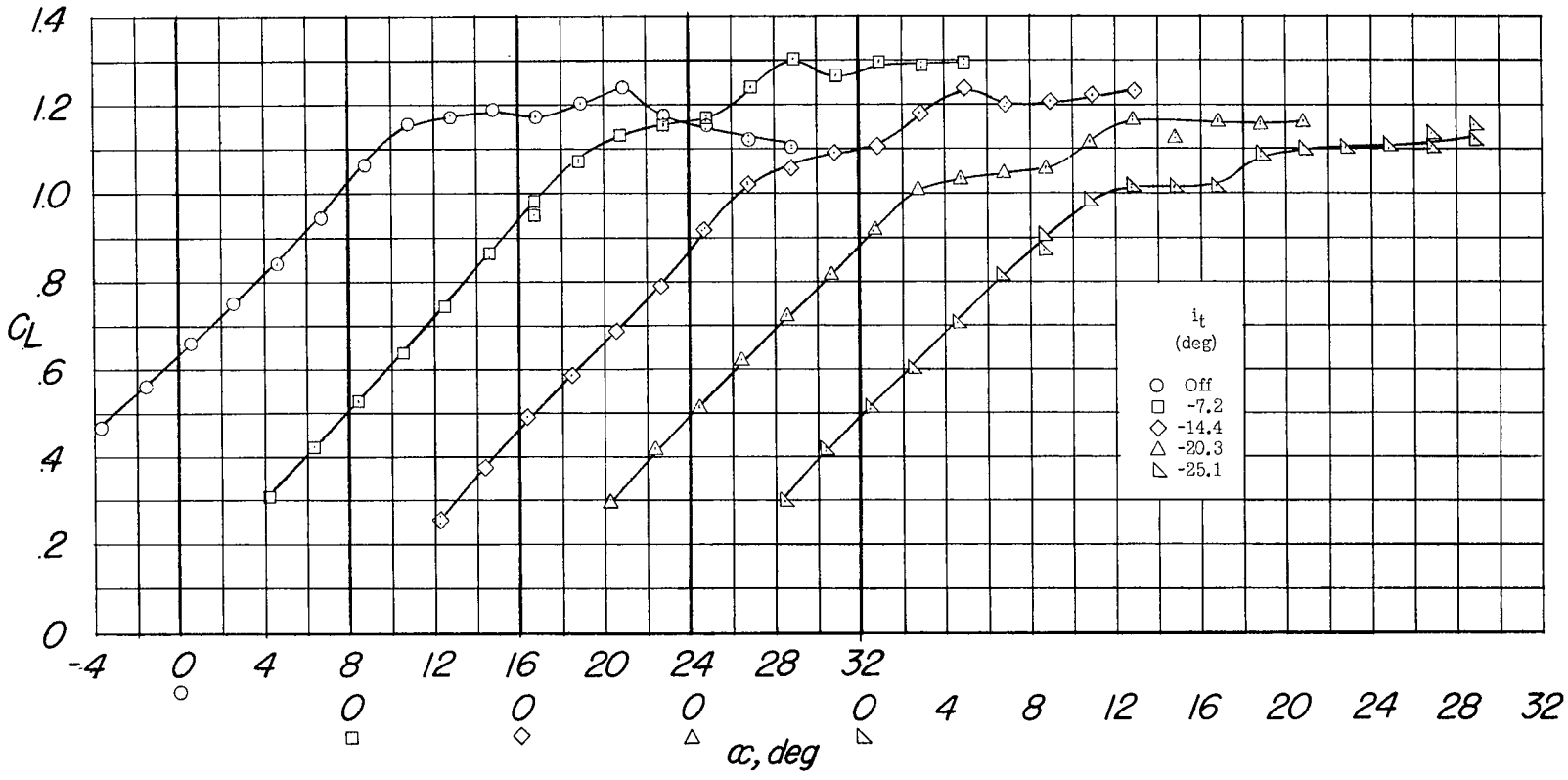

(a) C_L against α.

Figure 15.- Longitudinal characteristics of the model with the trailing-edge flaps deflected and the leading-edge flap drooped 20°. Configuration A + V + I_{SE} + (-0.123)T + 0.80F_{46} + N_{20}.

[redacted]

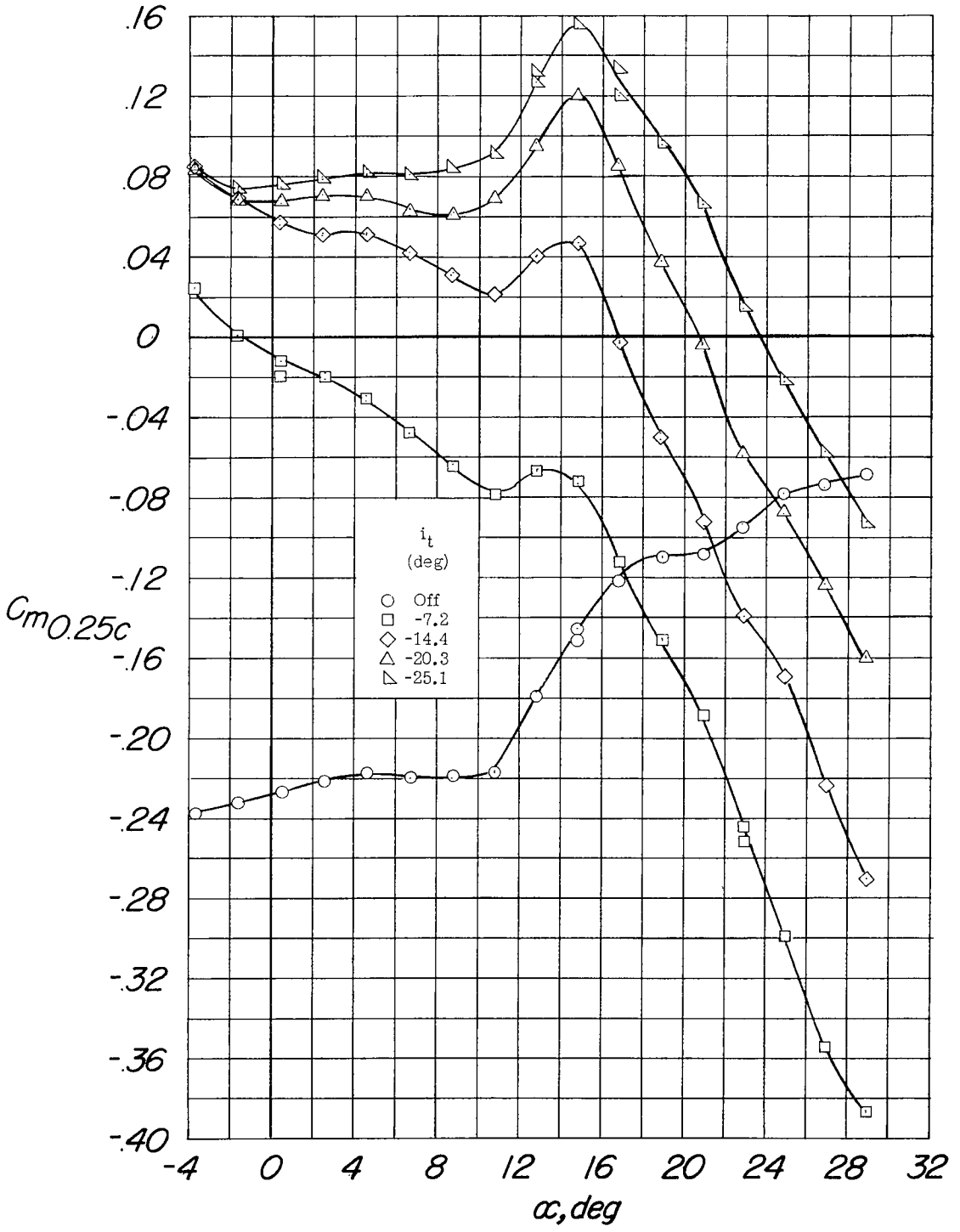

(b) C_m against α.

Figure 15.- Continued.

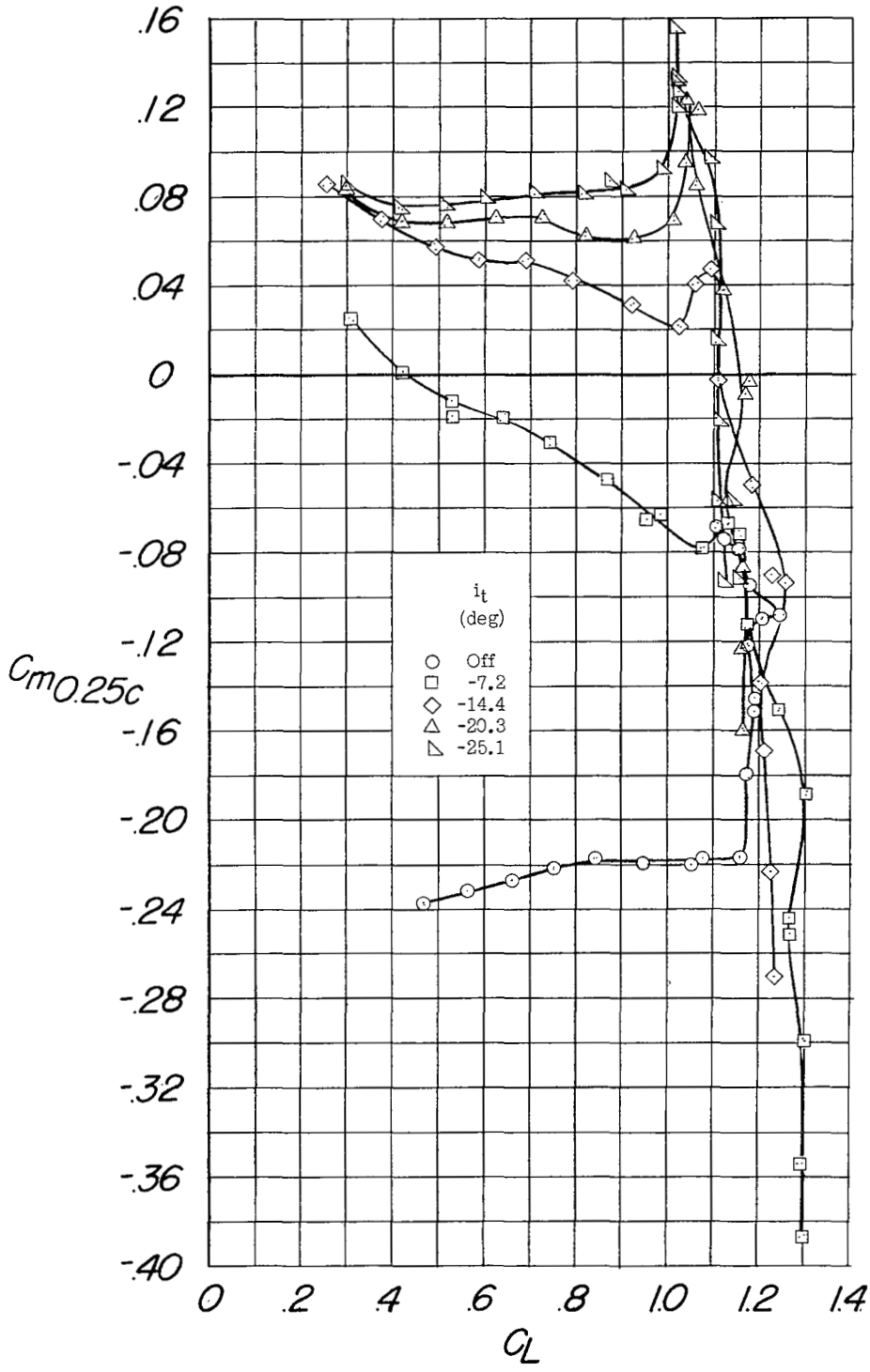

(c) C_m against C_L.

Figure 15.- Continued.

[redacted]

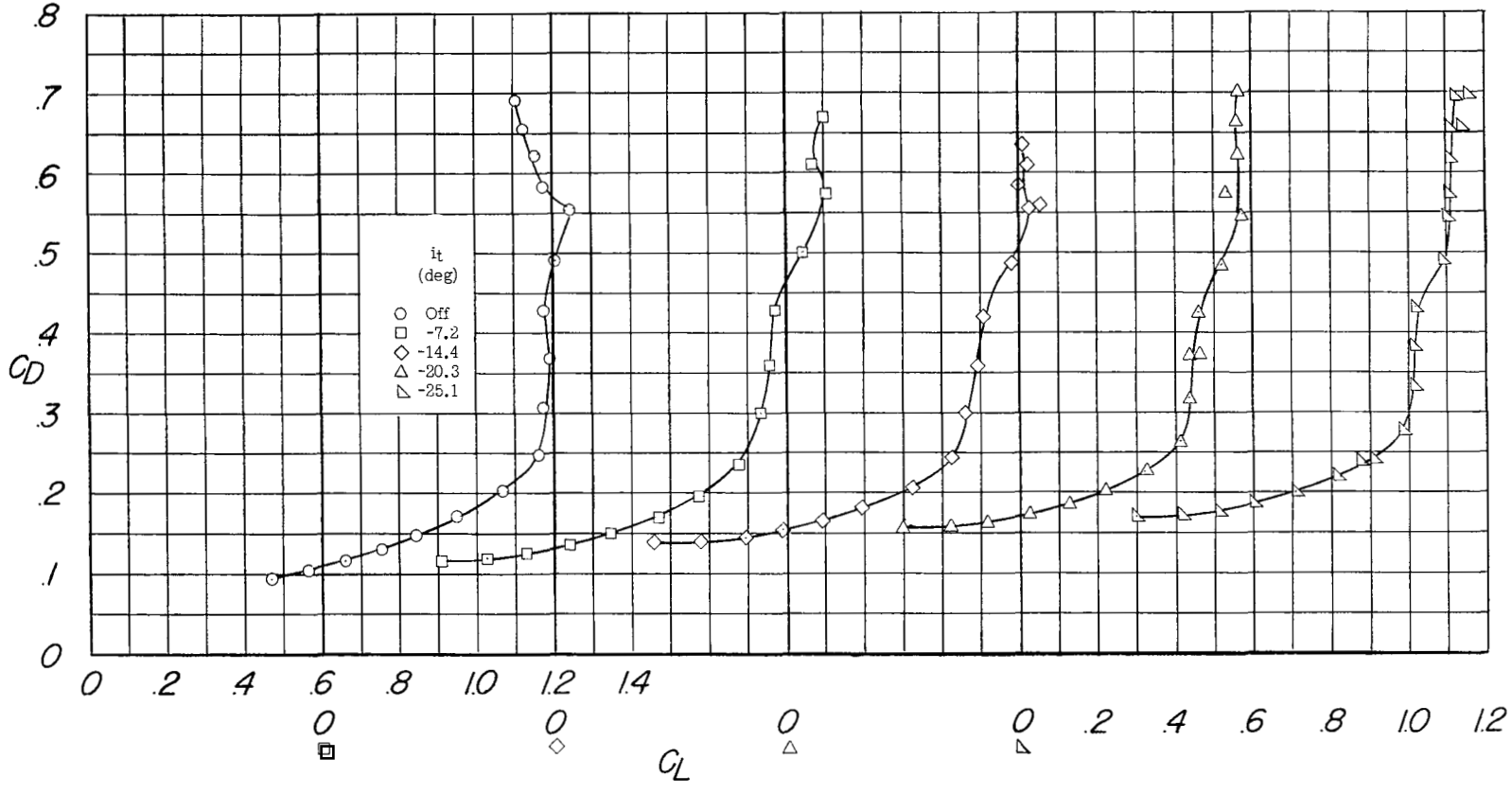

(d) C_D against C_L.

Figure 15.- Concluded.

[redacted]

[redacted]

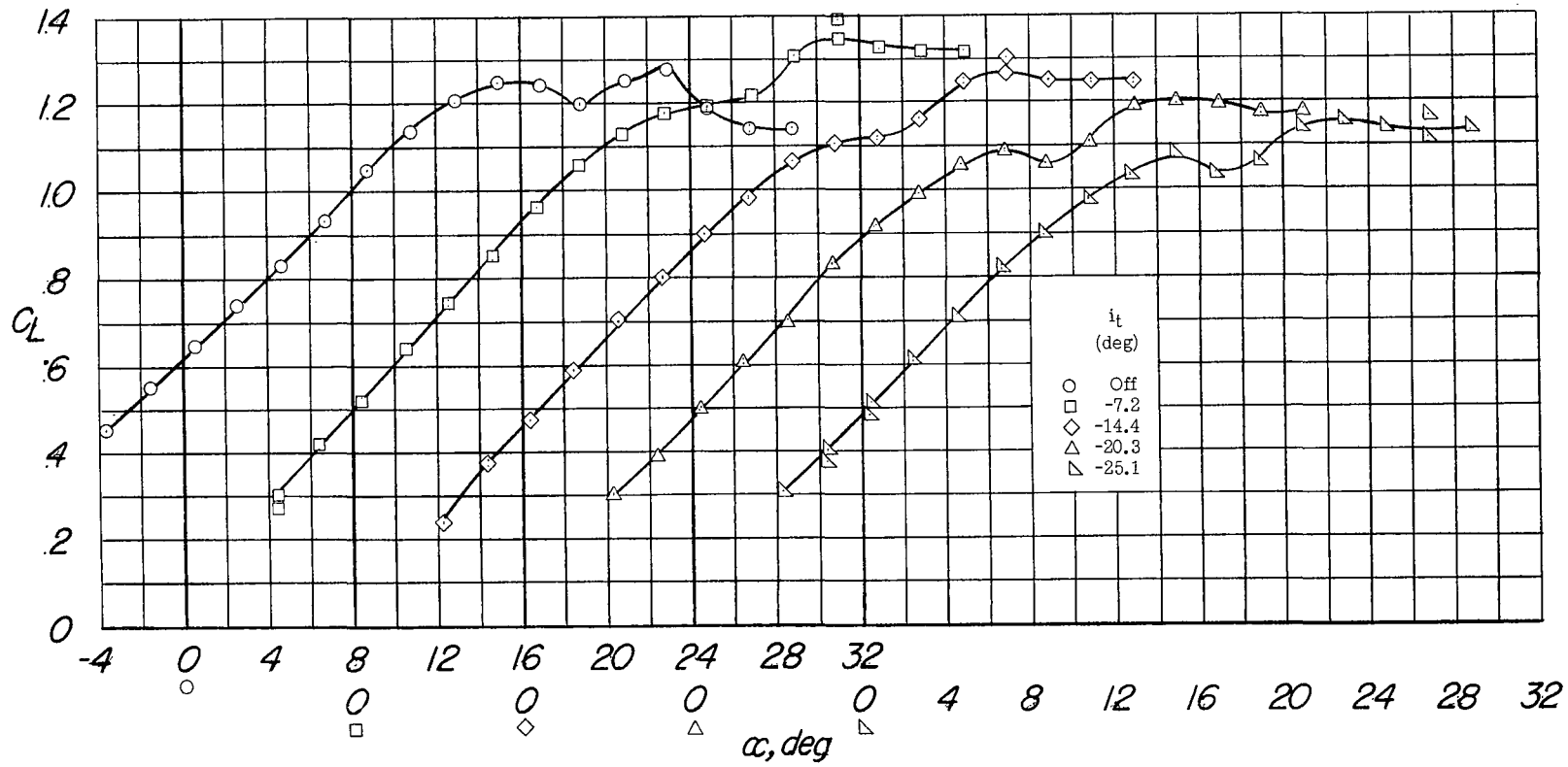

(a) C_L against α.

Figure 16.- Longitudinal characteristics of the model with the trailing-edge flaps deflected and the leading-edge flap drooped 30°. Configuration A + V + I_{SE} + (-0.123)T + 0.80F_{46} + N_{30}.

[redacted]

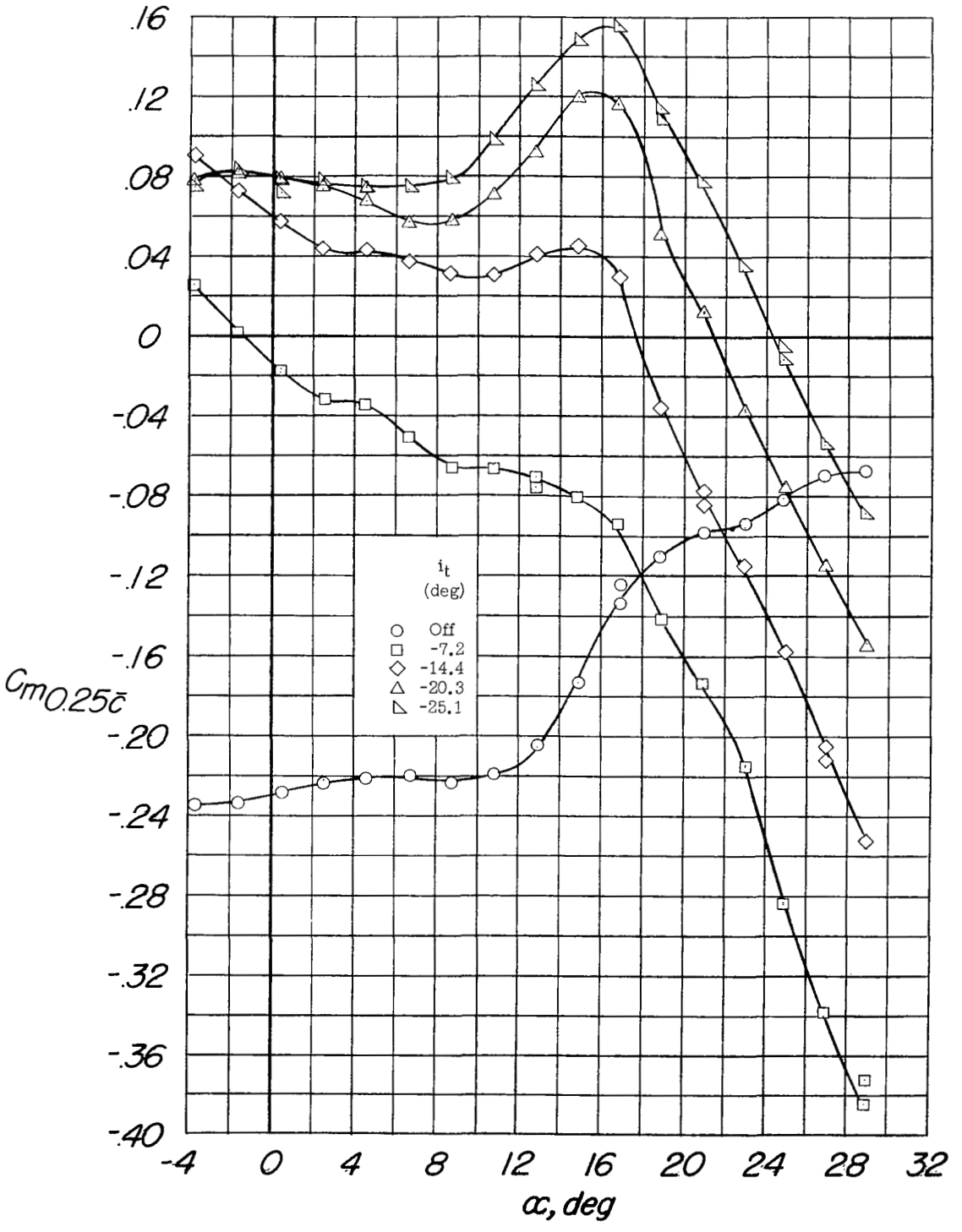

(b) C_m against α.

Figure 16.- Continued.

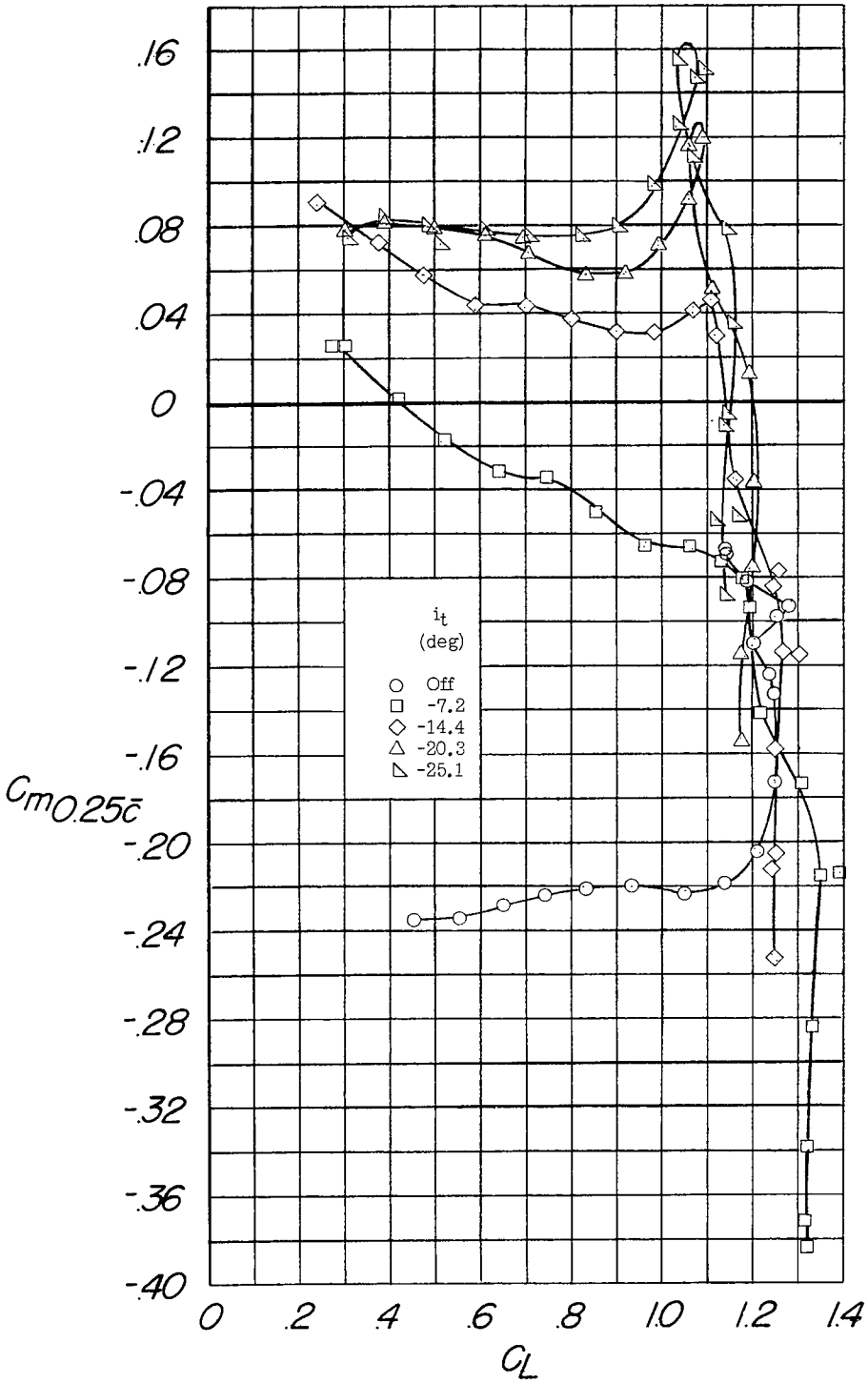

(c) C_m against C_L.

Figure 16.- Continued.

[redacted]

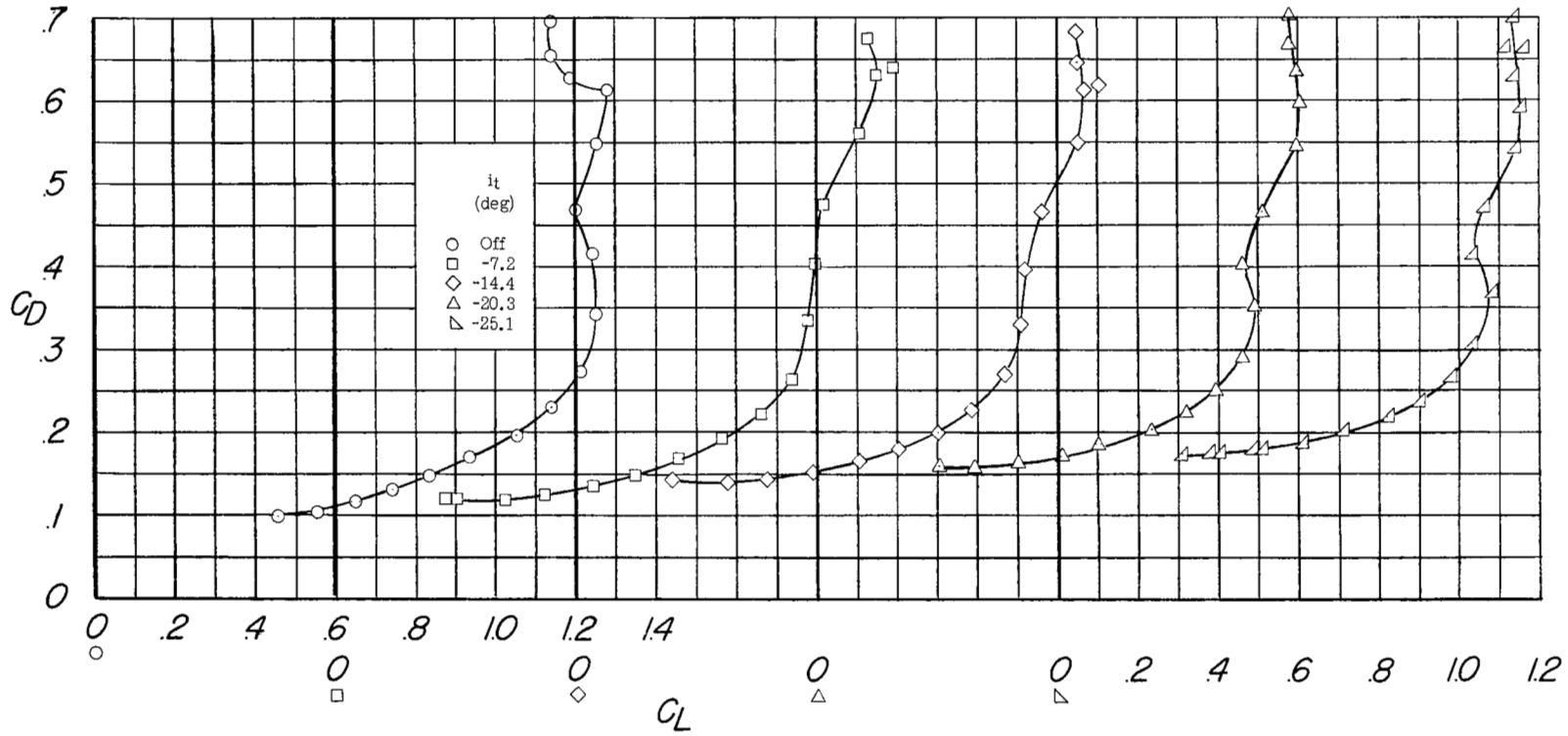

(d) C_D against C_L.

Figure 16.- Concluded.

[redacted]

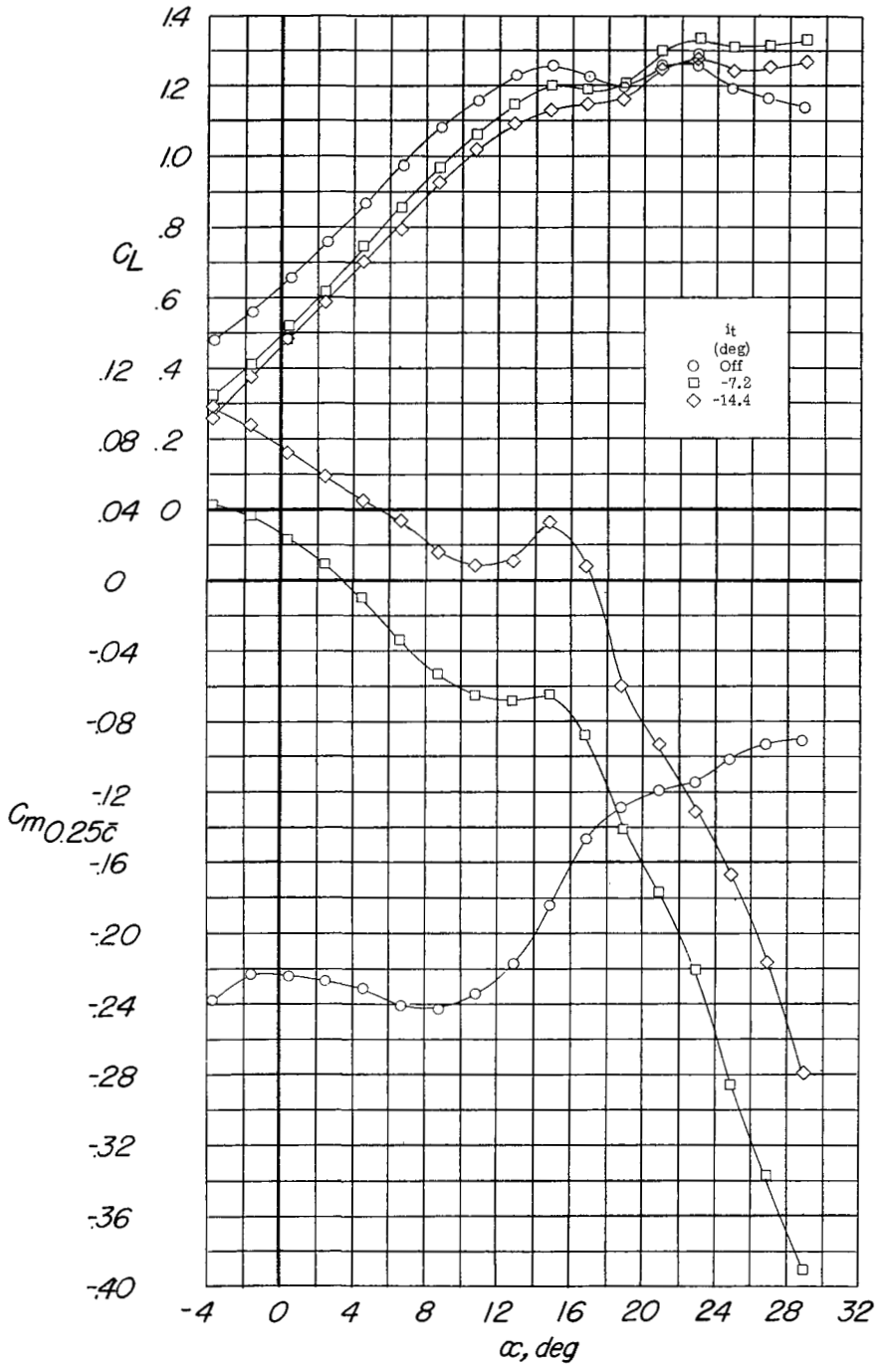

(a) C_L and C_m against α.

Figure 17.- Longitudinal characteristics of the model with the side speed brakes deflected 40°, trailing-edge flaps deflected, and leading-edge flap drooped 30°. Configuration A + V + I_{SE} + (-0.123)T + 0.80F_{46} + N_{30} + $B_{0,40}$.

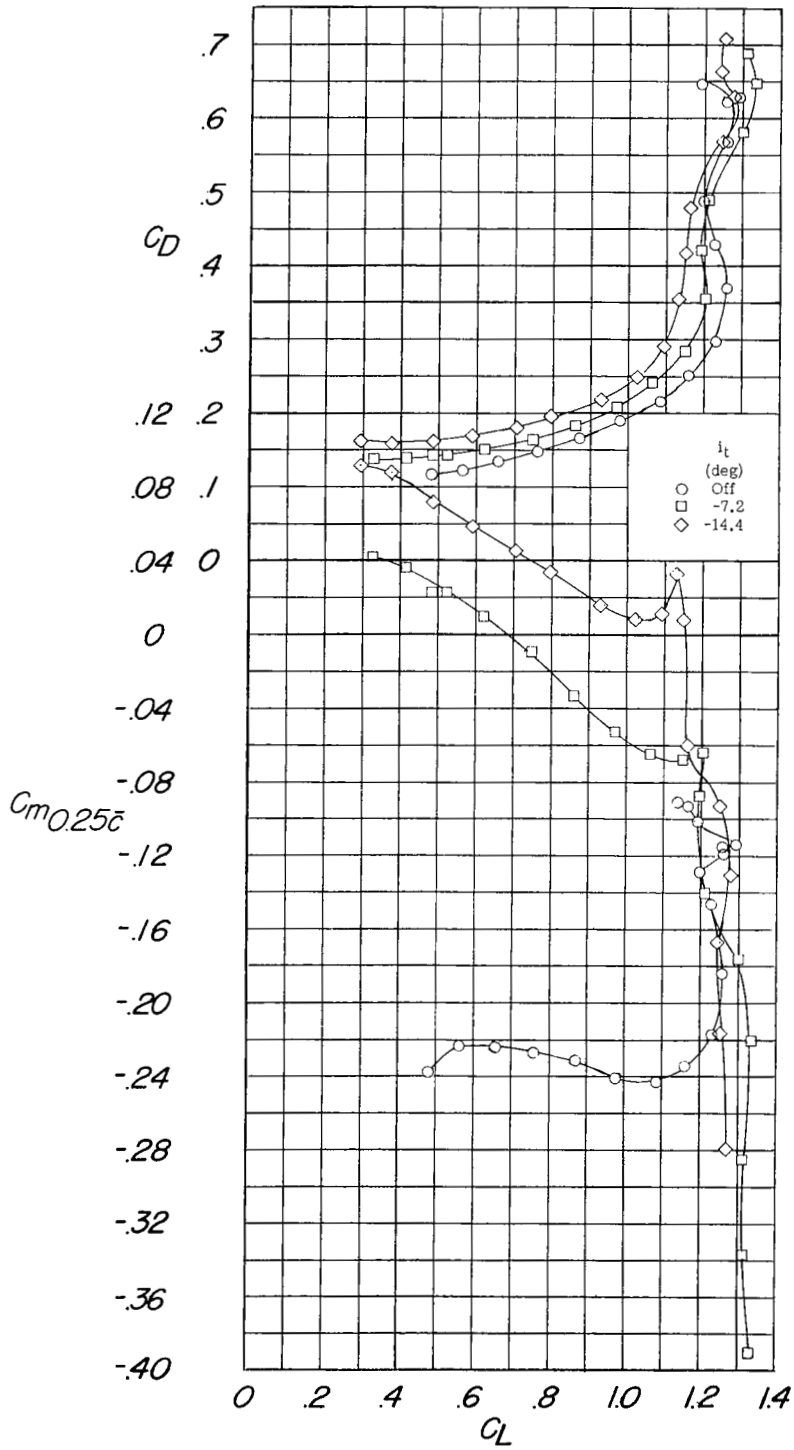

(b) C_D and C_m against C_L.

Figure 17.- Concluded.

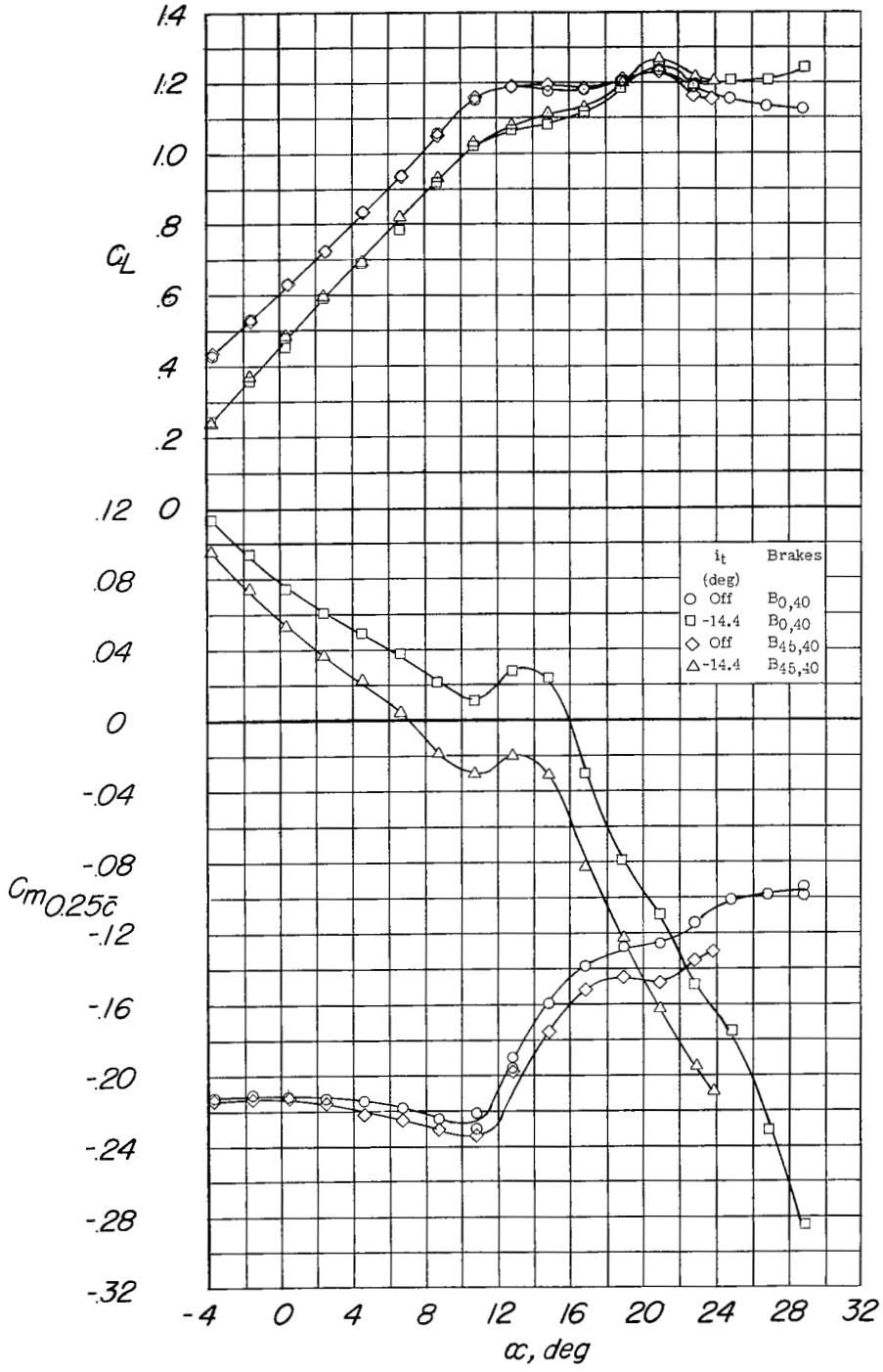

(a) C_L and C_m against α.

Figure 18.- Longitudinal characteristics of the model with the speed brakes deflected, trailing-edge flaps deflected, and leading-edge flap drooped 20°. Configuration A + V + I_{SE} + (-0.123)T + 0.80F_{46} + N_{20} + B.

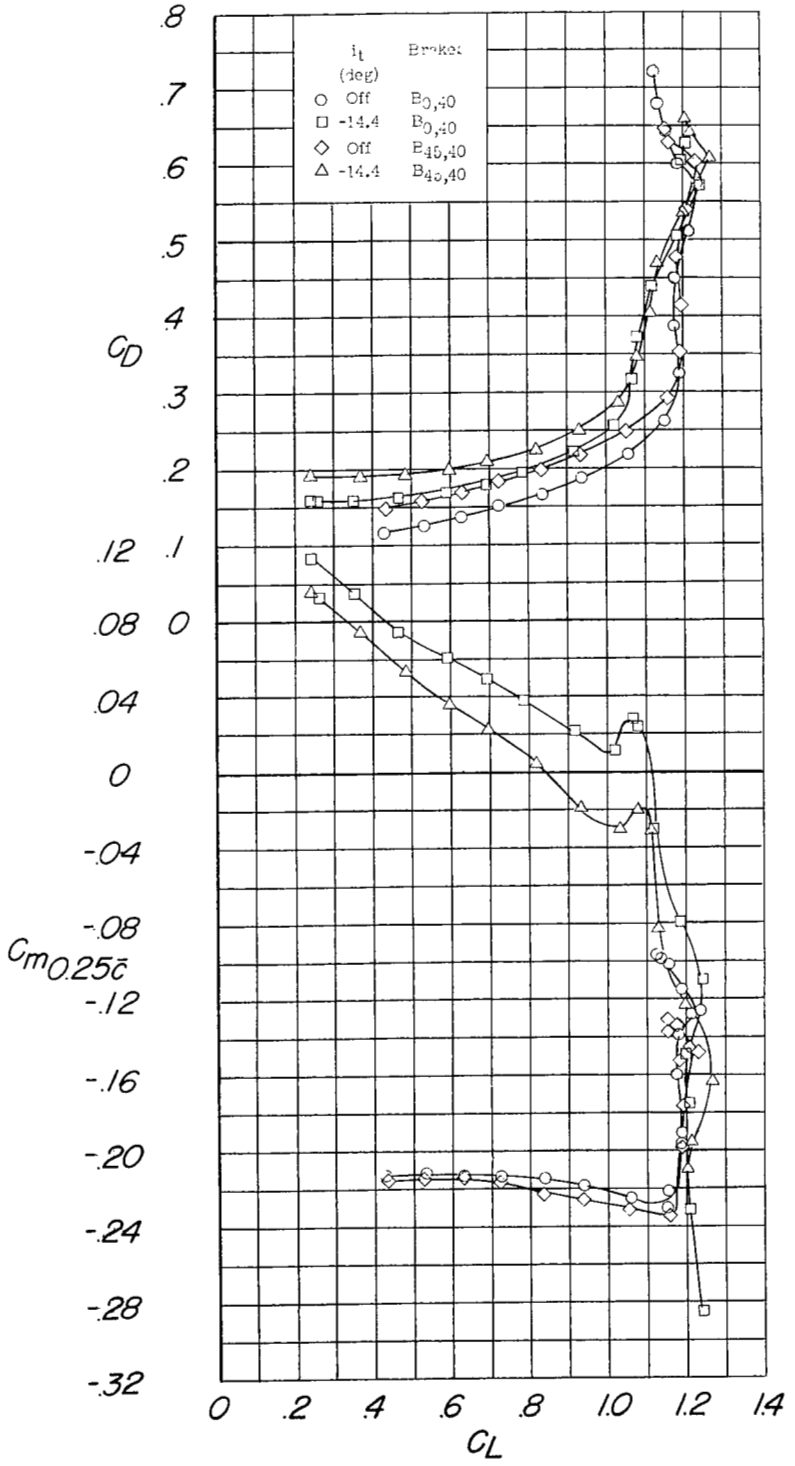

(b) C_D and C_m against C_L.

Figure 18.- Concluded.

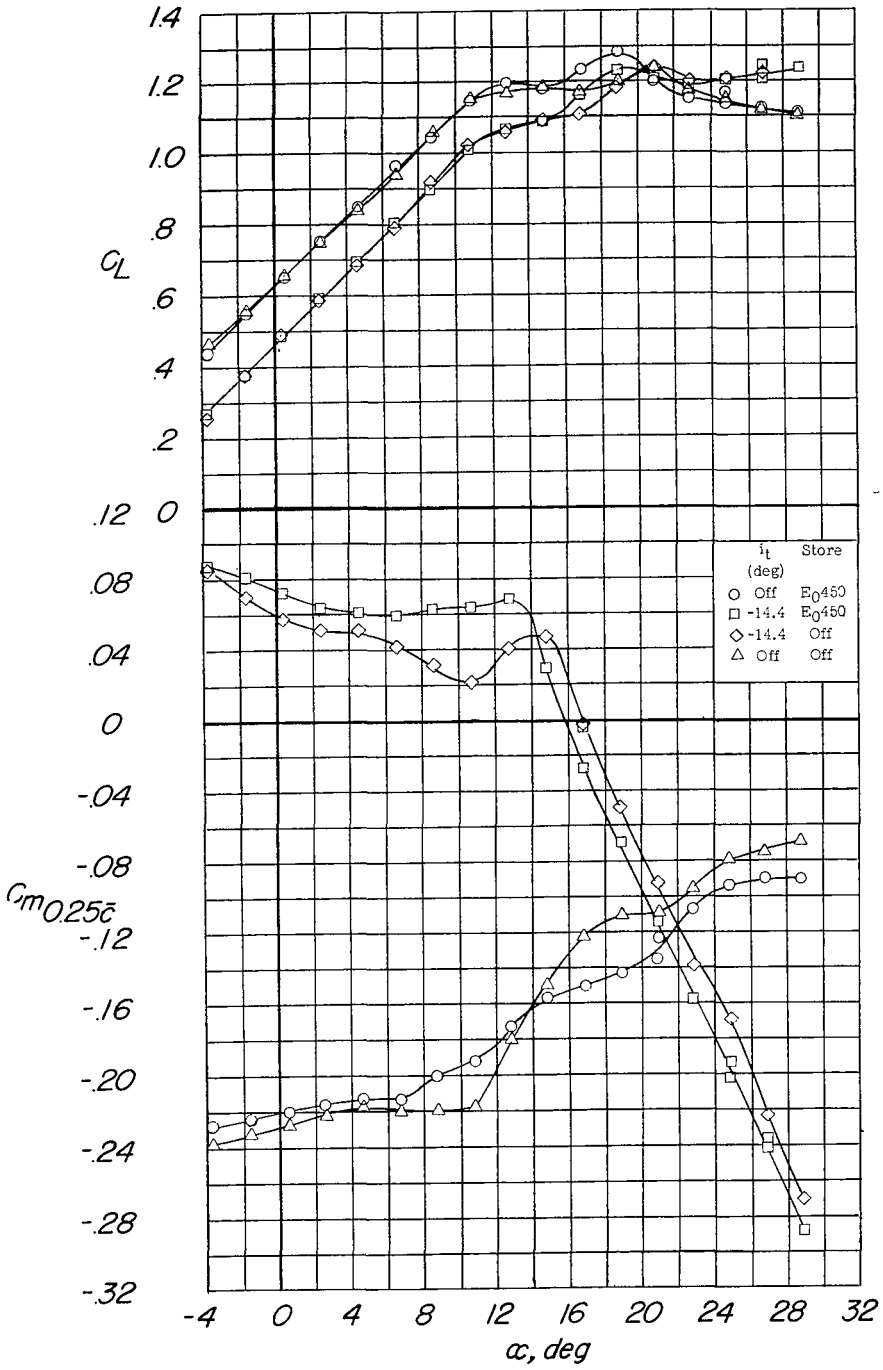

(a) C_L and C_m against α.

Figure 19.- Longitudinal characteristics of the model equipped with pylon-mounted external stores; trailing-edge flaps deflected and leading-edge flap drooped 20°. Configuration A + V + I_{SE} + (-0.123)$T_{-14.4}$ + 0.80F_{46} + N_{20} + E_0450.

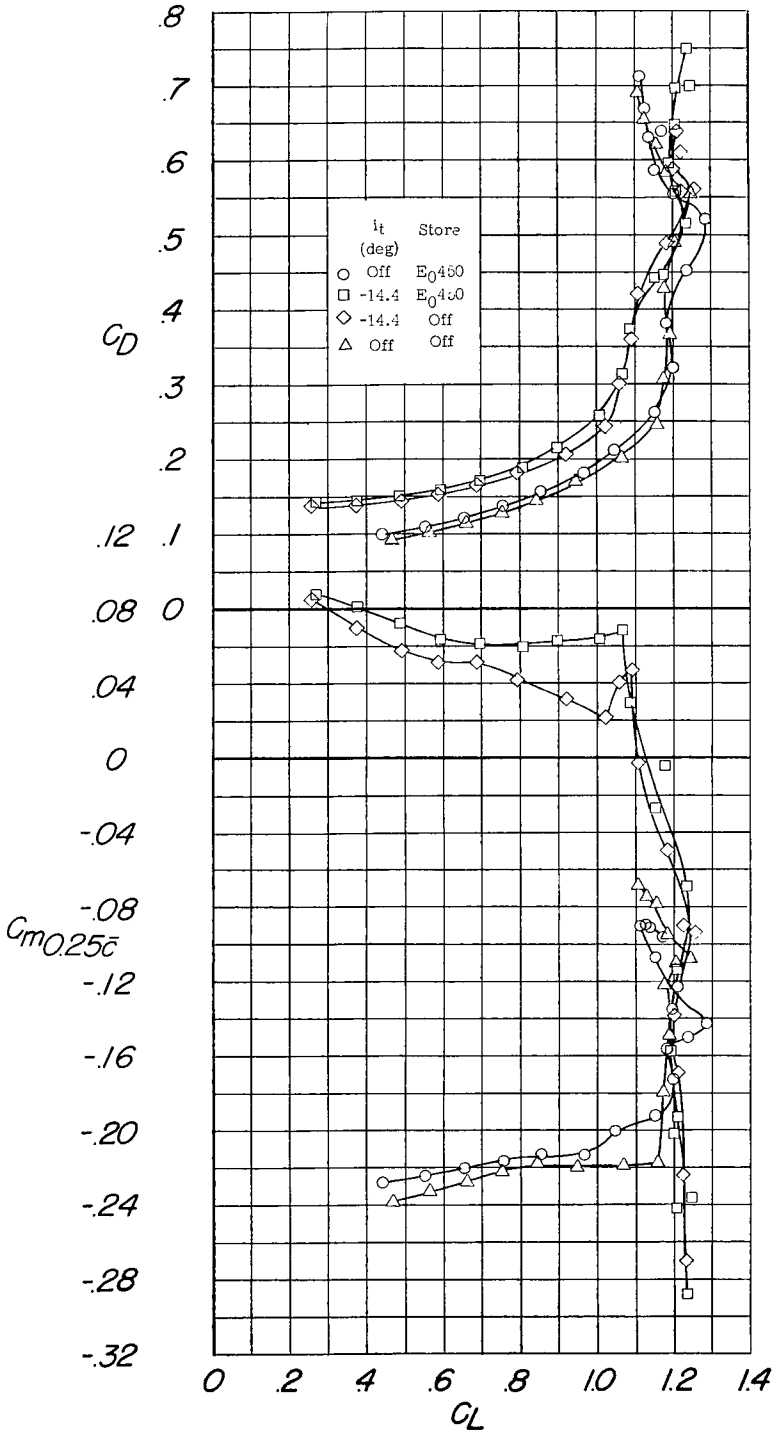

(b) C_D and C_m against C_L.

Figure 19.- Concluded.

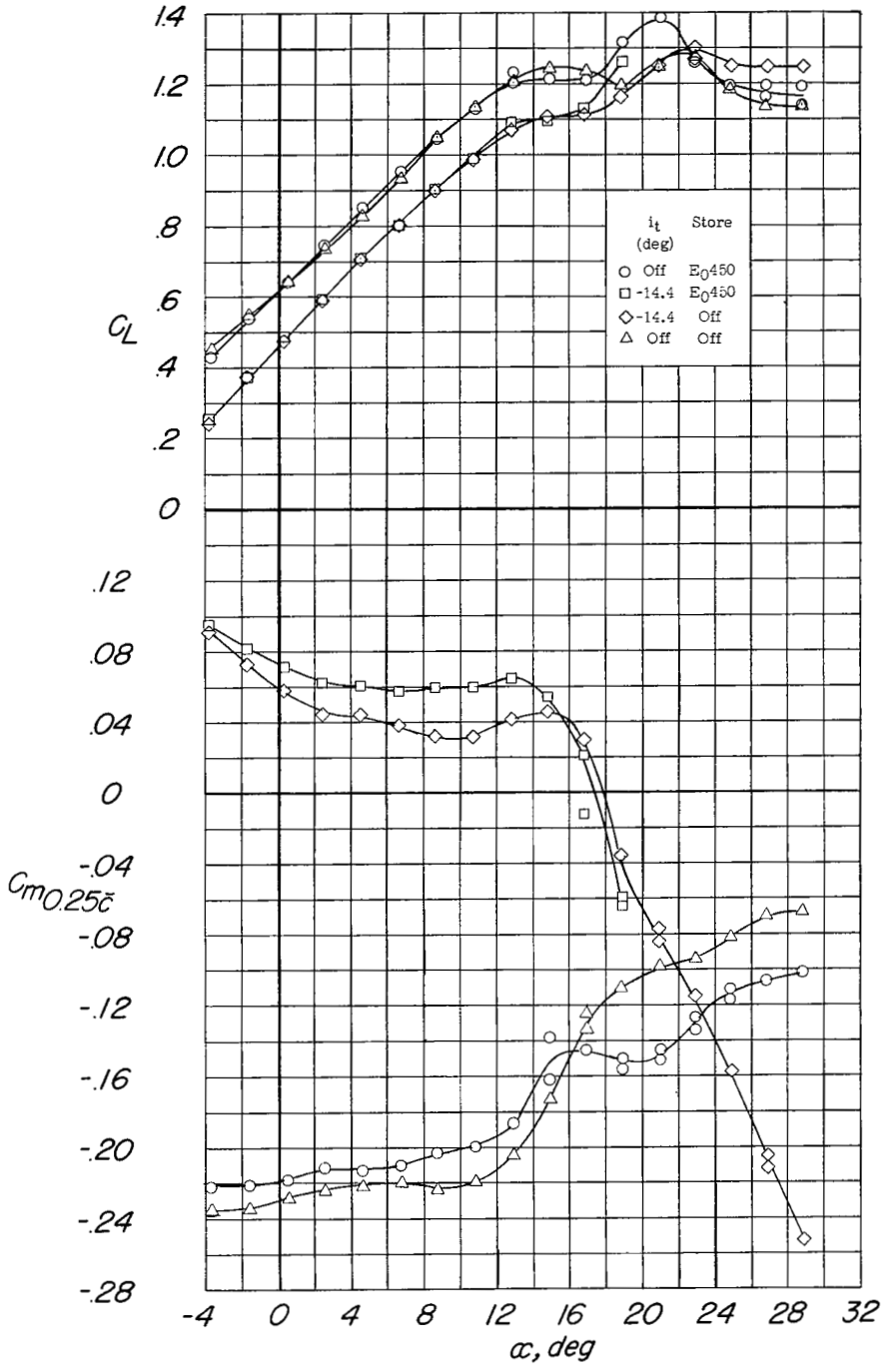

(a) C_L and C_m against α.

Figure 20.- Longitudinal characteristics of the model equipped with pylon-mounted external stores; trailing-edge flaps deflected and leading-edge flap drooped 30°. Configuration A + V + I_{SE} + (-0.123)$T_{-14.4}$ + 0.80F_{46} + N_{30} + E_0450.

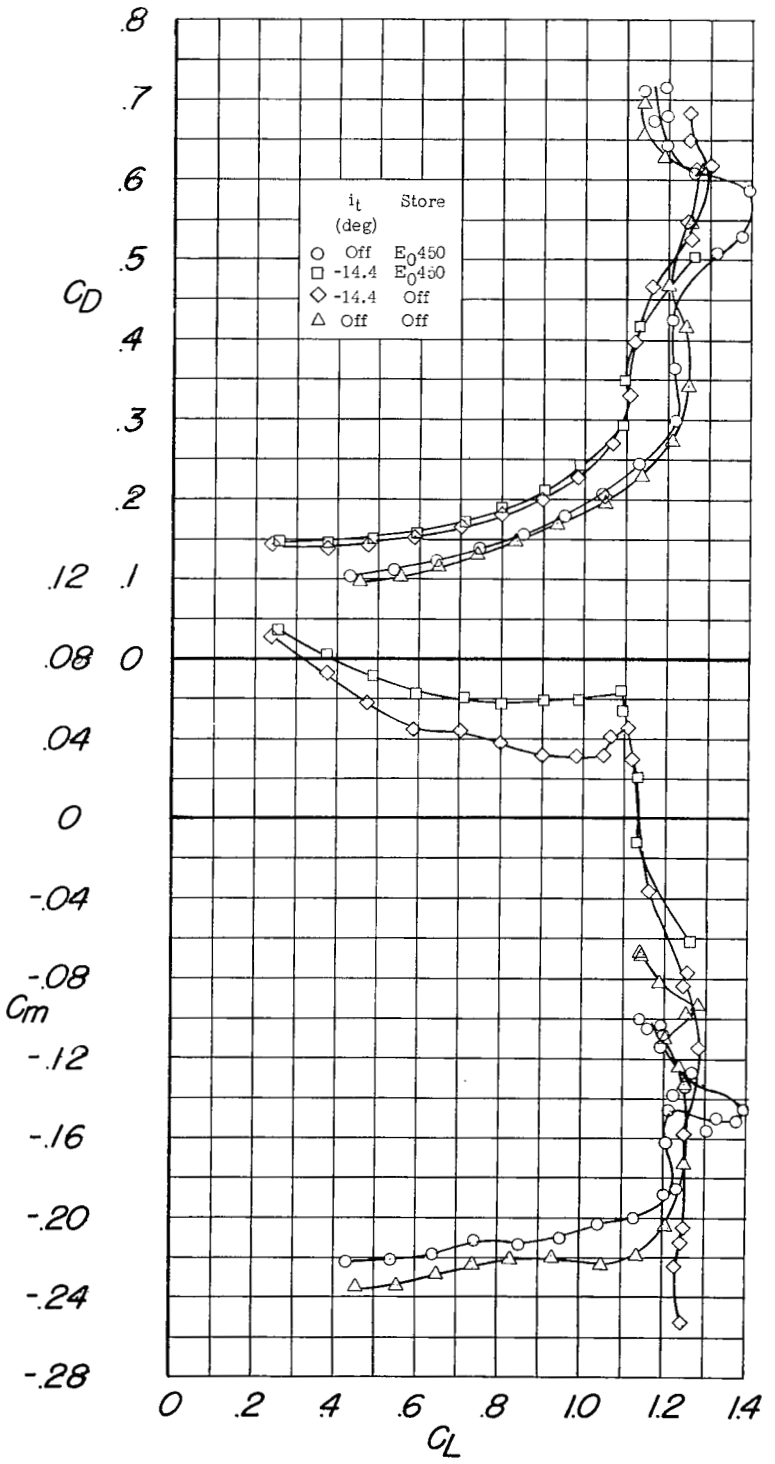

(b) C_D and C_m against C_L.

Figure 20.- Concluded.

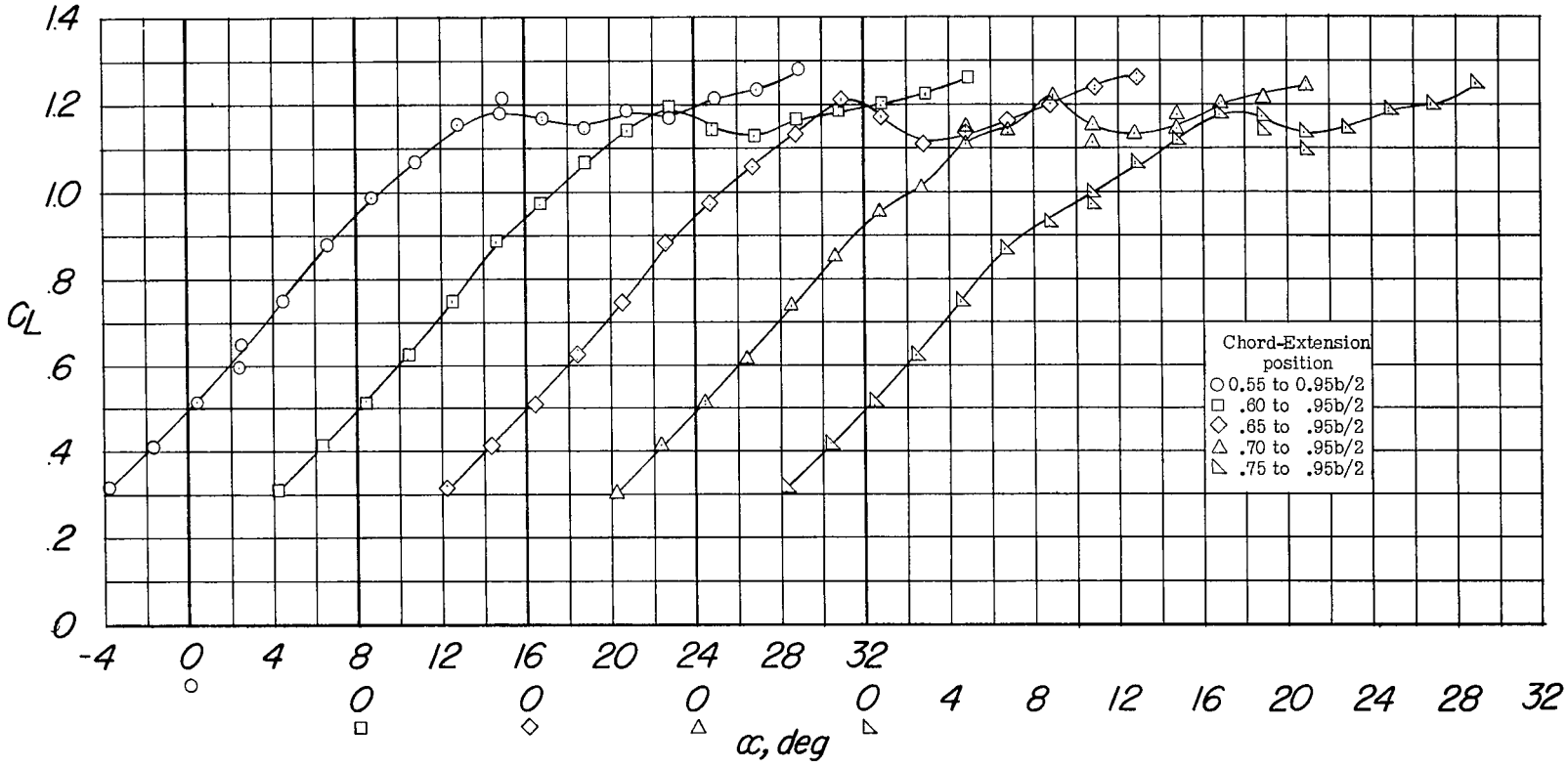

(a) C_L against α.

Figure 21.- Longitudinal characteristics of the model equipped with chord-extensions; trailing-edge flaps deflected. Configuration A + V + I_{SE} + $(-0.123)T_{-14.4}$ + $0.80F_{46}$ + C.

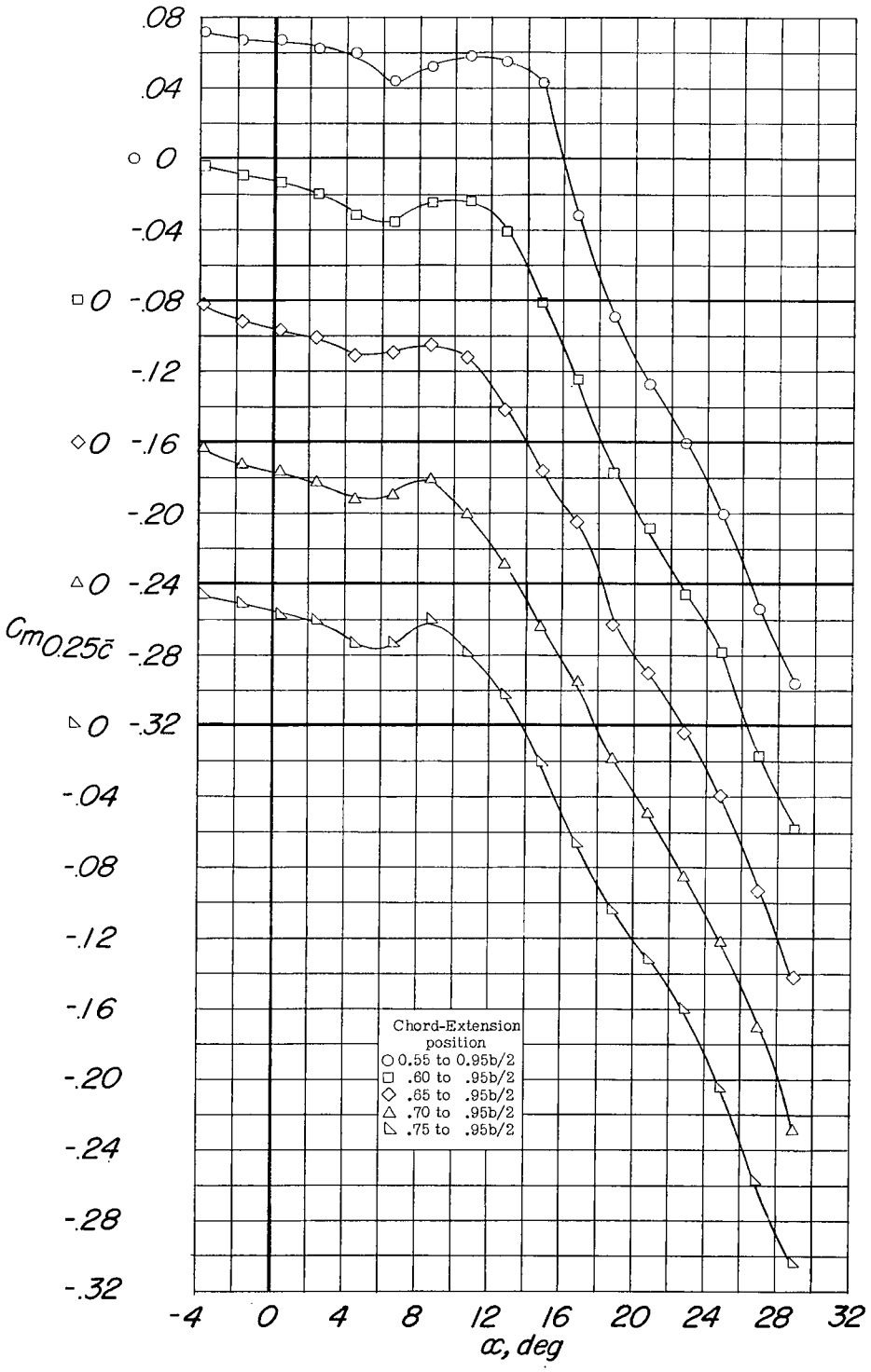

(b) C_m against α.

Figure 21.- Continued.

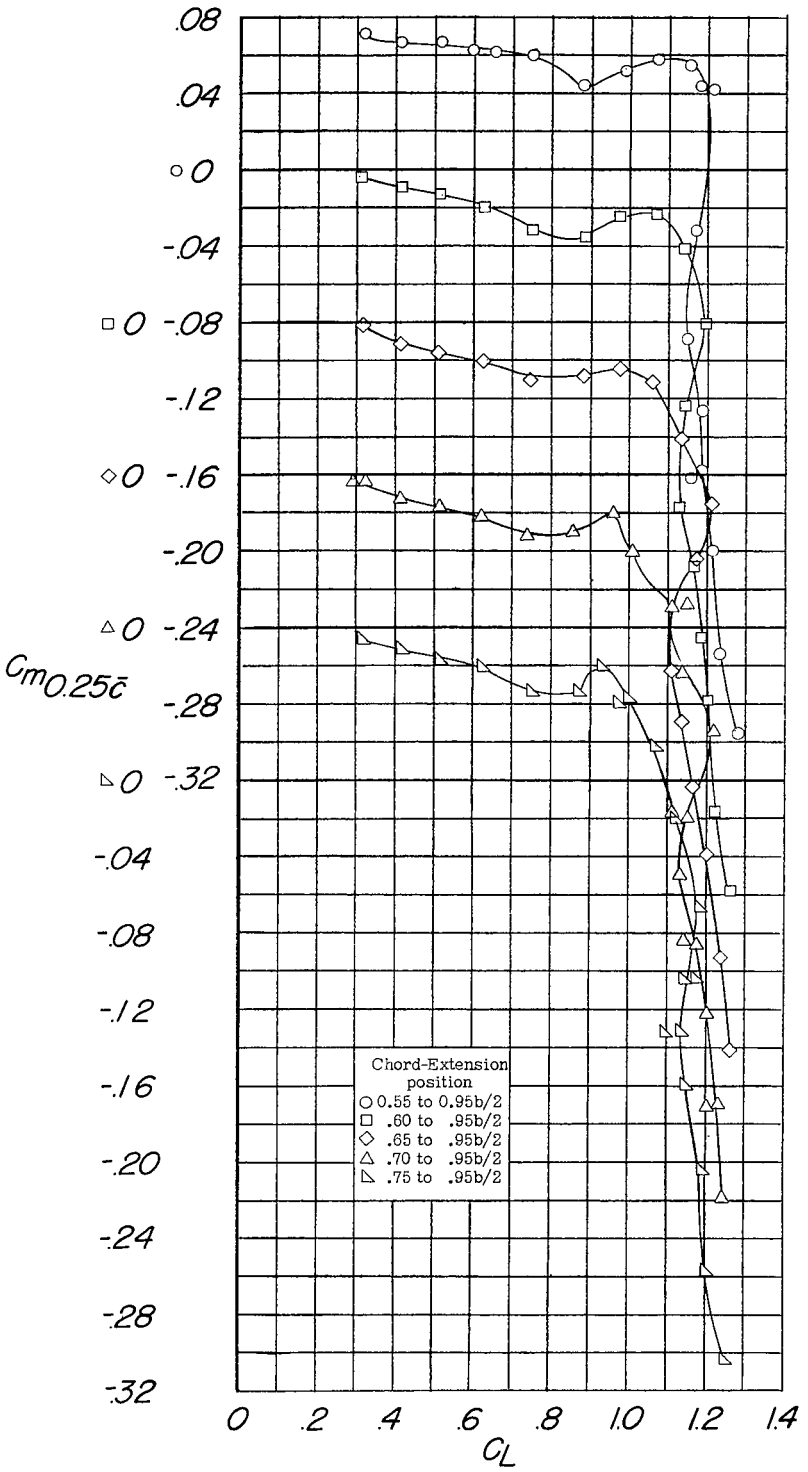

(c) C_m against C_L.

Figure 21.- Continued.

[redacted]

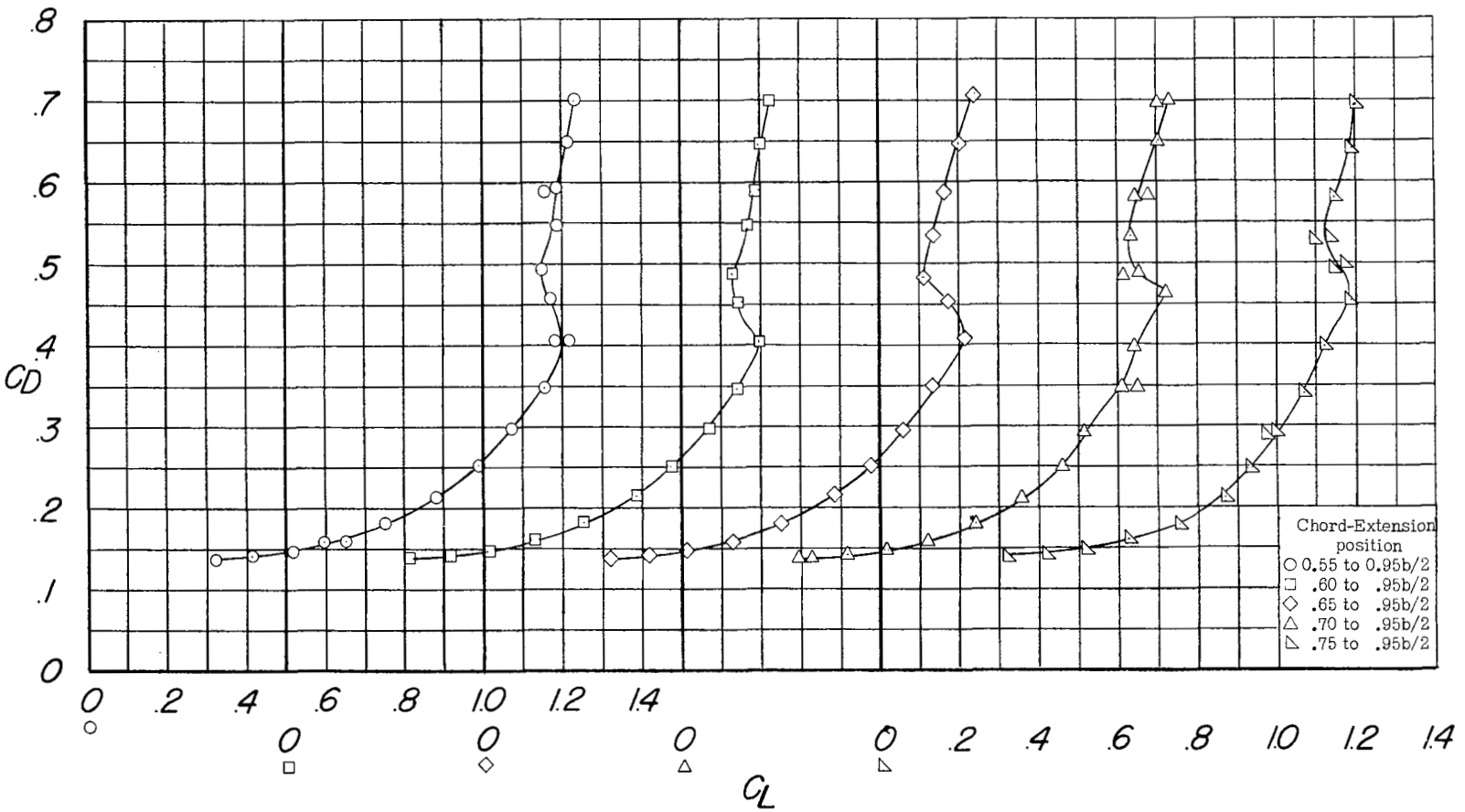

(d) C_D against C_L.

Figure 21.- Concluded.

[redacted]

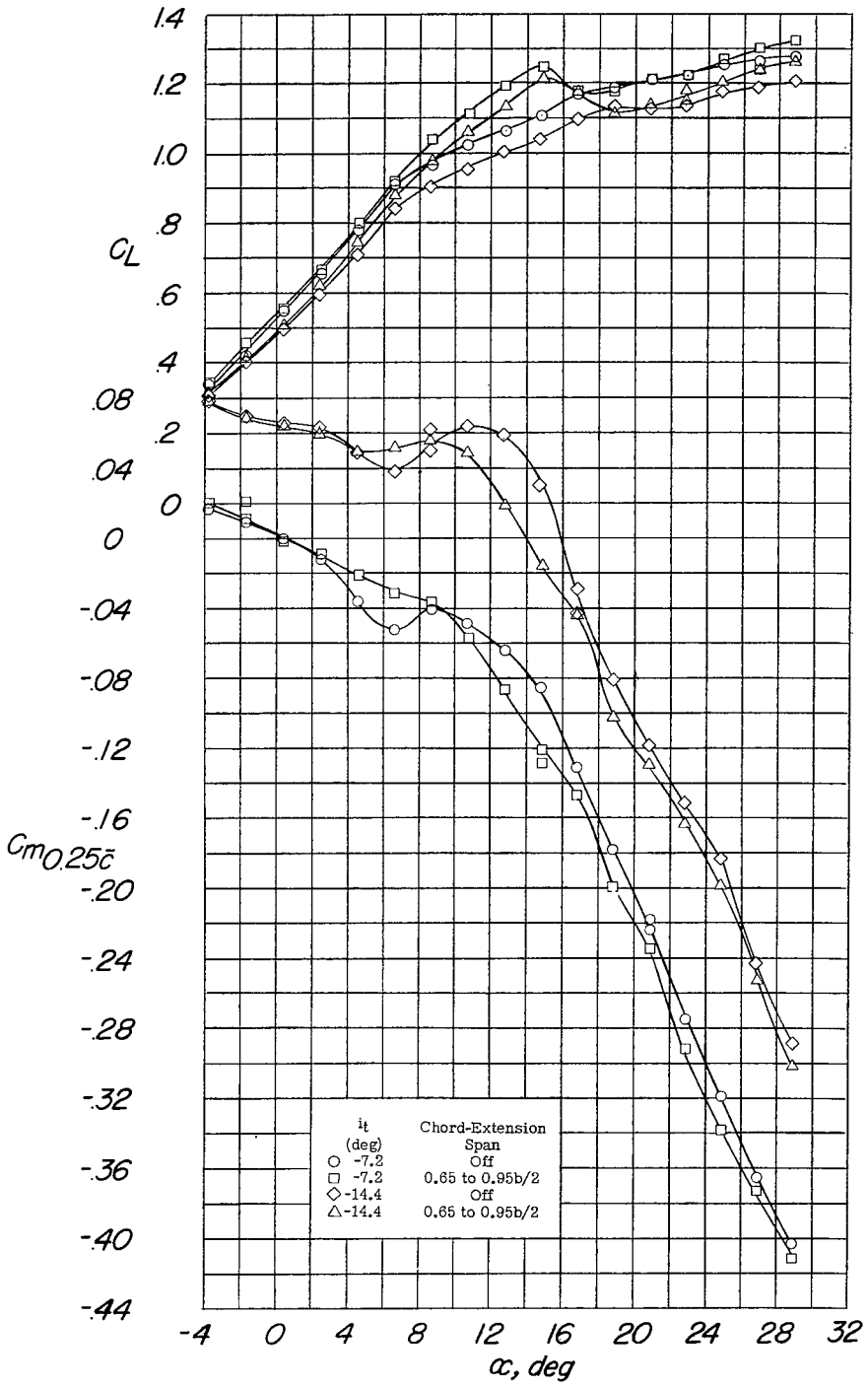

(a) C_L and C_m against α.

Figure 22.- Longitudinal characteristics of the model equipped with chord-extensions; trailing-edge flaps deflected. Configuration A + V + I_{SE} + $(-0.123)T_{-14.4}$ + $0.80F_{46}$ + C(0.65 to 0.95).

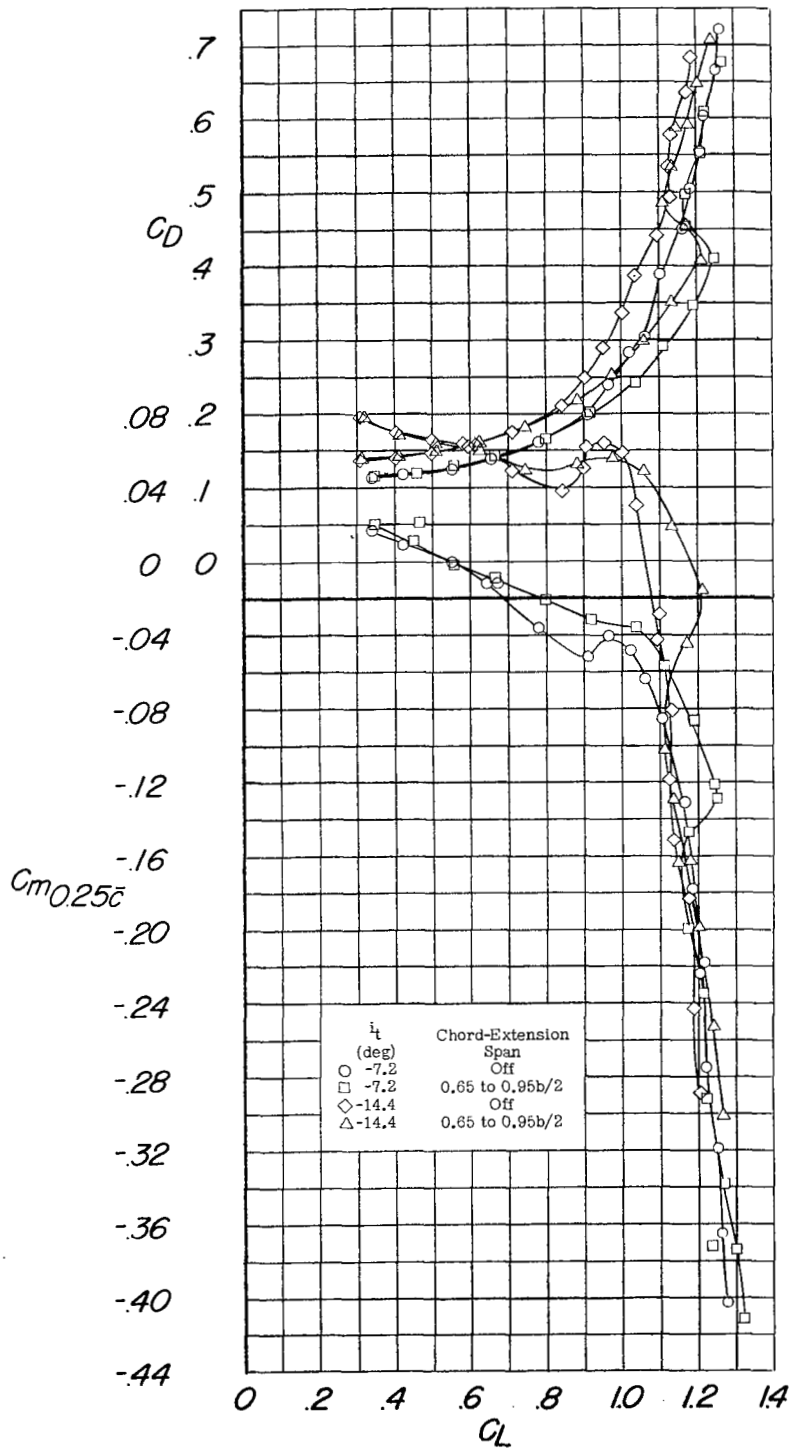

(b) C_D and C_m against C_L.

Figure 22.- Concluded.

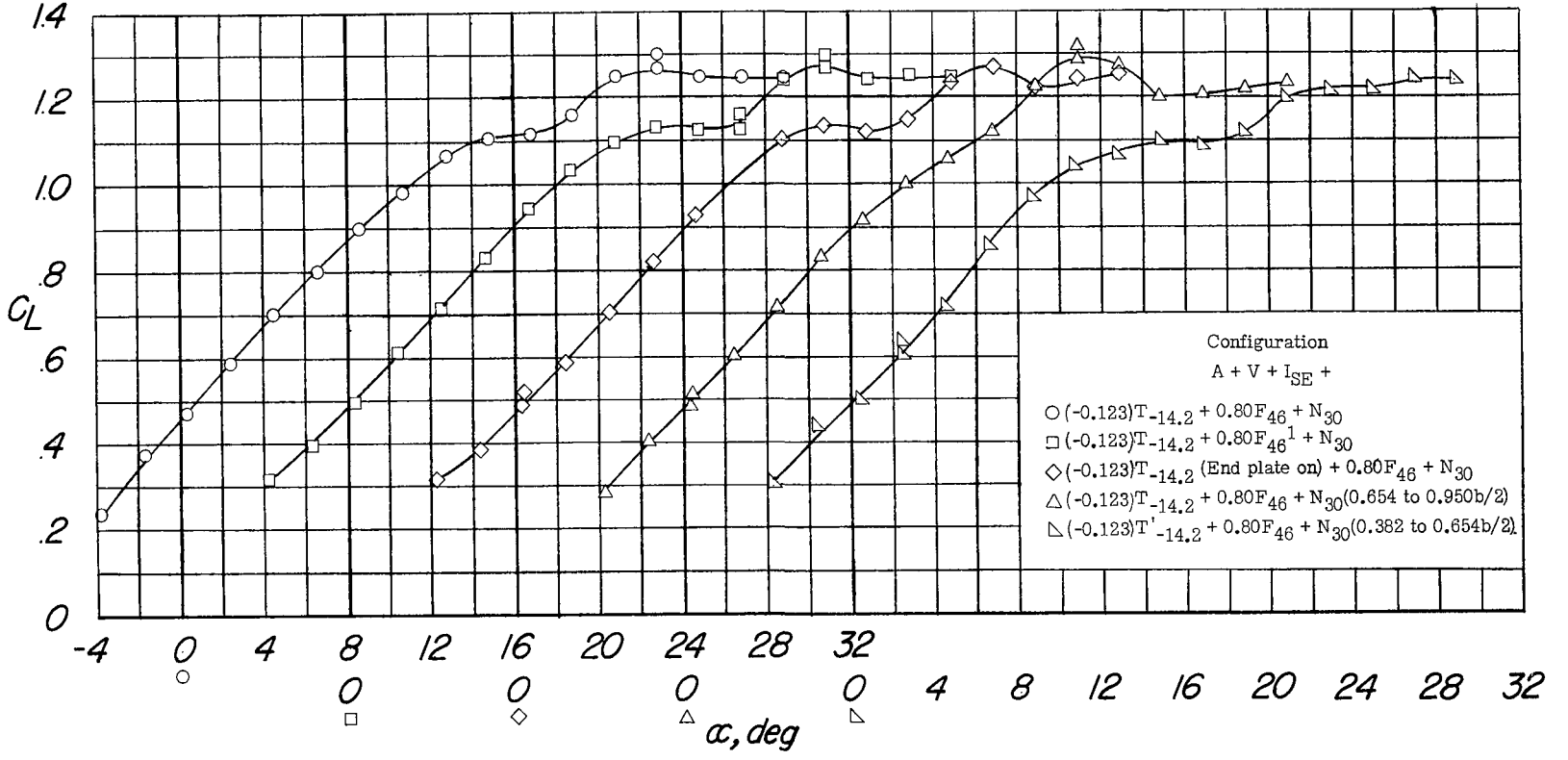

(a) C_L against α.

Figure 23.- Longitudinal characteristics of the model equipped with various flap and tail modifications. Configuration A + V + I_{SE} + (-0.123)$T_{-14.2}$ + 0.80F_{46} + N_{30}.

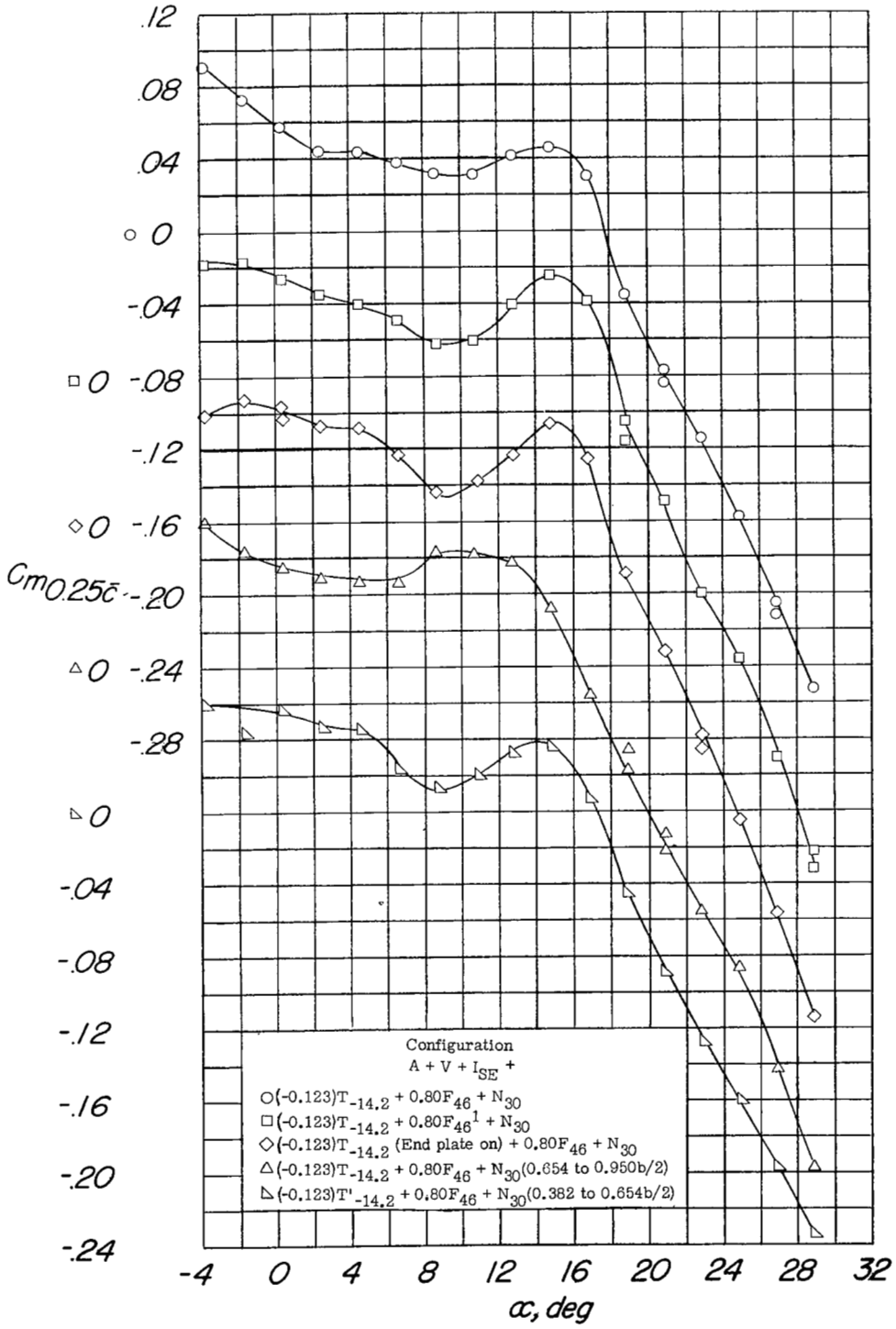

(b) C_m against α.

Figure 23.- Continued.

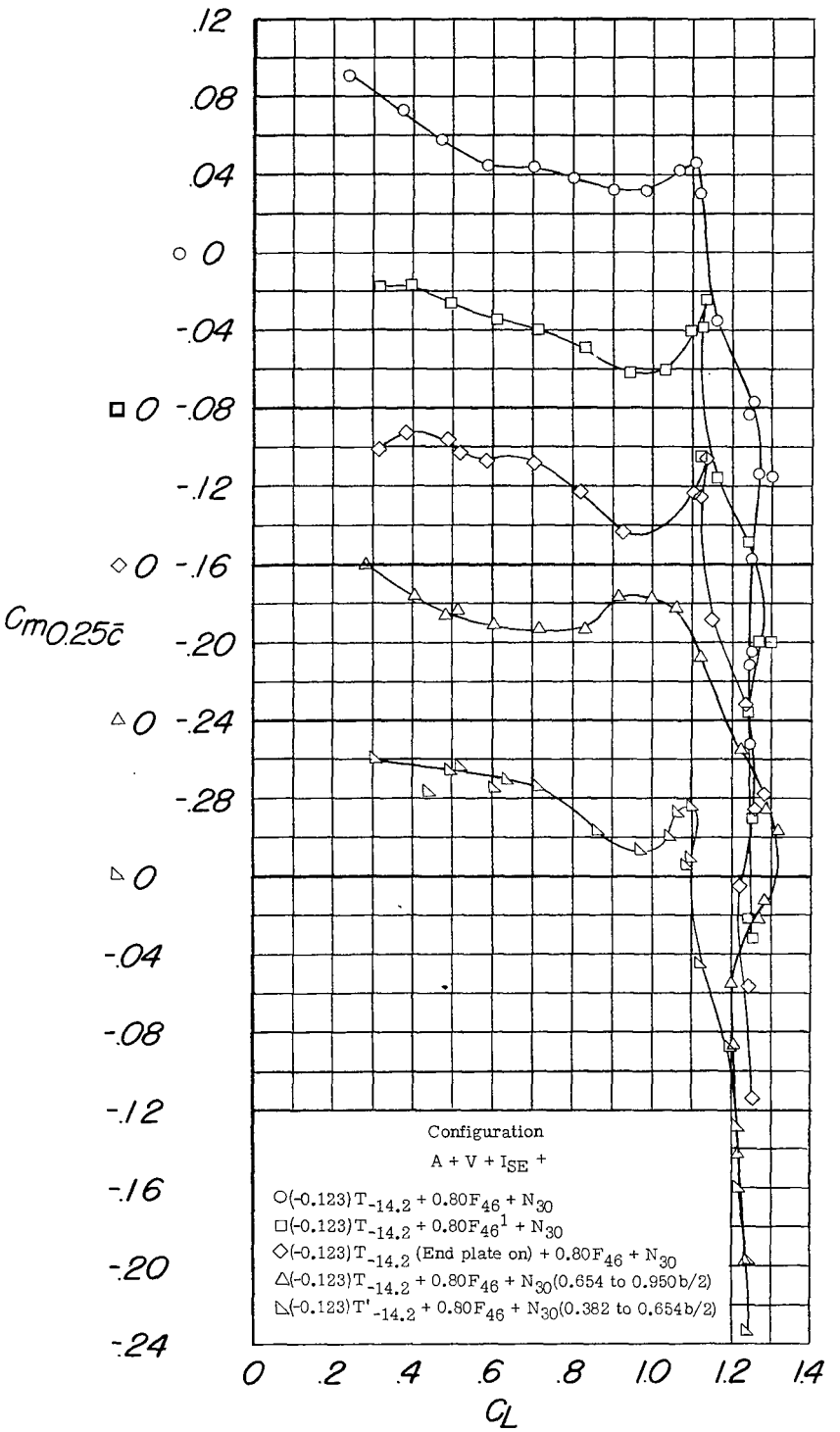

(c) C_m against C_L.

Figure 23.- Continued.

[redacted]

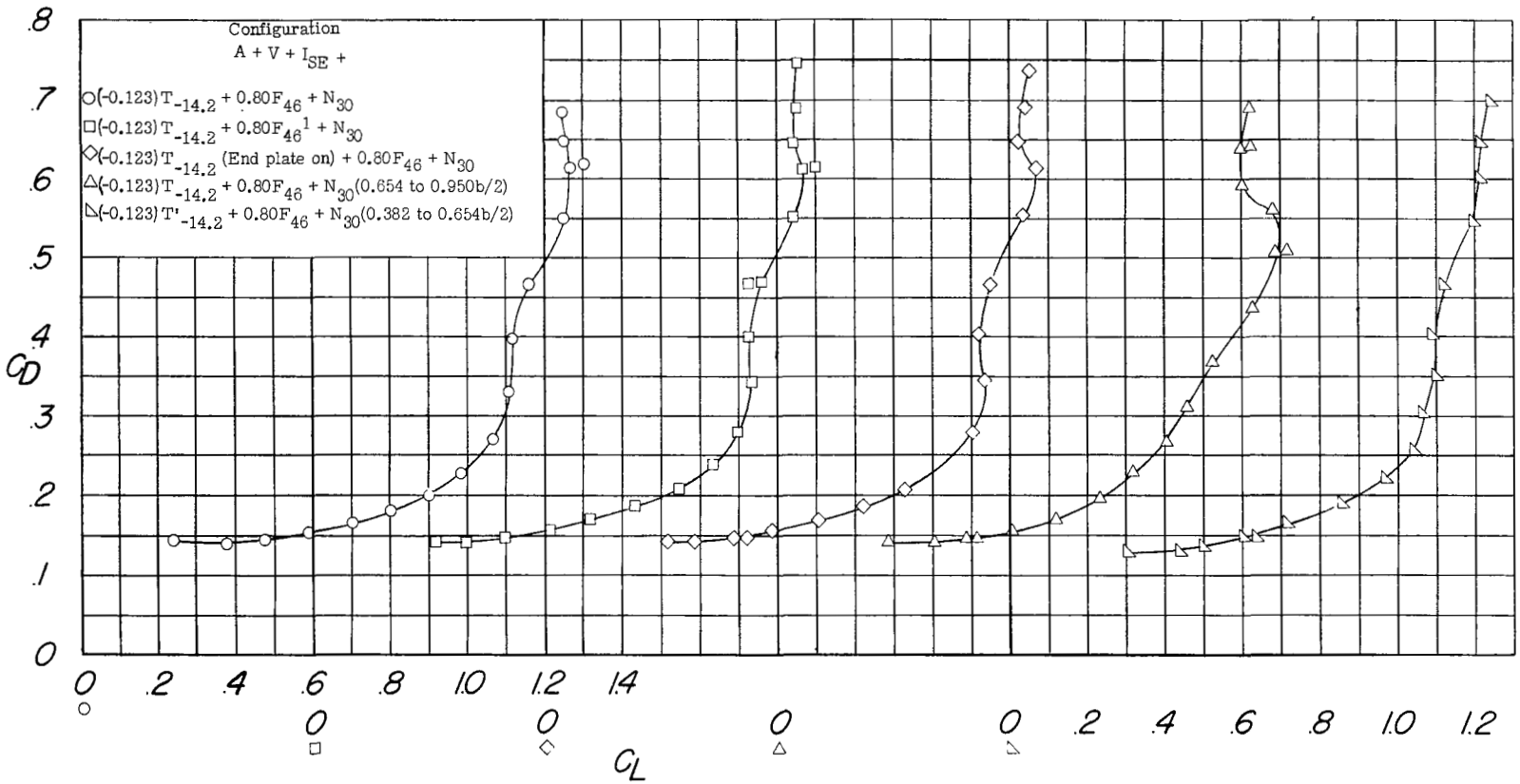

(d) C_D against C_L.

Figure 23.- Concluded.

[redacted]

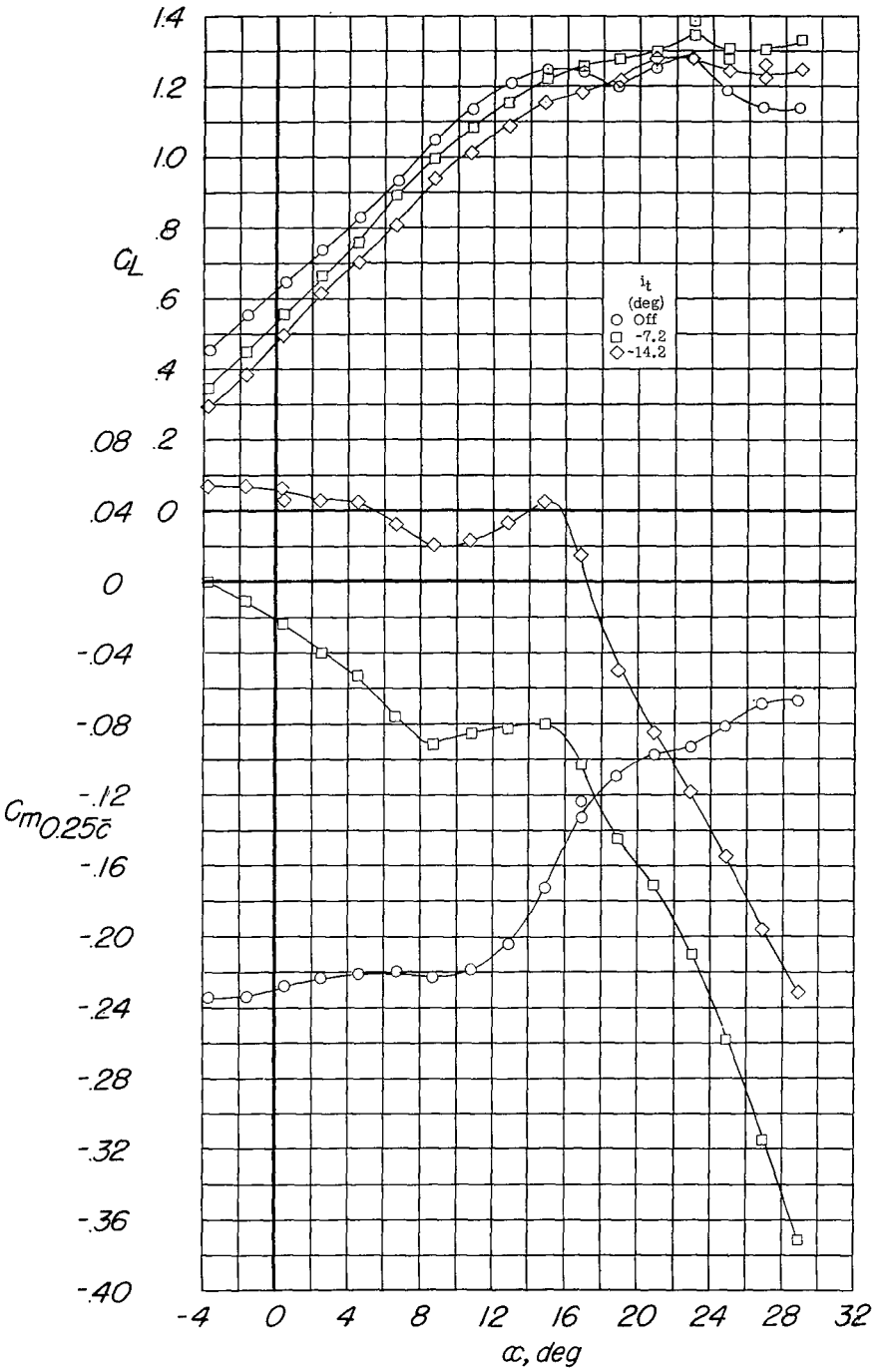

(a) C_L and C_m against α.

Figure 24.- Longitudinal characteristics of the model equipped with a modified horizontal tail; trailing-edge flaps deflected and leading-edge flap drooped 30°. Configuration A + V + I_{SE} + (-0.123)T' + $0.80F_{46}$ + N_{30}.

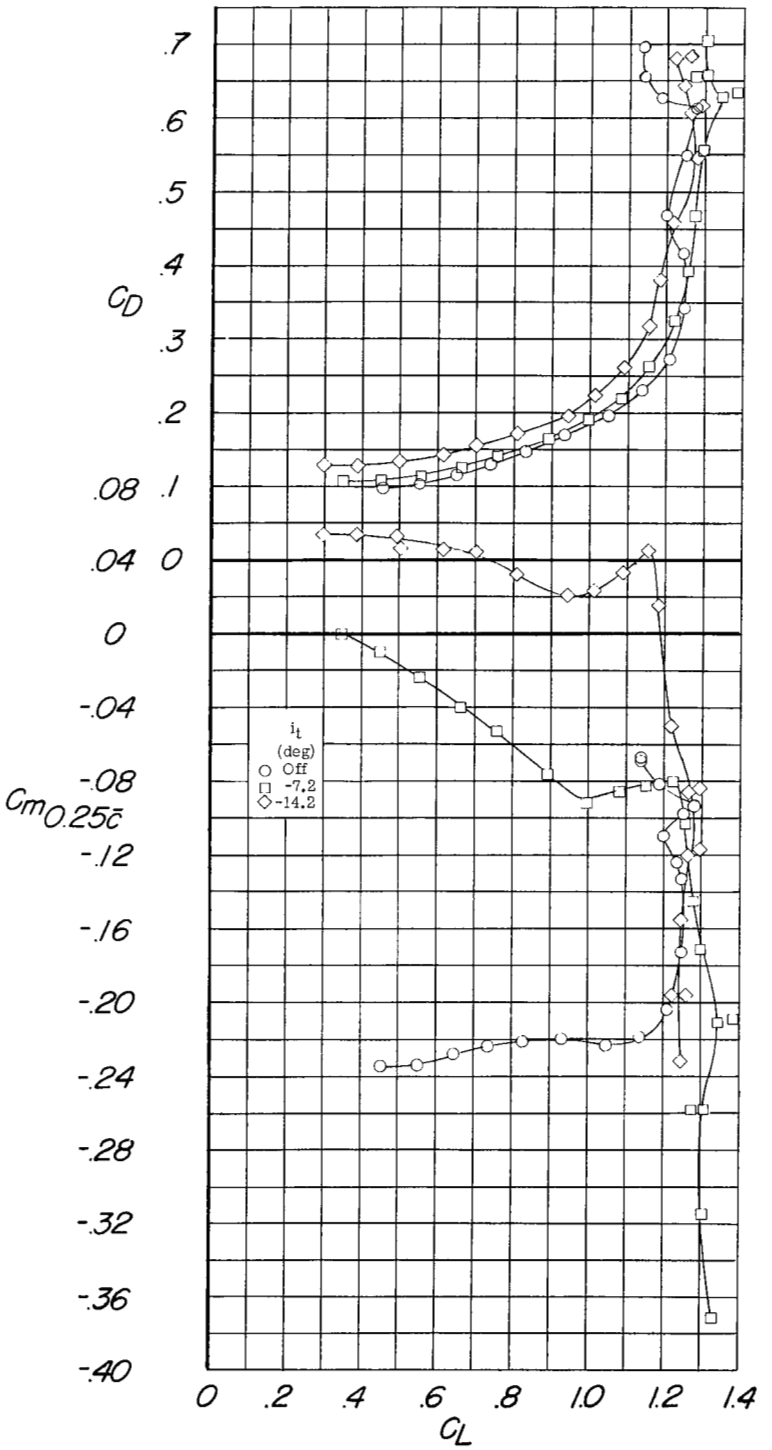

(b) C_D and C_m against C_L.

Figure 24.- Concluded.

[redacted]

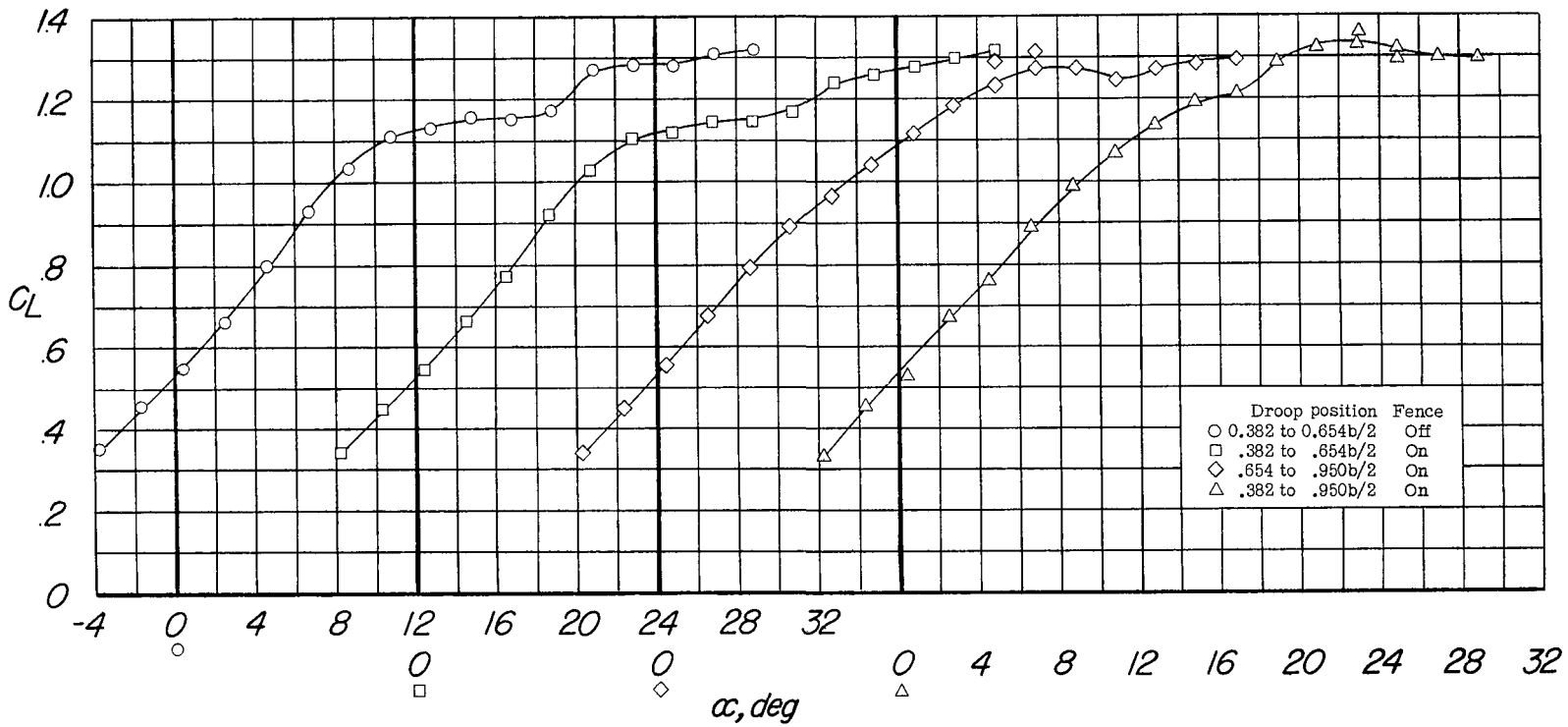

(a) C_L against α.

Figure 25.- Longitudinal characteristics of the model with various portions of the leading-edge flap deflected; model equipped with a modified horizontal tail; trailing-edge flaps deflected. Configuration $A + V + I_{SE} + (-0.123)T'_{-7.2} + 0.80F_{46} + N_{30} + 1W_{0.654}$.

[redacted]

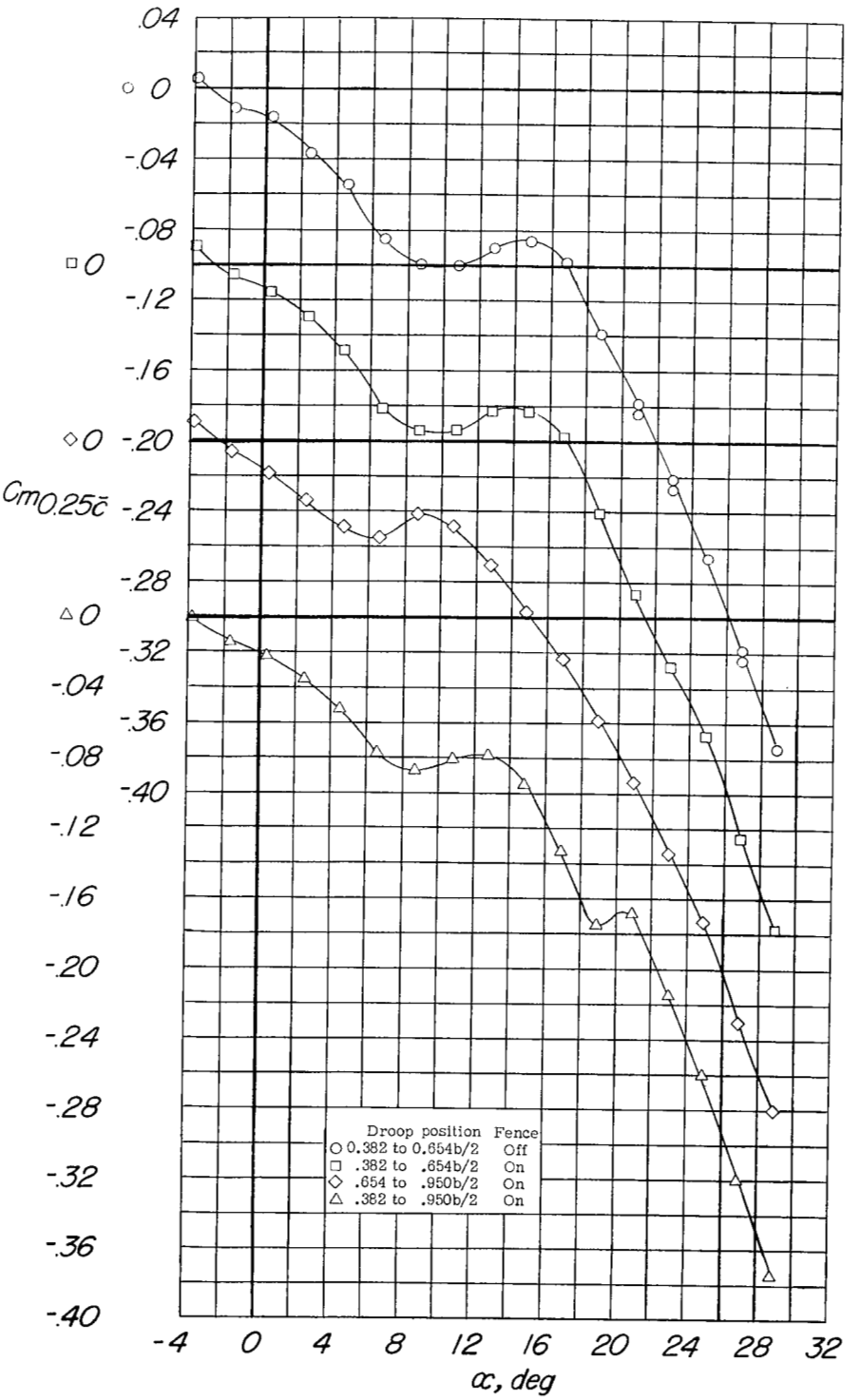

(b) C_m against α.

Figure 25.- Continued.

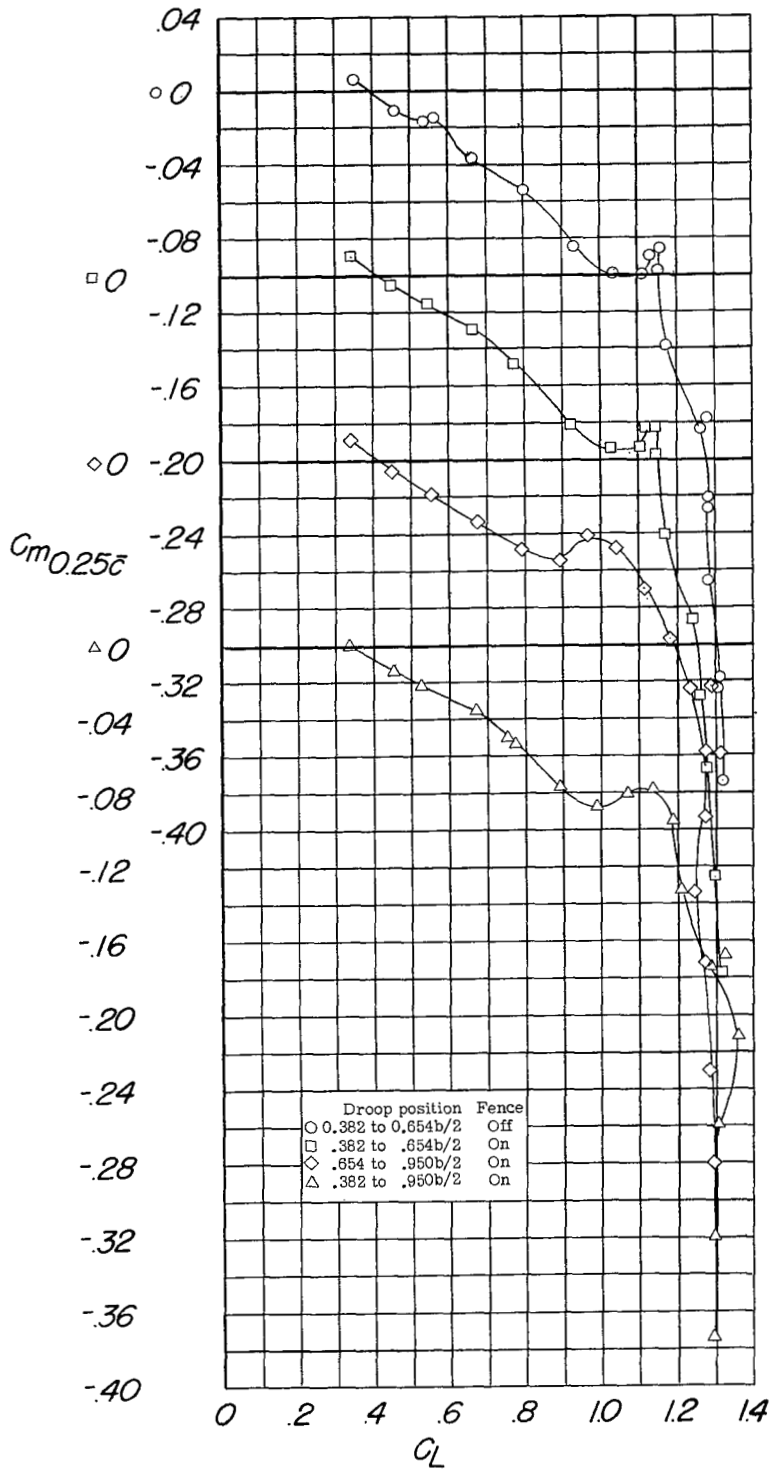

(c) C_m against C_L.

Figure 25.- Continued.

[redacted]

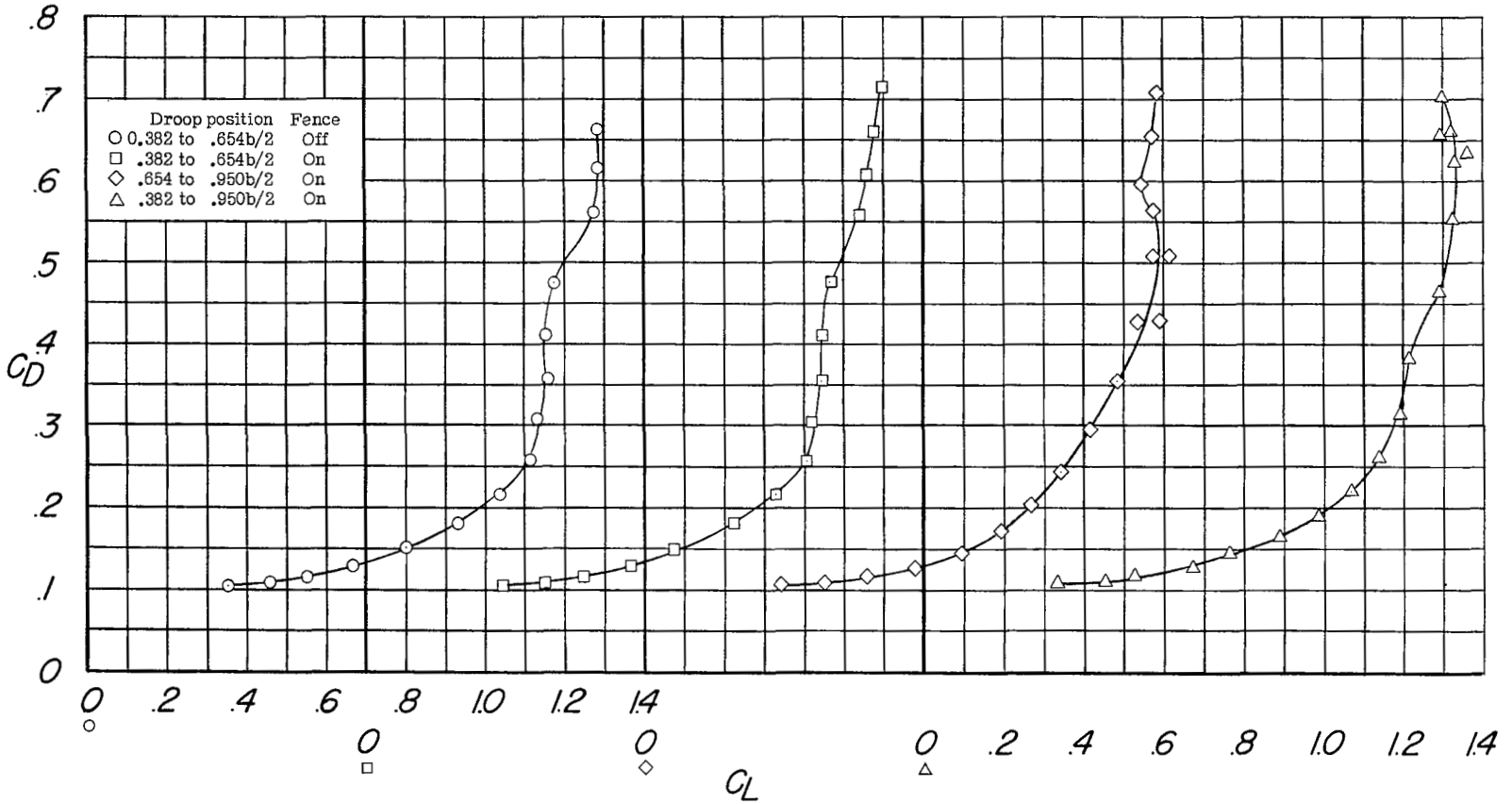

(d) C_D against C_L.

Figure 25.- Concluded.

[redacted]

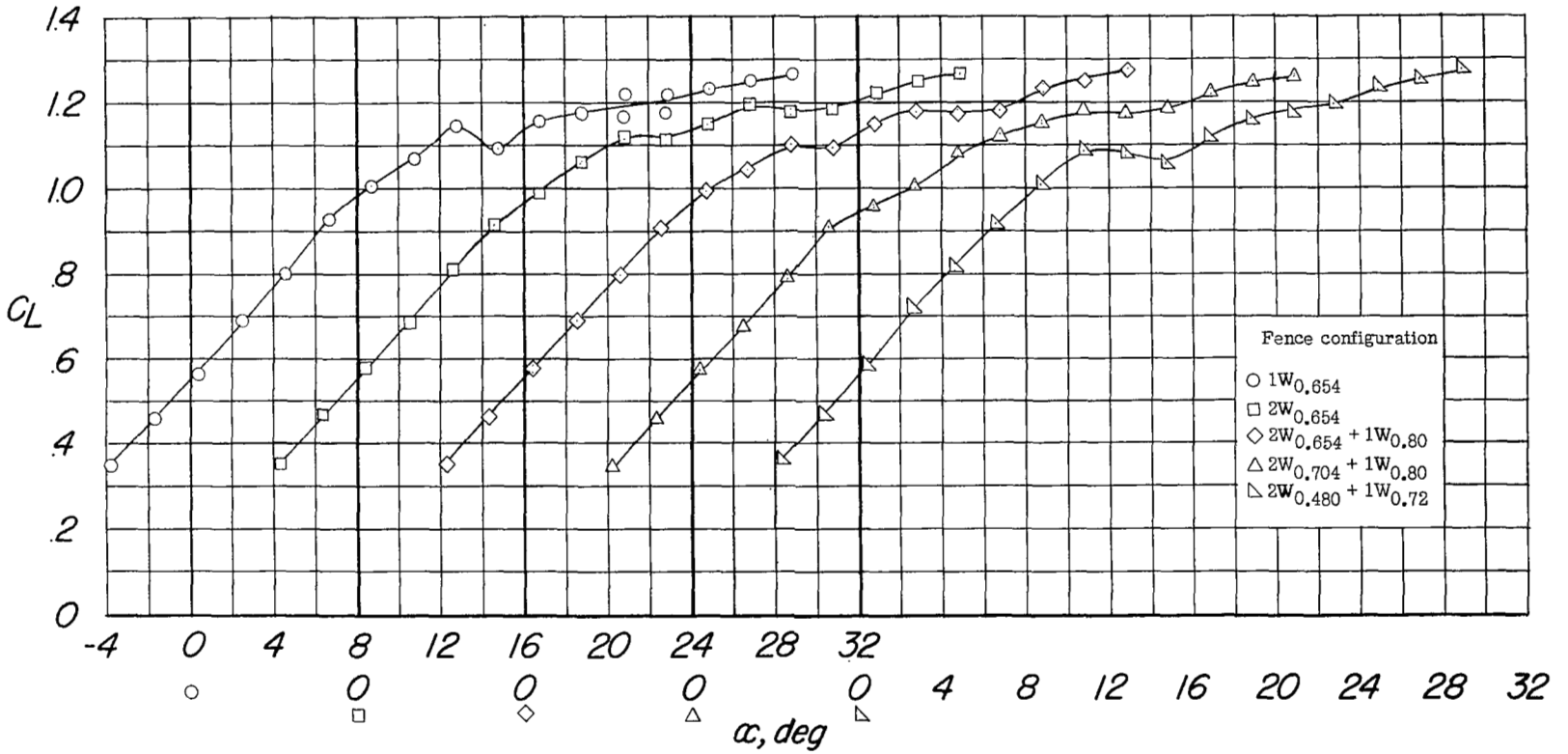

(a) C_L against α.

Figure 26.- Longitudinal characteristics of the model equipped with various fence configurations, a modified horizontal tail, and deflected trailing-edge flaps. Configuration $A + V + I_{SE} + (-0.123)T'_{-7.2} + 0.80F_{46} + W$.

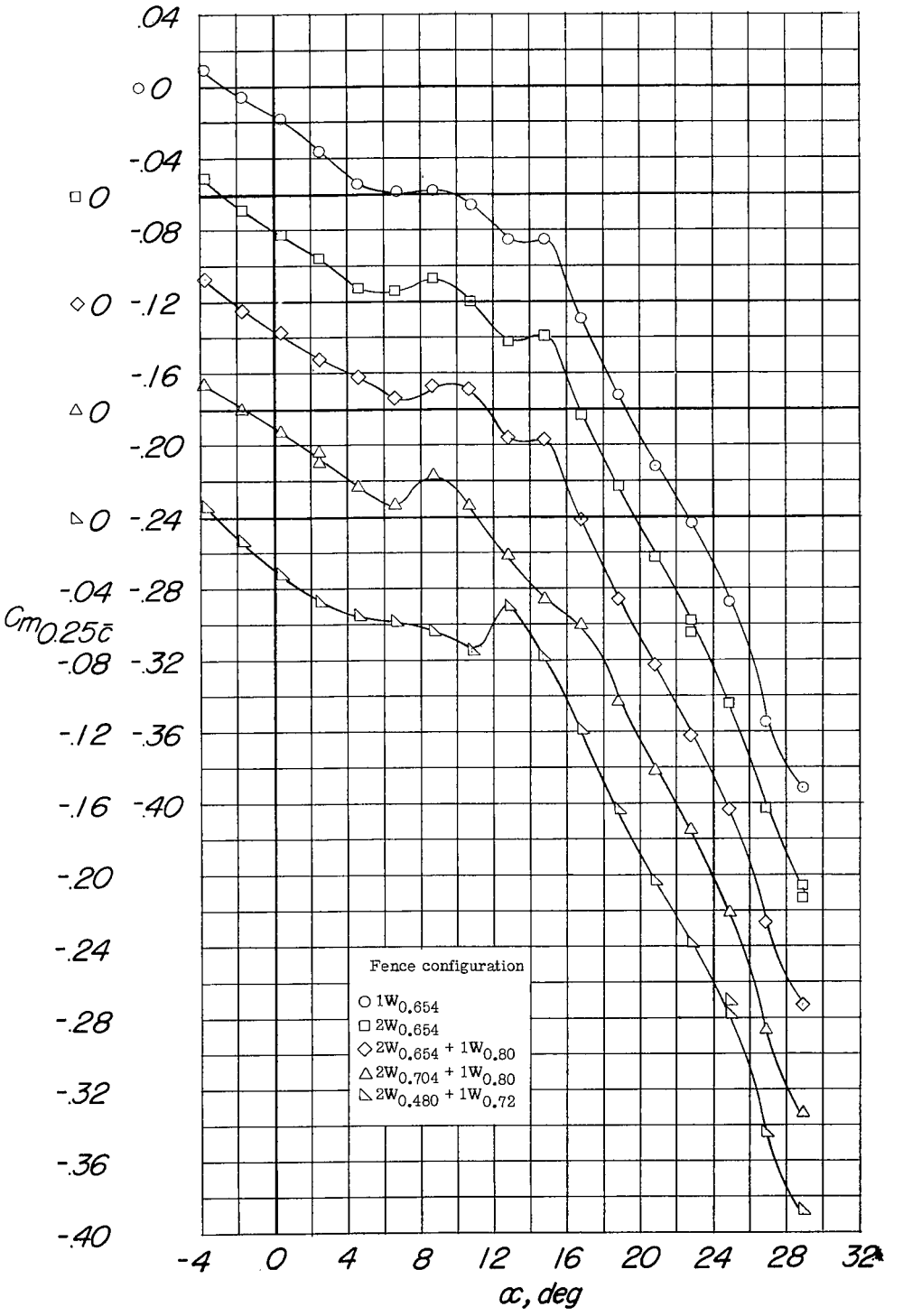

(b) C_m against α.

Figure 26.- Continued.

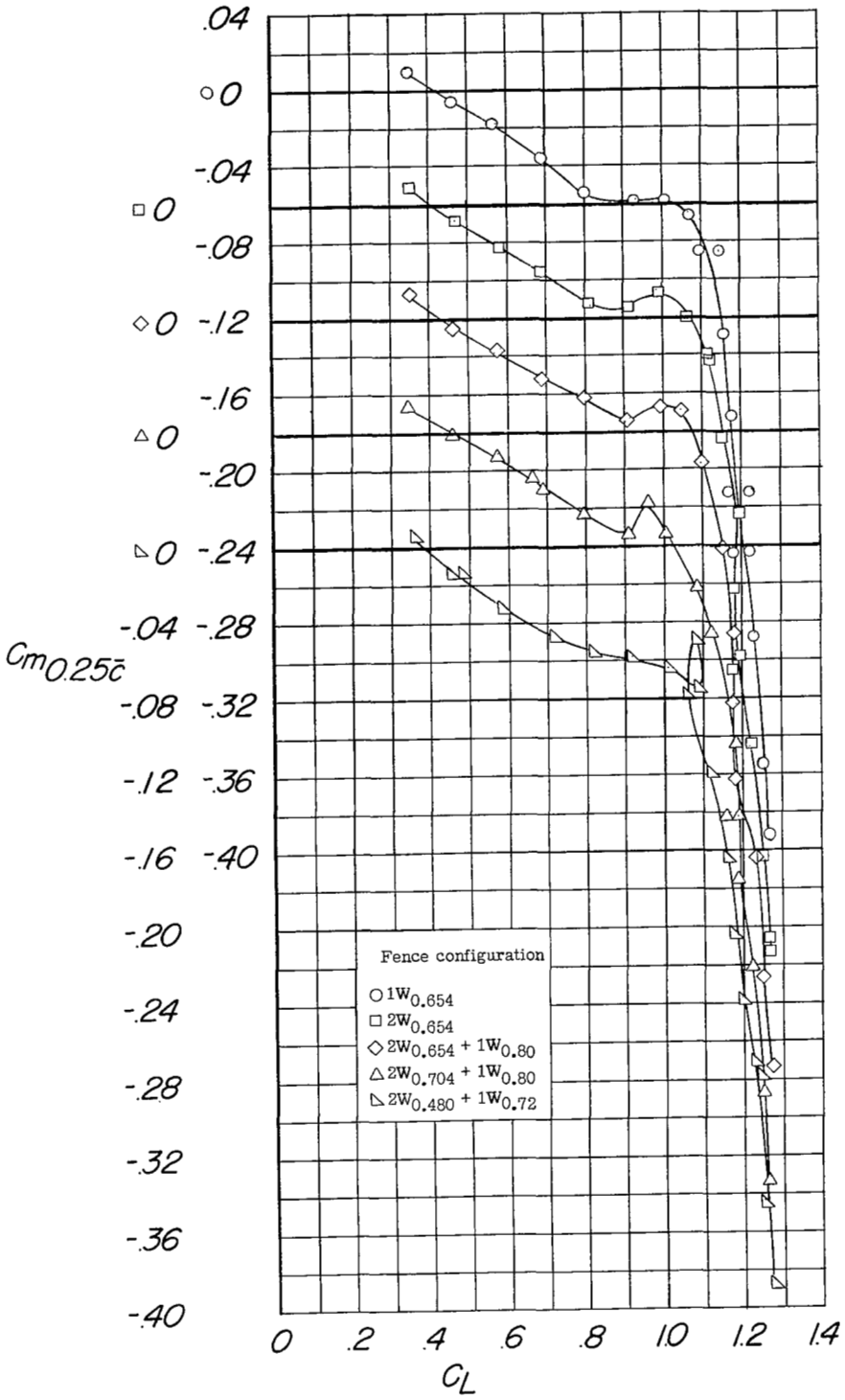

(c) C_m against C_L.

Figure 26.- Continued.

[redacted]

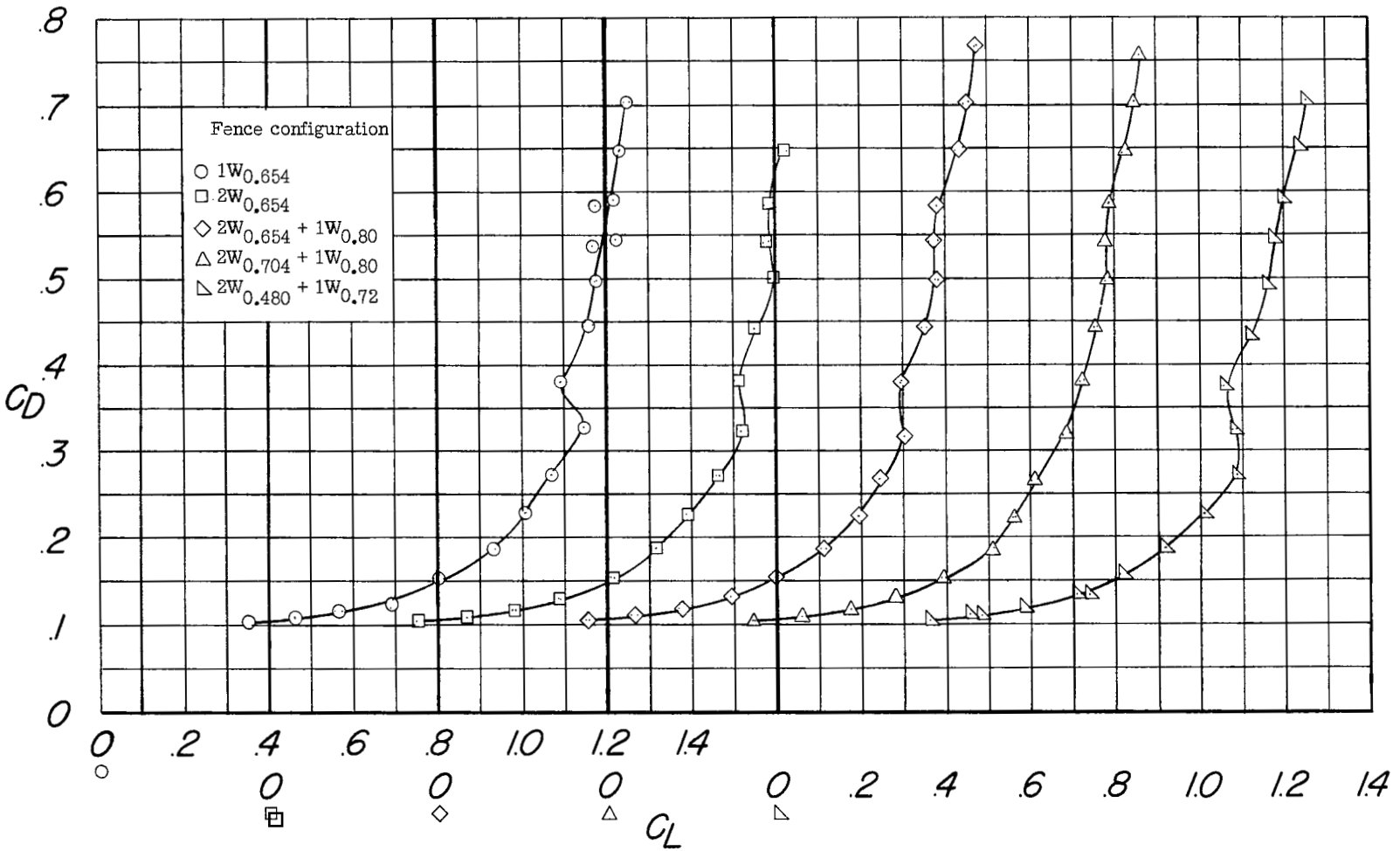

(d) C_D against C_L.

Figure 26.- Concluded.

[redacted]

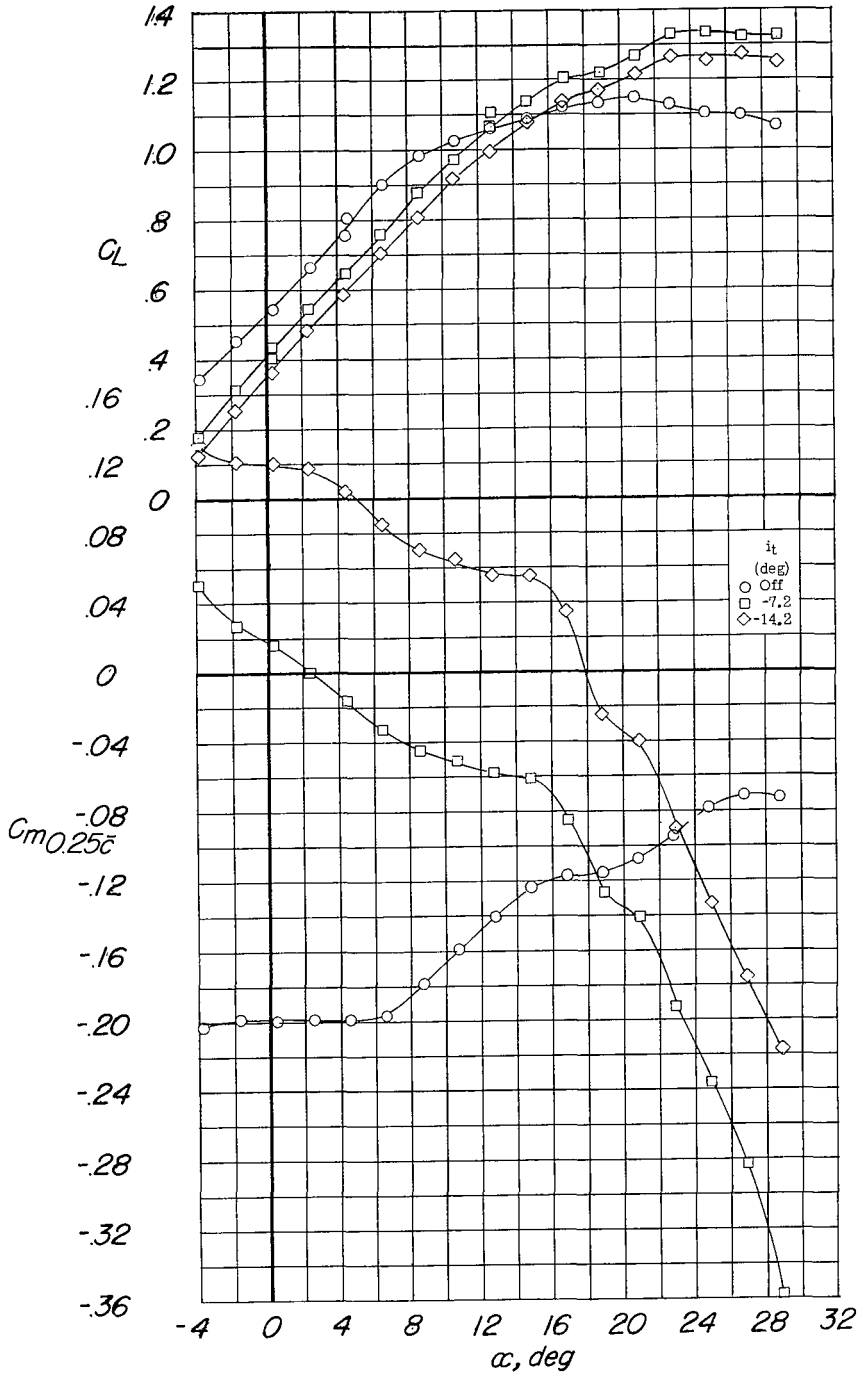

(a) C_L and C_m against α.

Figure 27.- Longitudinal characteristics of the model equipped with a modified horizontal tail; trailing-edge flaps deflected 35° and leading-edge flap drooped 30°. Configuration A + V + I_{SE} + (-0.123)T' + $0.80F_{35}$ + N_{30}.

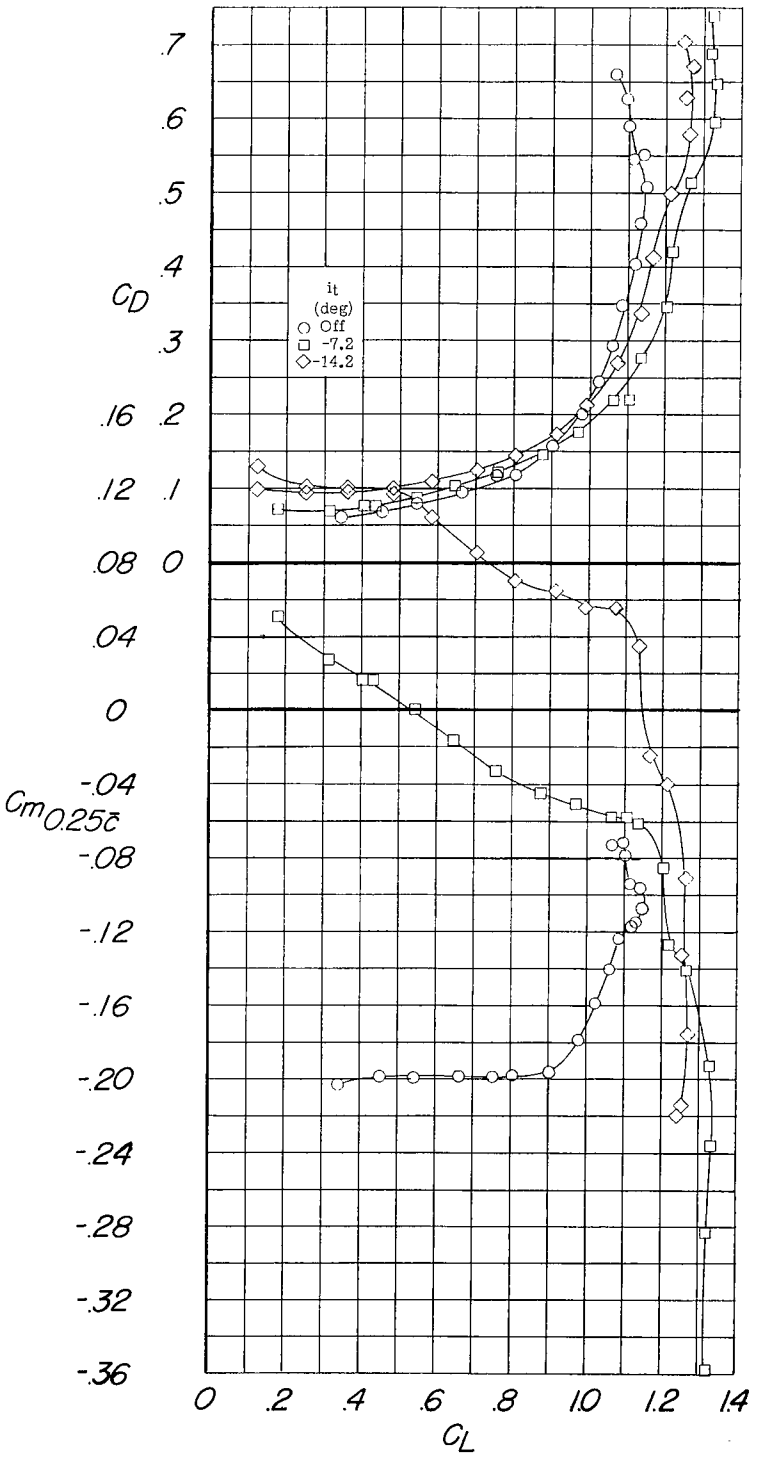

(b) C_D and C_m against C_L.

Figure 27.- Concluded.

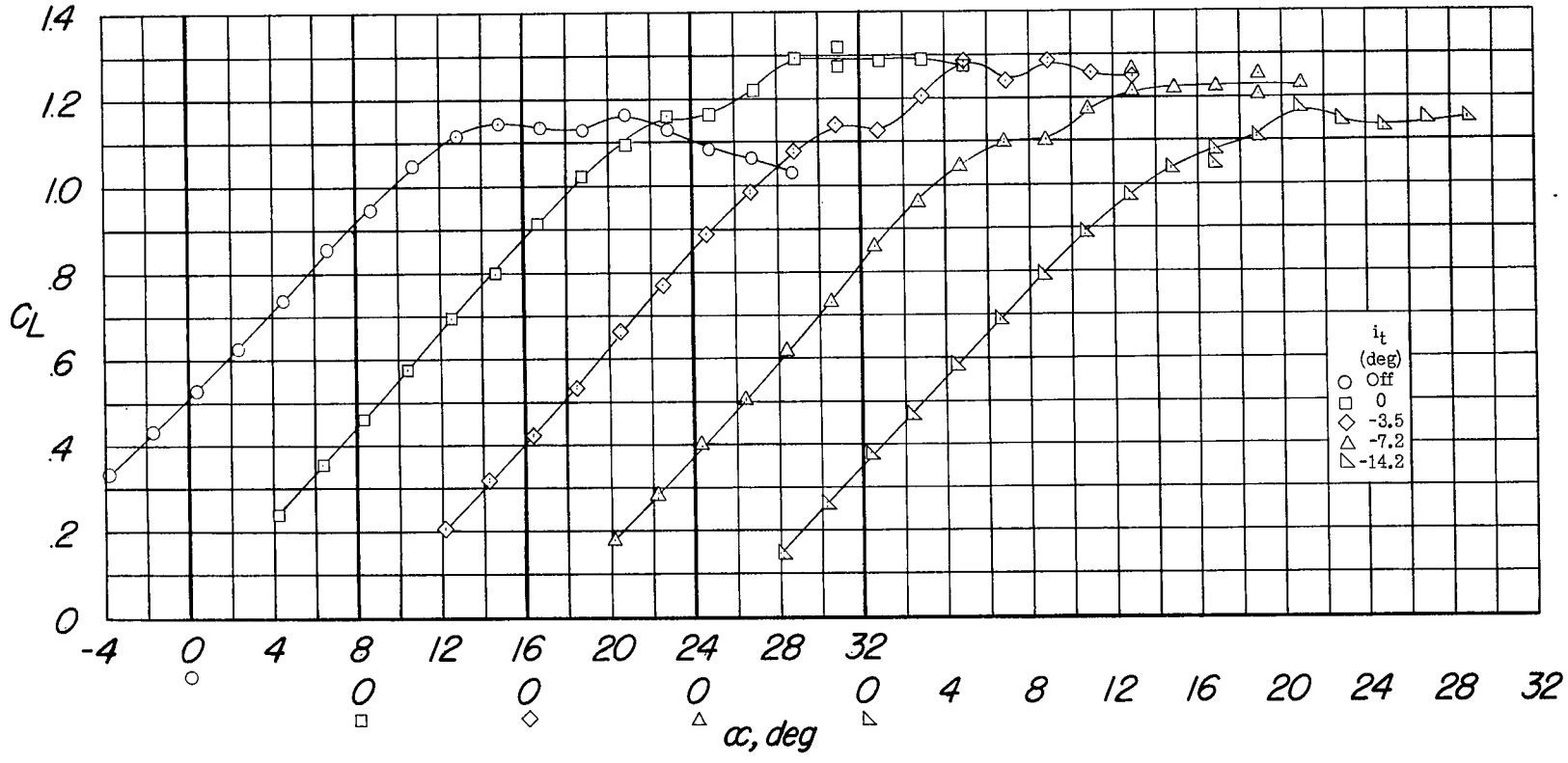

(a) C_L against α.

Figure 28.- Longitudinal characteristics of the model equipped with a modified horizontal tail; 60-percent-span trailing-edge flaps deflected 46° and leading-edge flap drooped 20°. Configuration A + V + I_{SE} + (-0.123)T' + 0.60F_{46} + N_{20}.

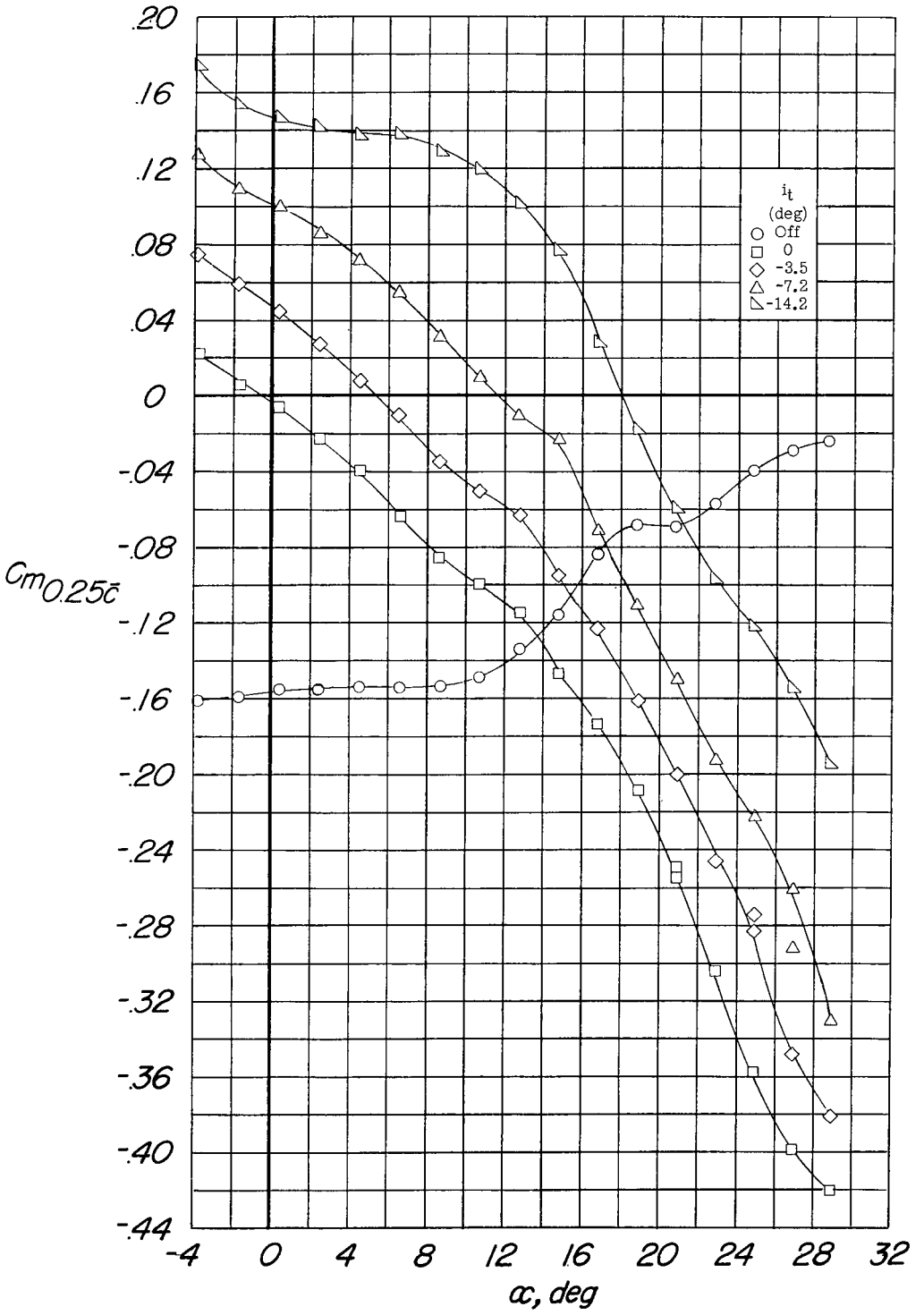

(b) C_m against α.

Figure 28.- Continued.

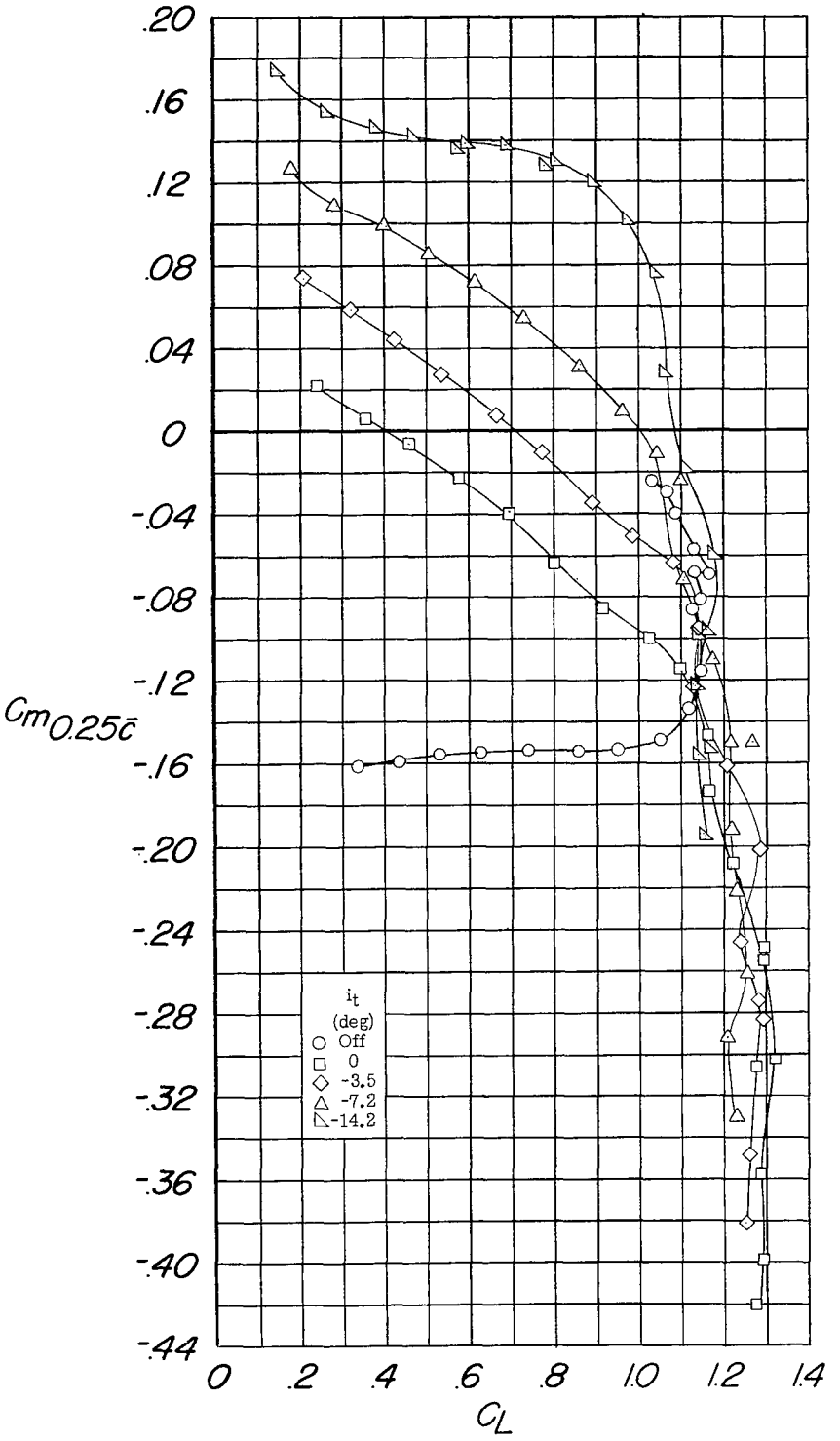

(c) C_m against C_L.

Figure 28.- Continued.

[redacted]

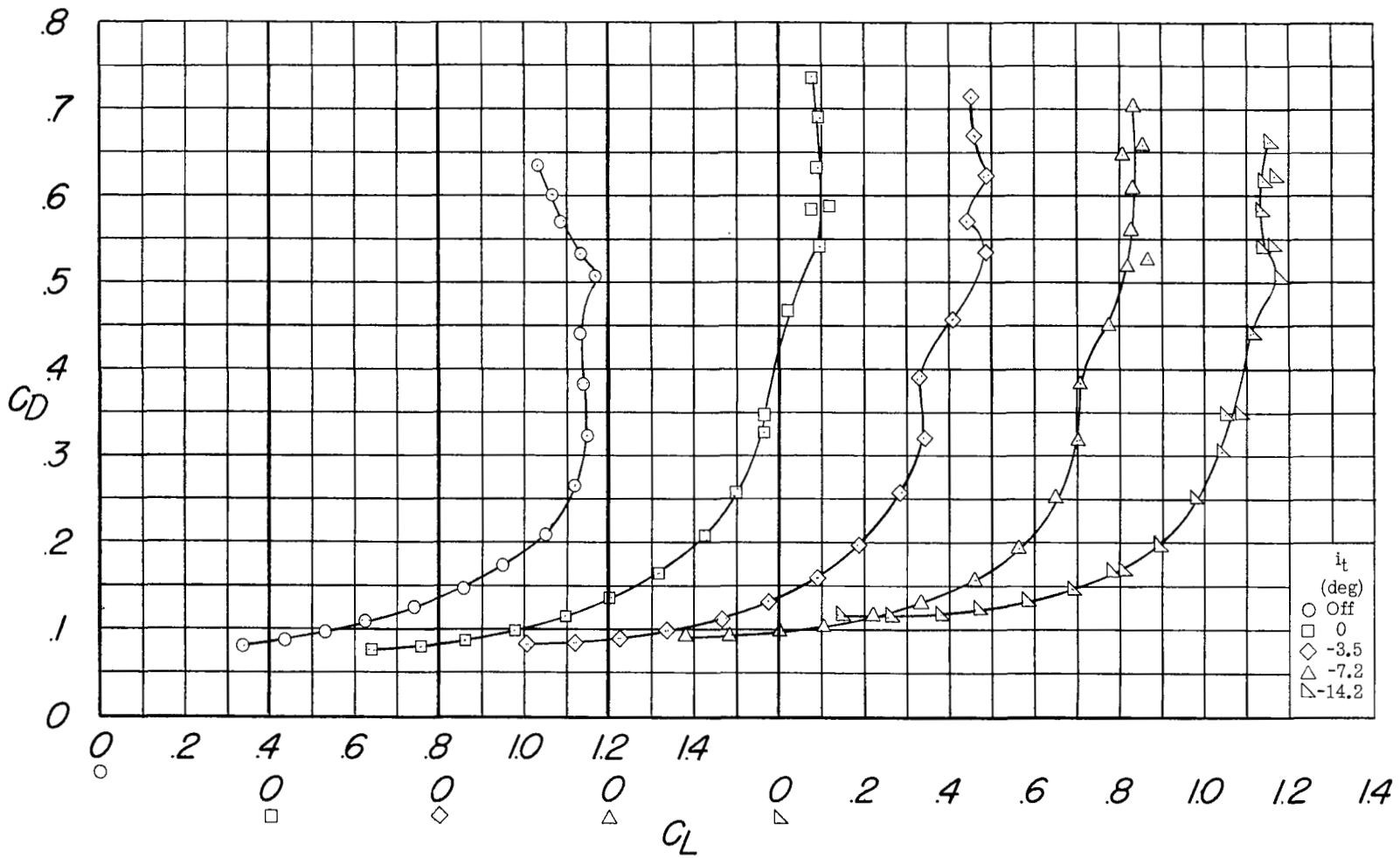

(d) C_D against C_L.

Figure 28.- Concluded.

[redacted]

[redacted]

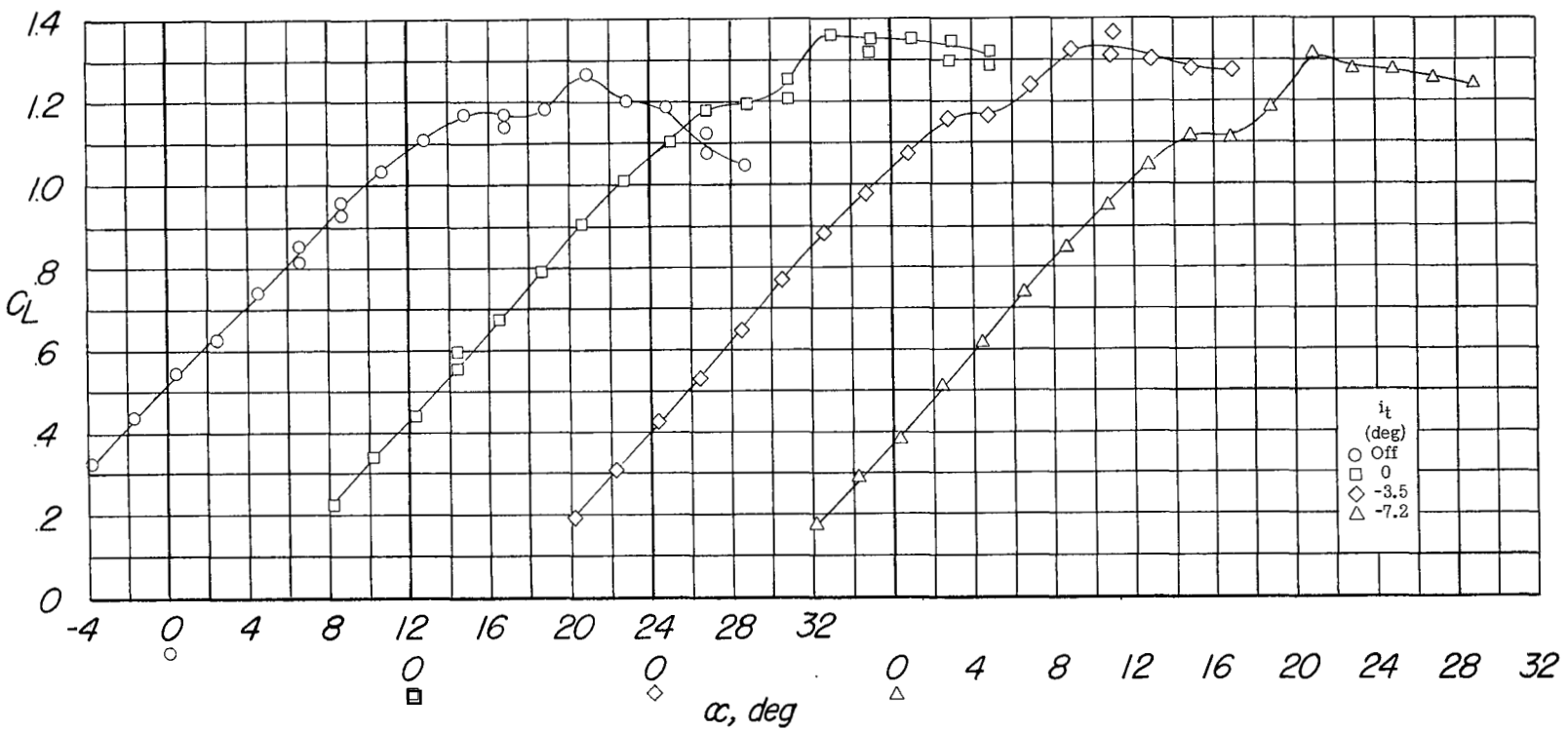

[redacted]

(a) C_L against α.

Figure 29.- Longitudinal characteristics of the model equipped with a modified horizontal tail; 60-percent-span trailing-edge flaps deflected 46° and leading-edge flap drooped 30°. Configuration A + V + I_{SE} + (-0.123)T' + 0.60F_{46} + N_{30}.

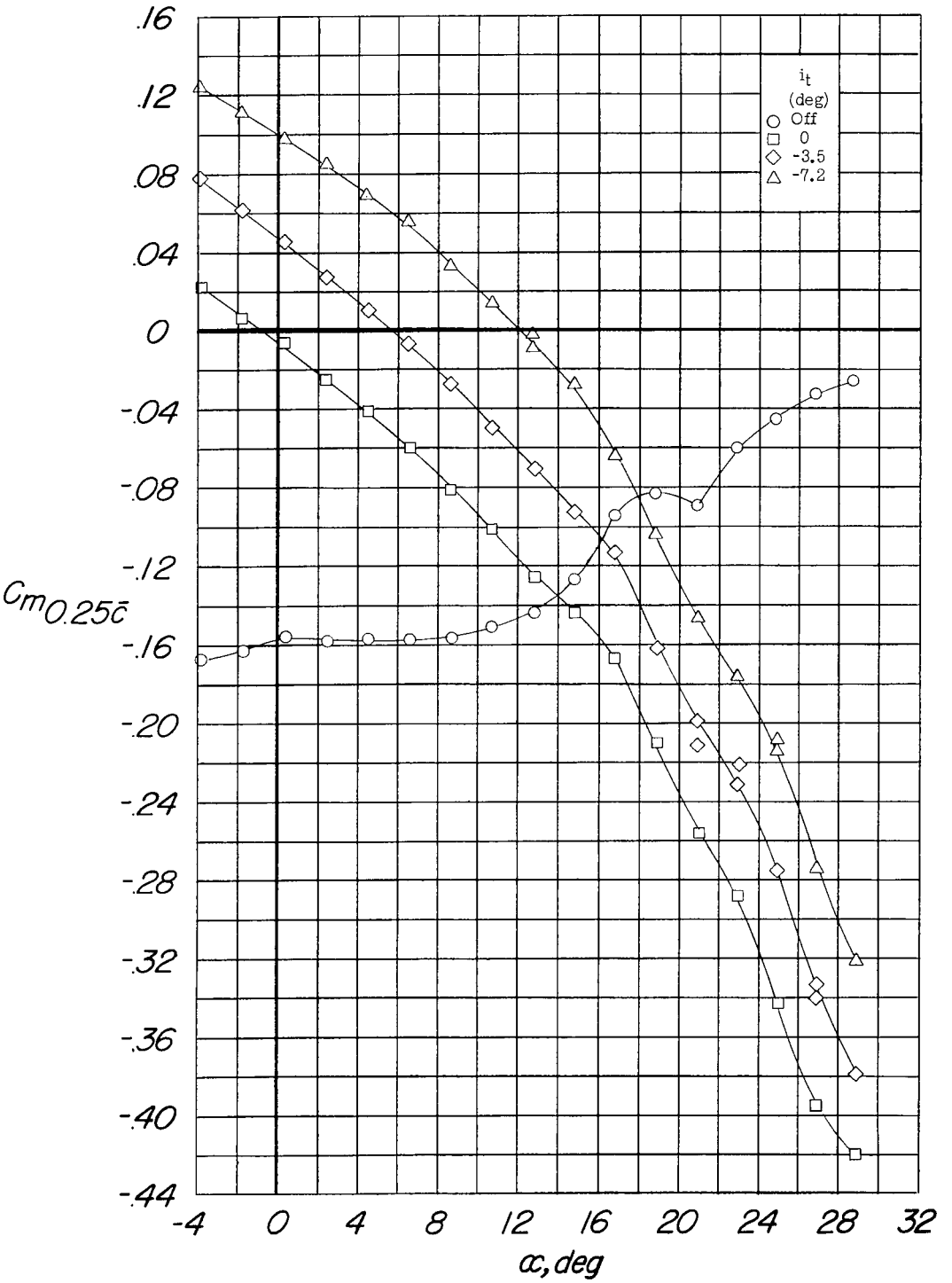

(b) C_m against α.

Figure 29.- Continued.

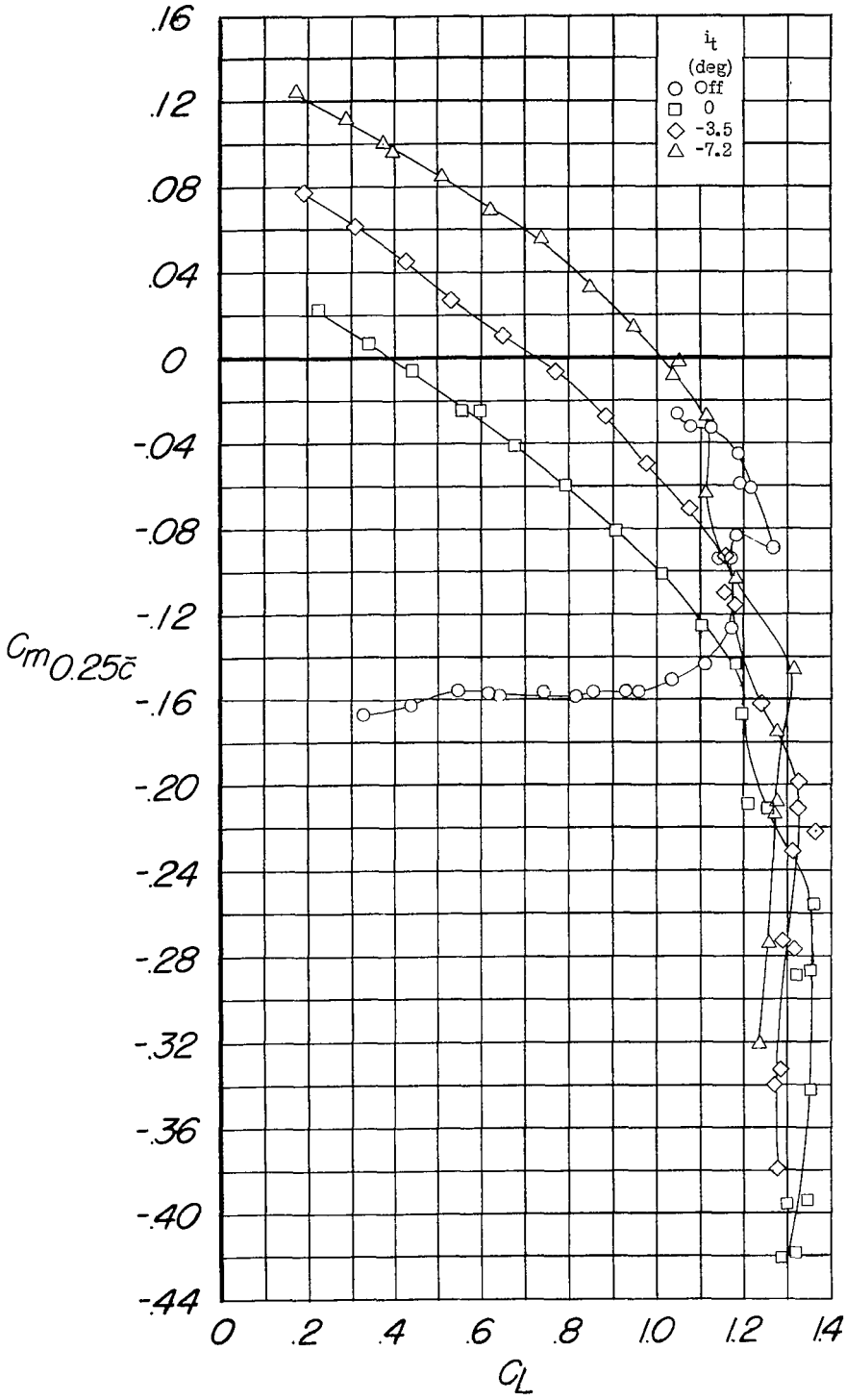

(c) C_m against C_L.

Figure 29.- Continued.

[redacted]

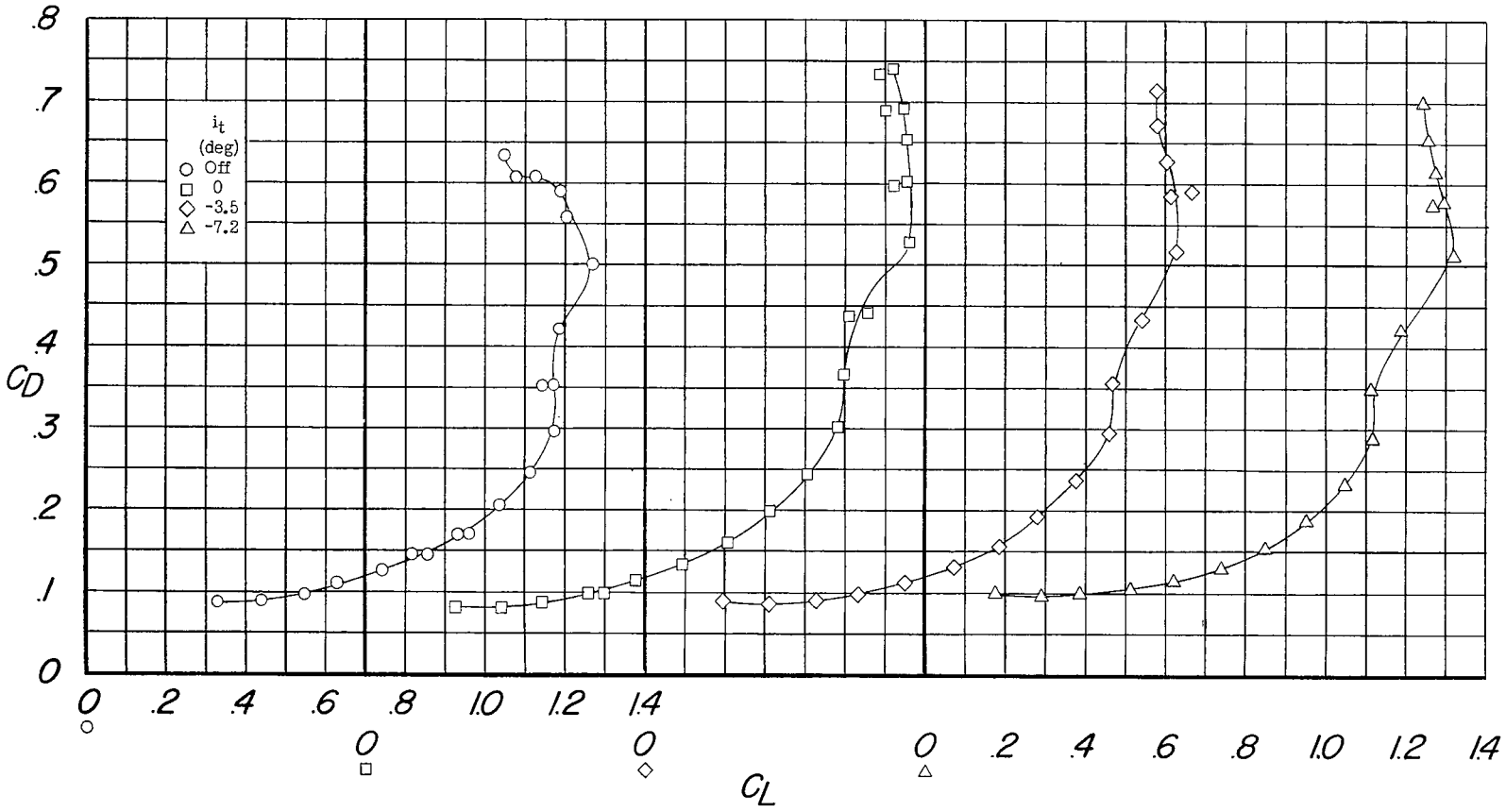

(d) C_D against C_L.

Figure 29.- Concluded.

[redacted]

[redacted]

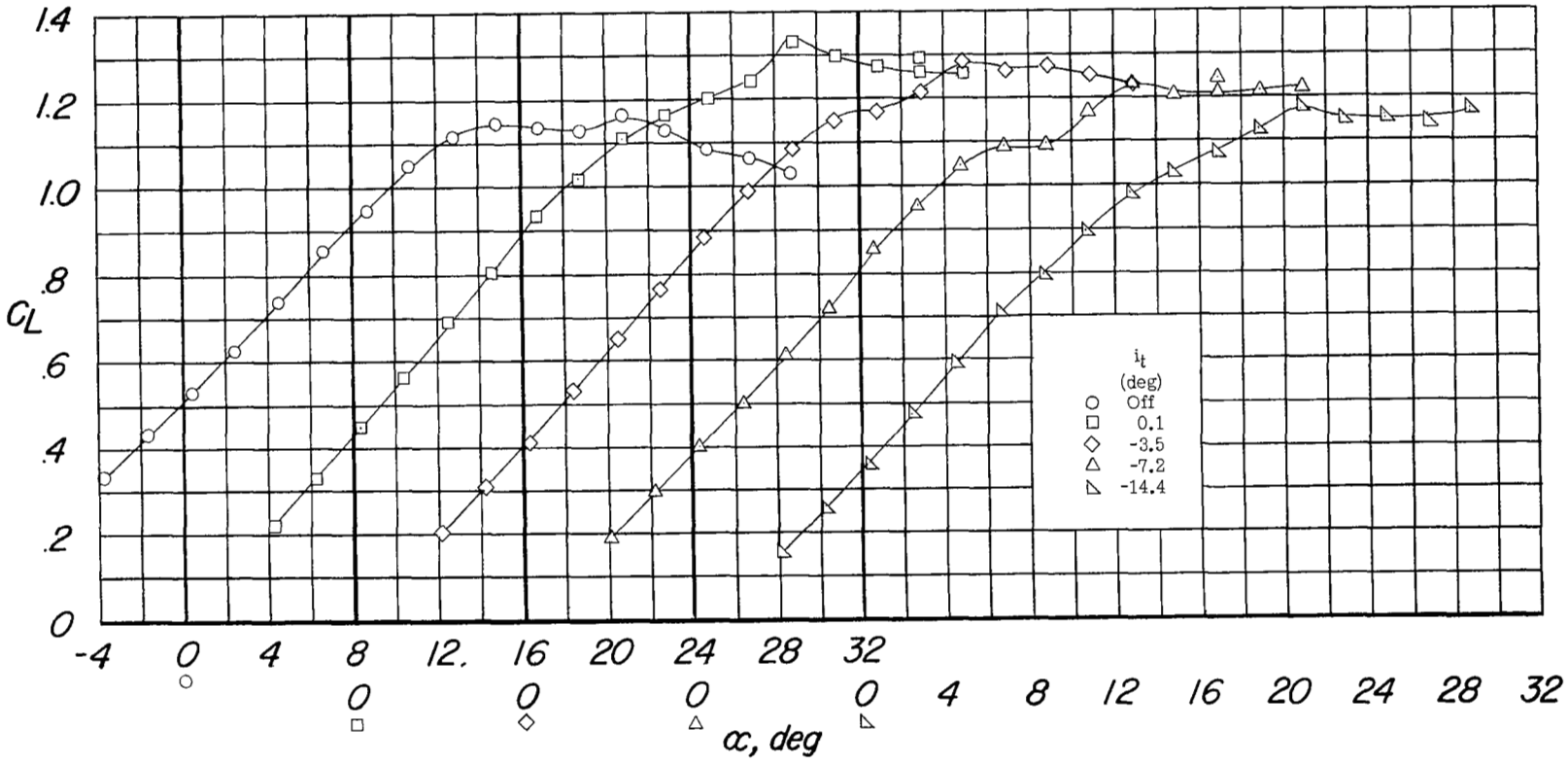

(a) C_L against α.

Figure 30.- Longitudinal characteristics of the model with 60-percent-span trailing-edge flaps deflected 46° and leading-edge flap drooped 20°. Configuration A + V + I_{SE} + (-0.123)T + 0.60F_{46} + N_{20}.

[redacted]

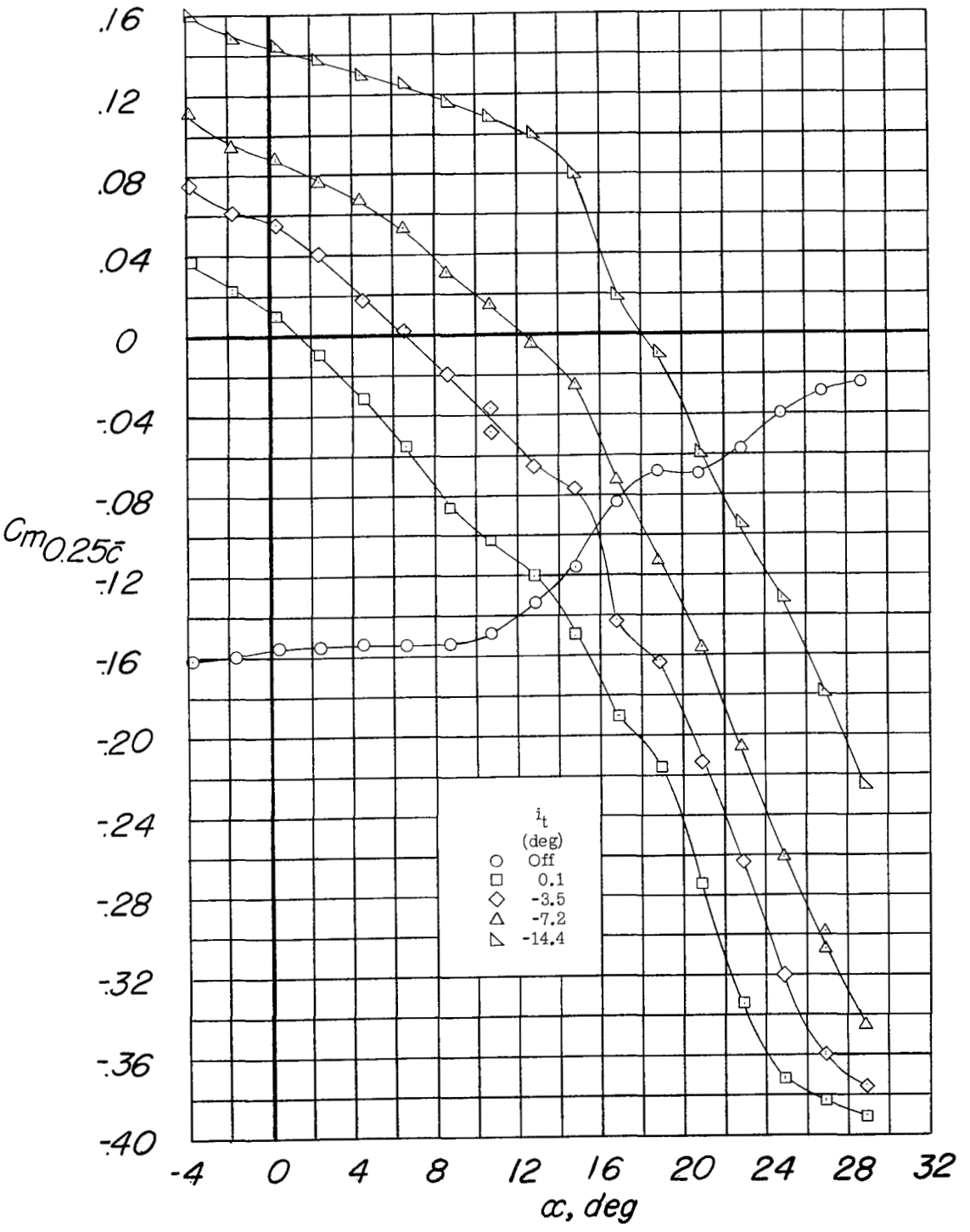

(b) C_m against α.

Figure 30.- Continued.

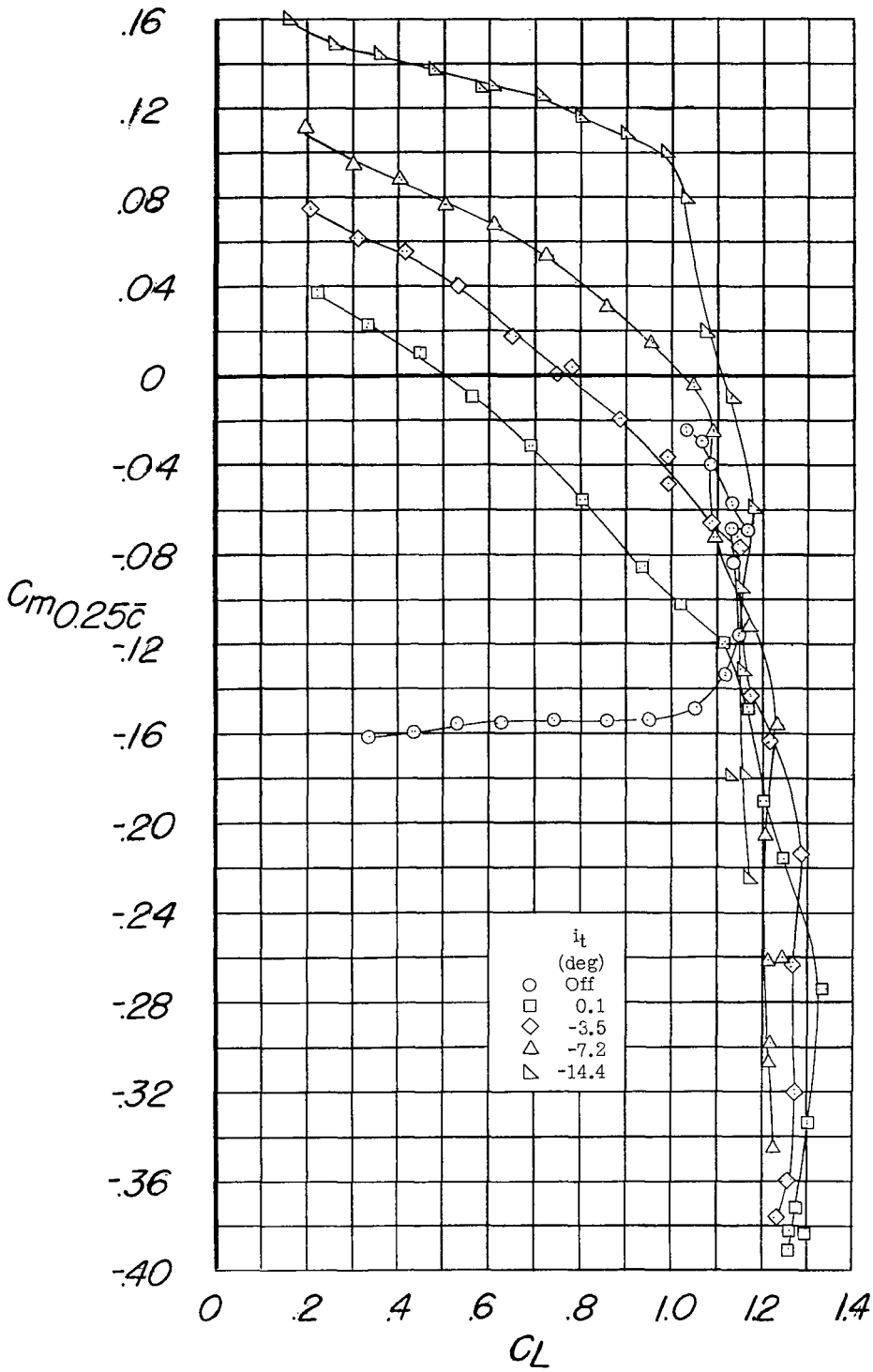

(c) C_m against C_L.

Figure 30.- Continued.

[redacted]

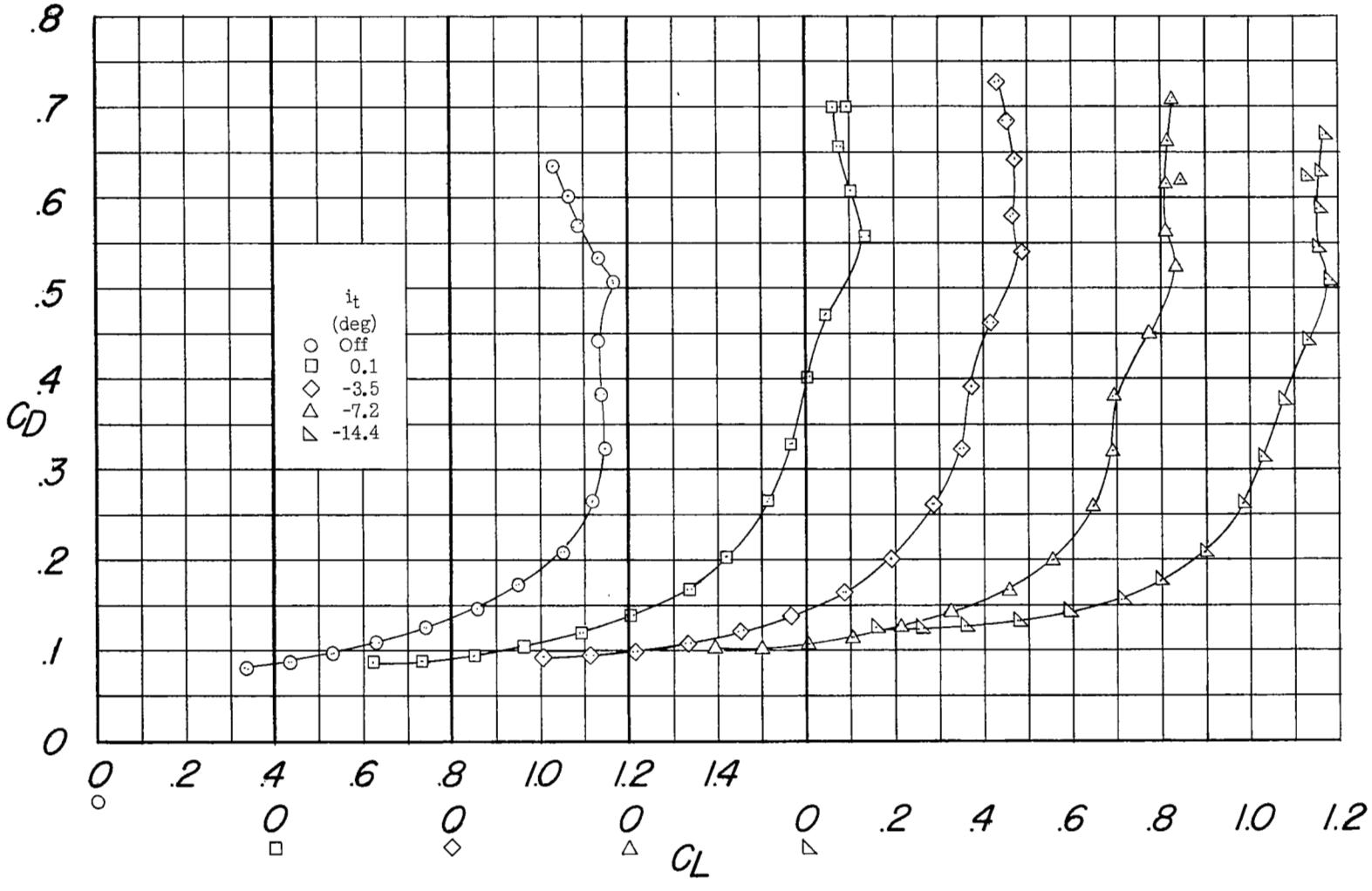

(d) C_D against C_L.

Figure 30.- Concluded.

[redacted]

[redacted]

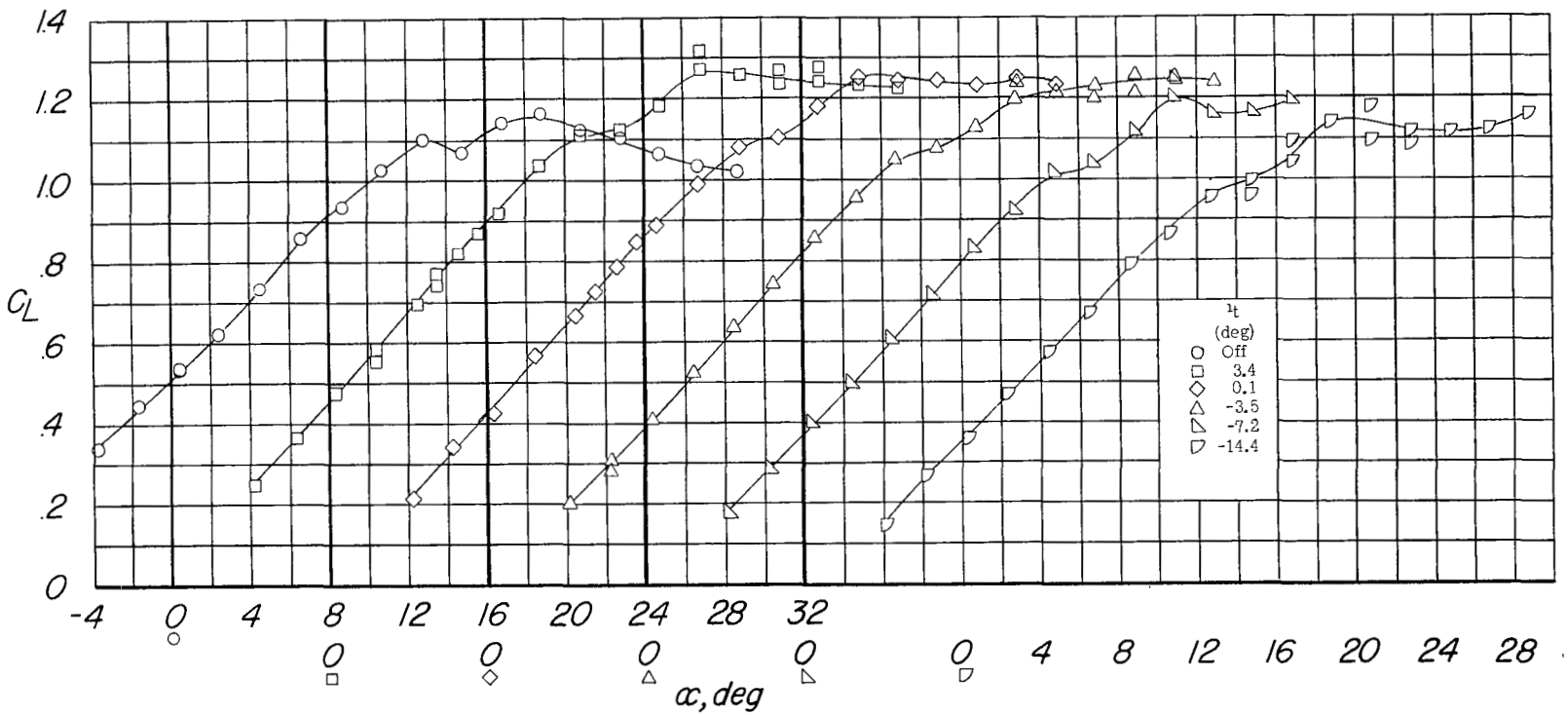

(a) C_L against α.

Figure 31.- Longitudinal characteristics of the model equipped with pylon-mounted external stores; 60-percent-span trailing-edge flaps deflected 46° and leading-edge flap drooped 20°. Configuration A + V + I_{SE} + (-0.123)T + $0.60F_{46}$ + N_{20} + E_0450.

[redacted]

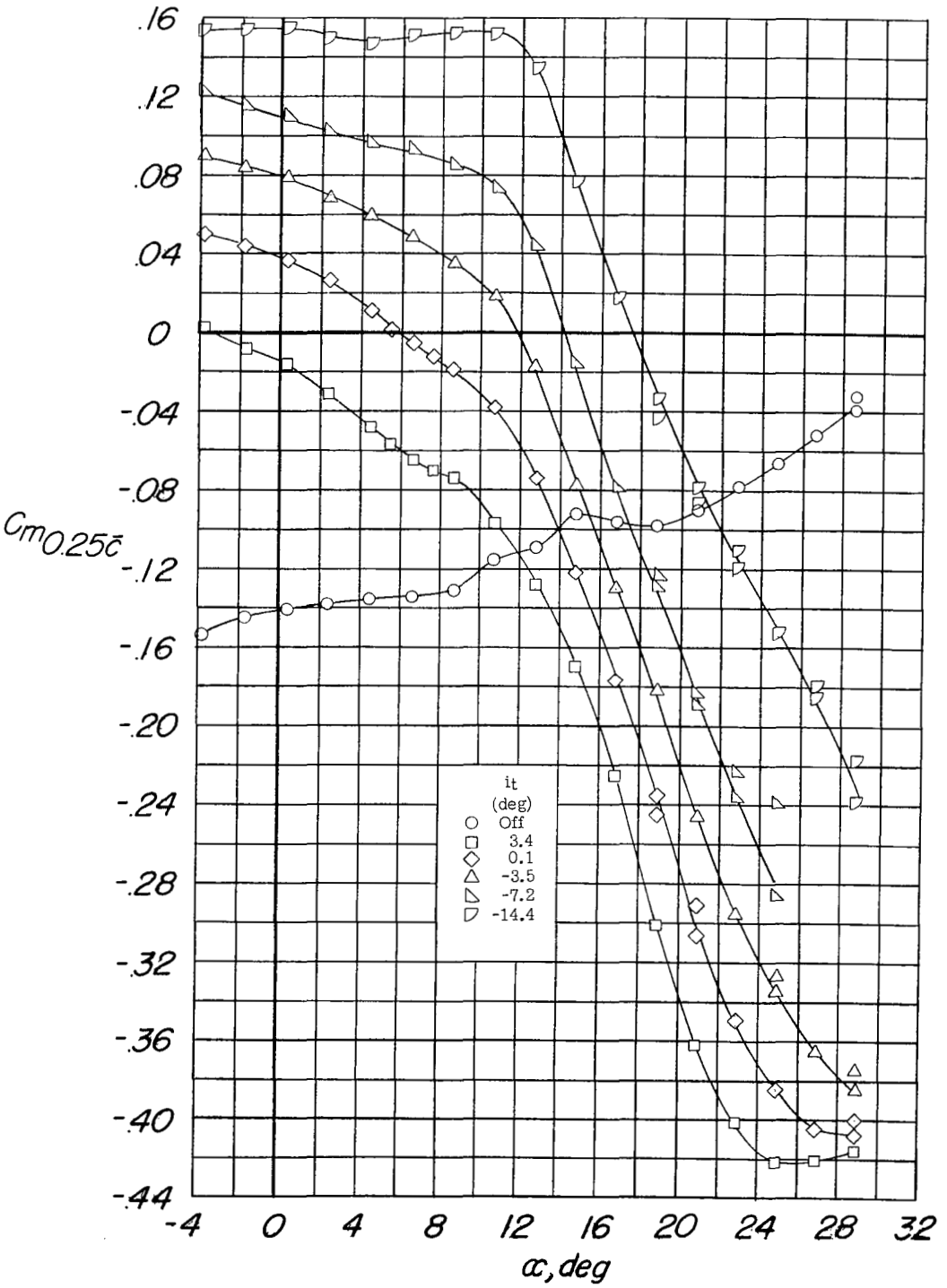

(b) C_m against α.

Figure 31.- Continued.

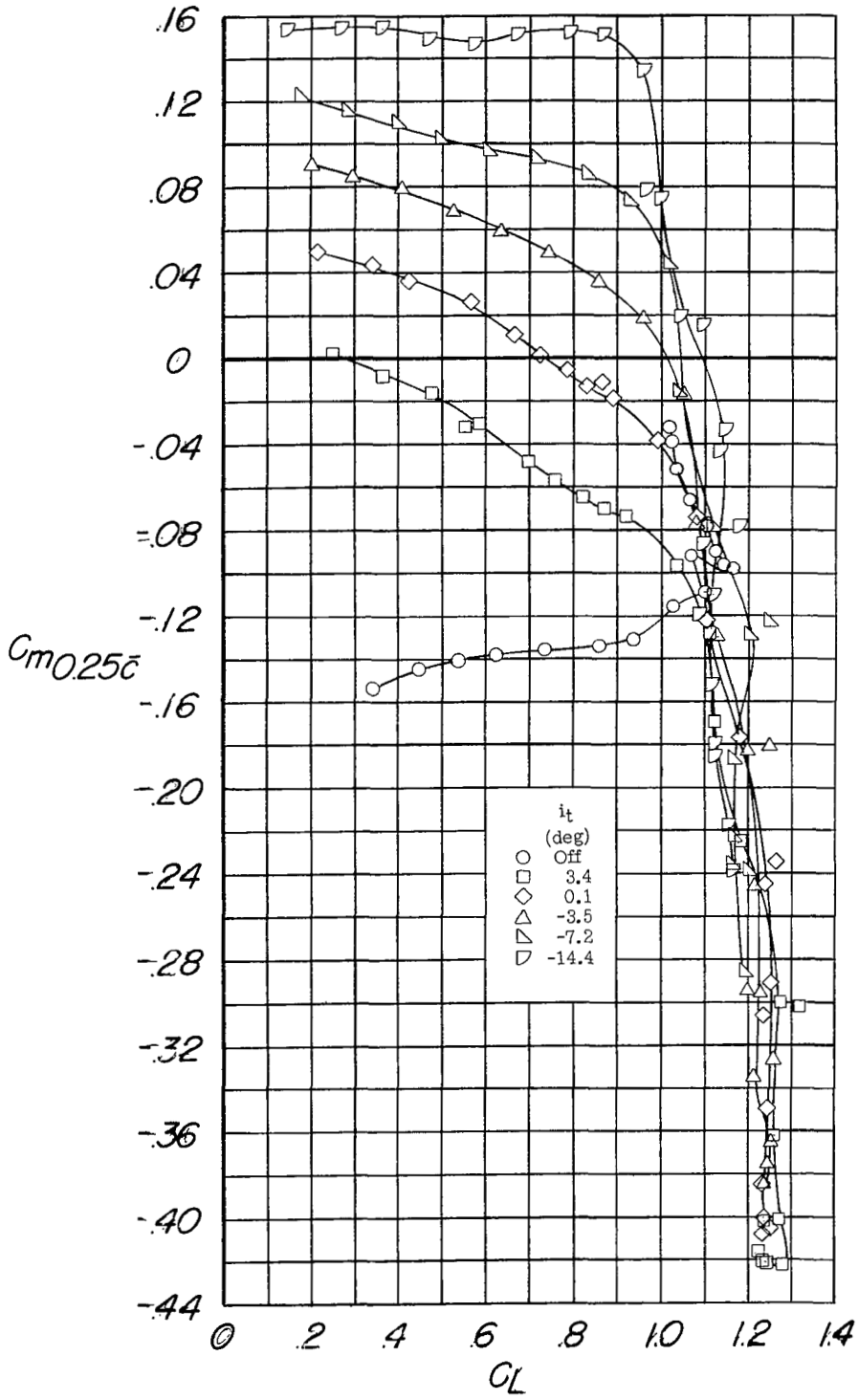

(c) C_m against C_L.

Figure 31.- Continued.

[redacted]

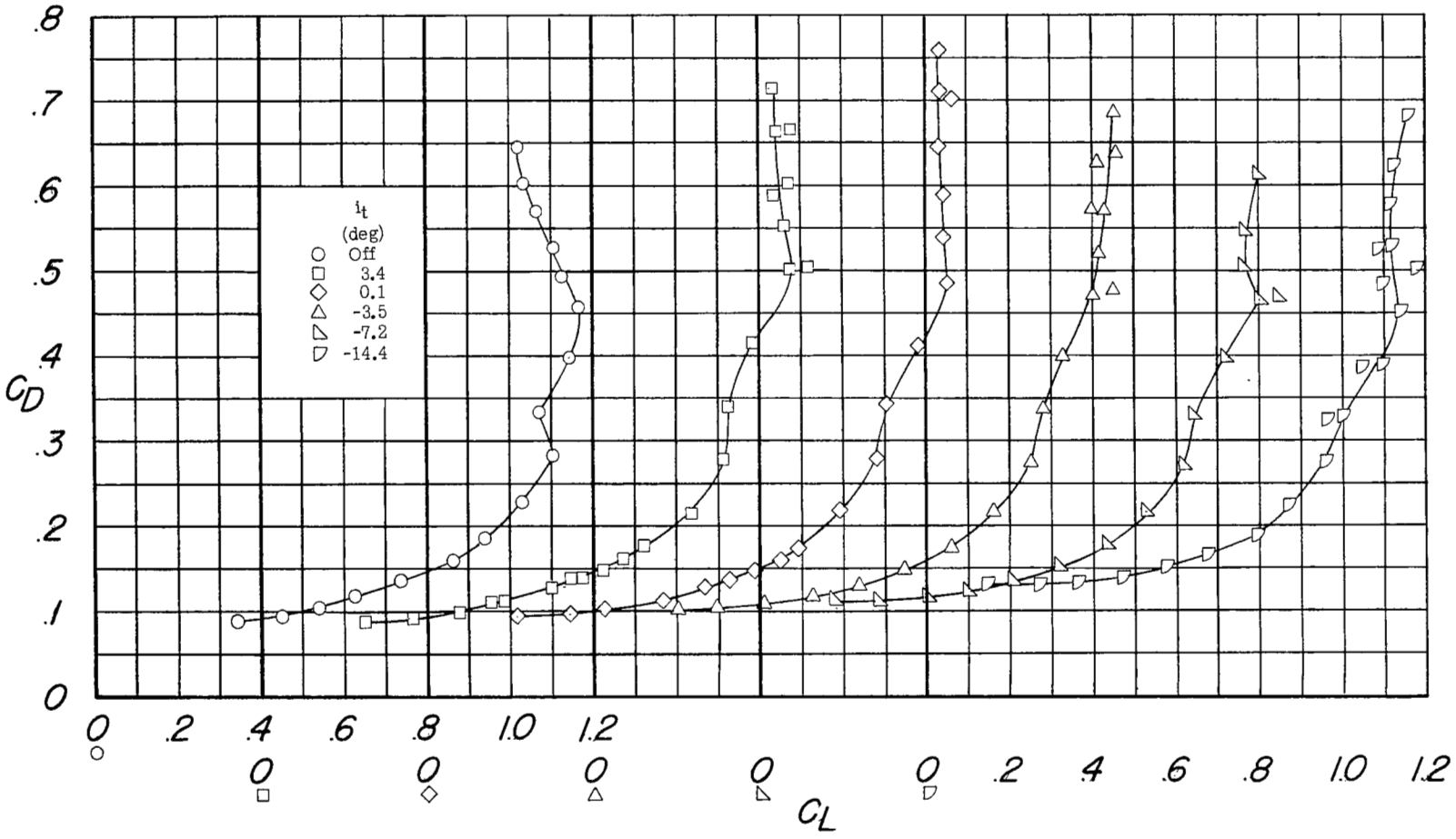

(d) C_D against C_L.

Figure 31.- Concluded.

[redacted]

[redacted]

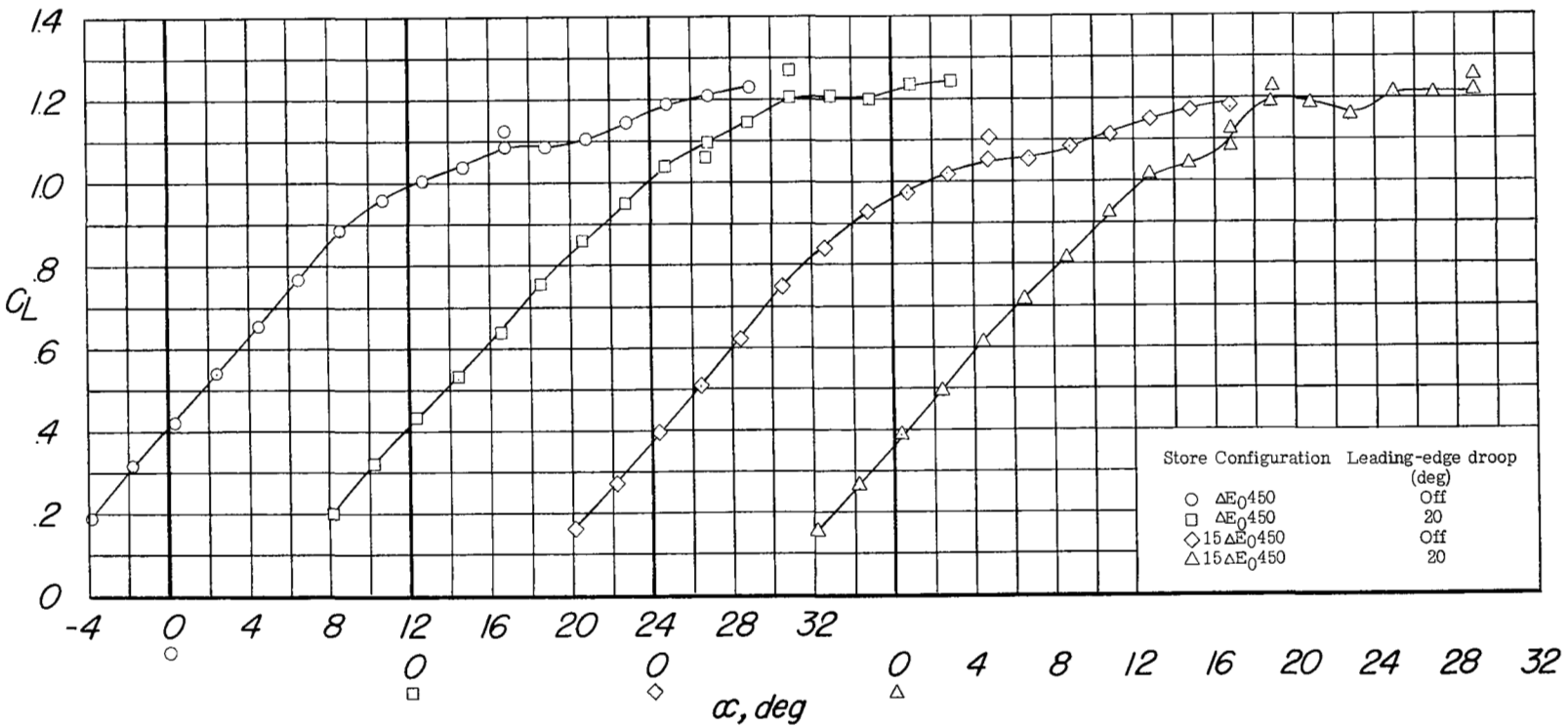

(a) C_L against α.

Figure 32.- Longitudinal characteristics of the model equipped with finned external stores; 60-percent-span trailing-edge flaps deflected 46°; with and without the leading-edge flap drooped 20°. Configuration A + V + I_{SE} + $(-0.123)T_{-7.2}$ + $0.60F_{46}$ + N + $\Delta E_0 450$.

[redacted]

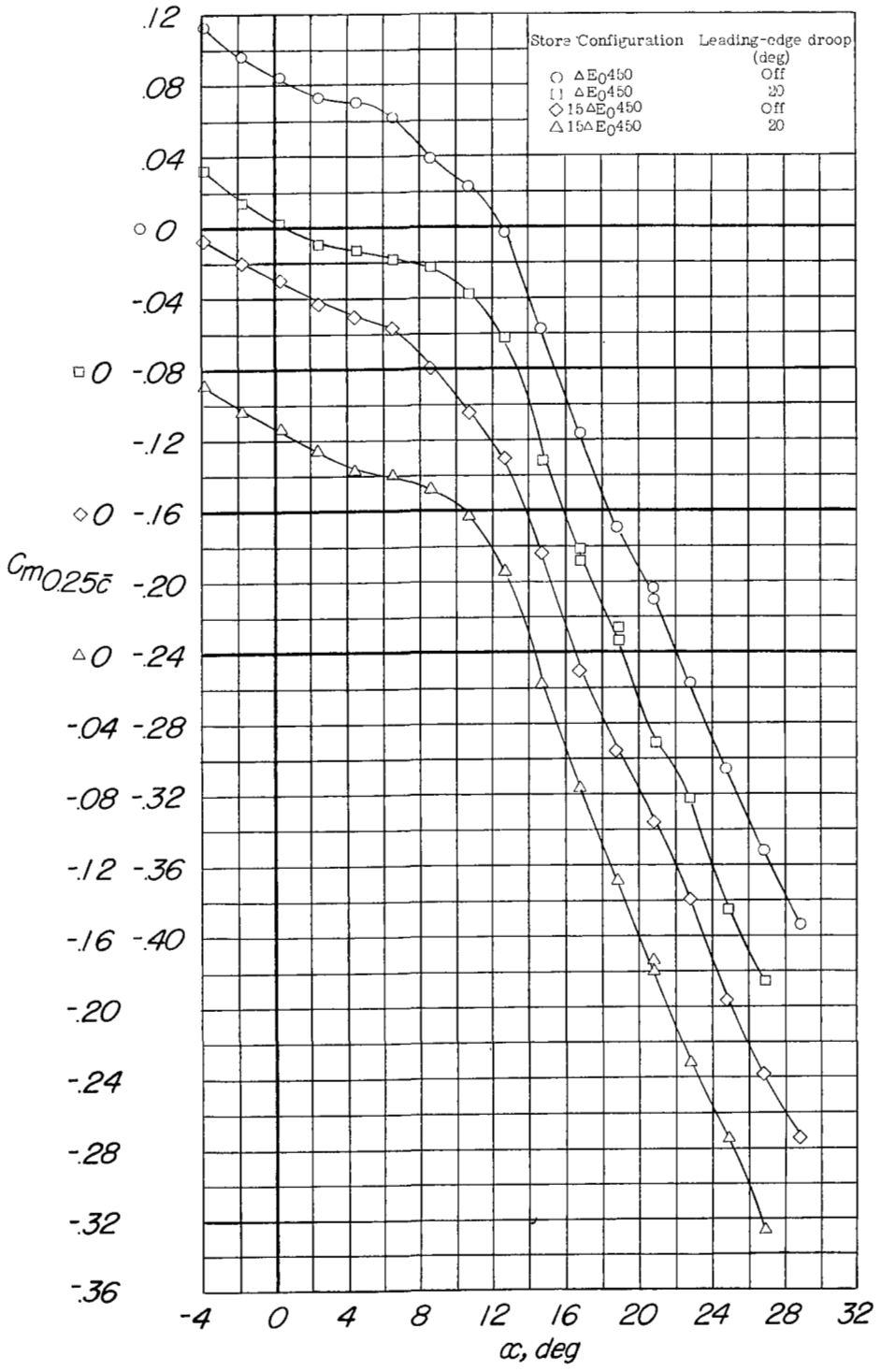

(b) C_m against α.

Figure 32.- Continued.

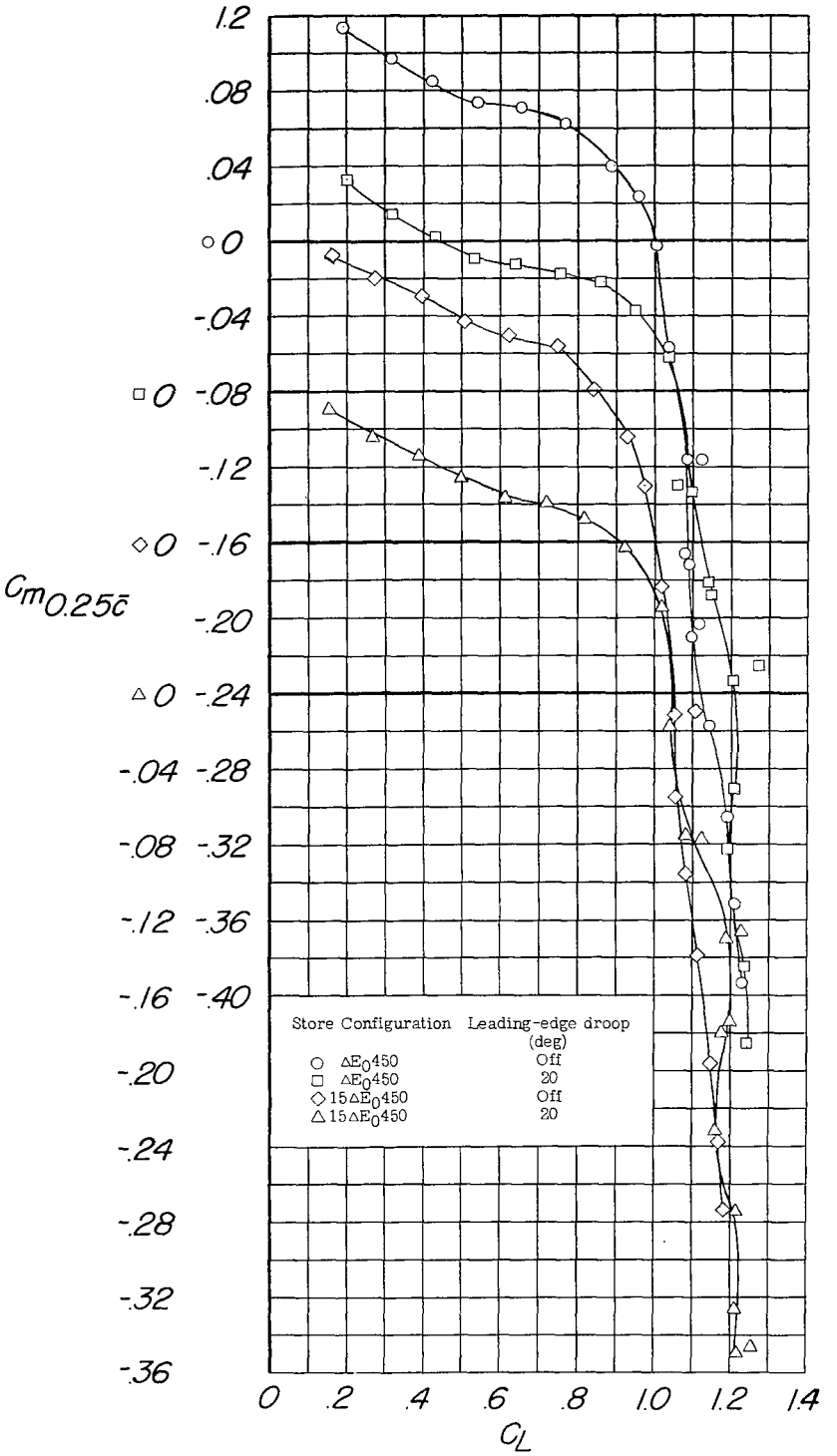

(c) C_m against C_L.

Figure 32.- Continued.

[redacted]

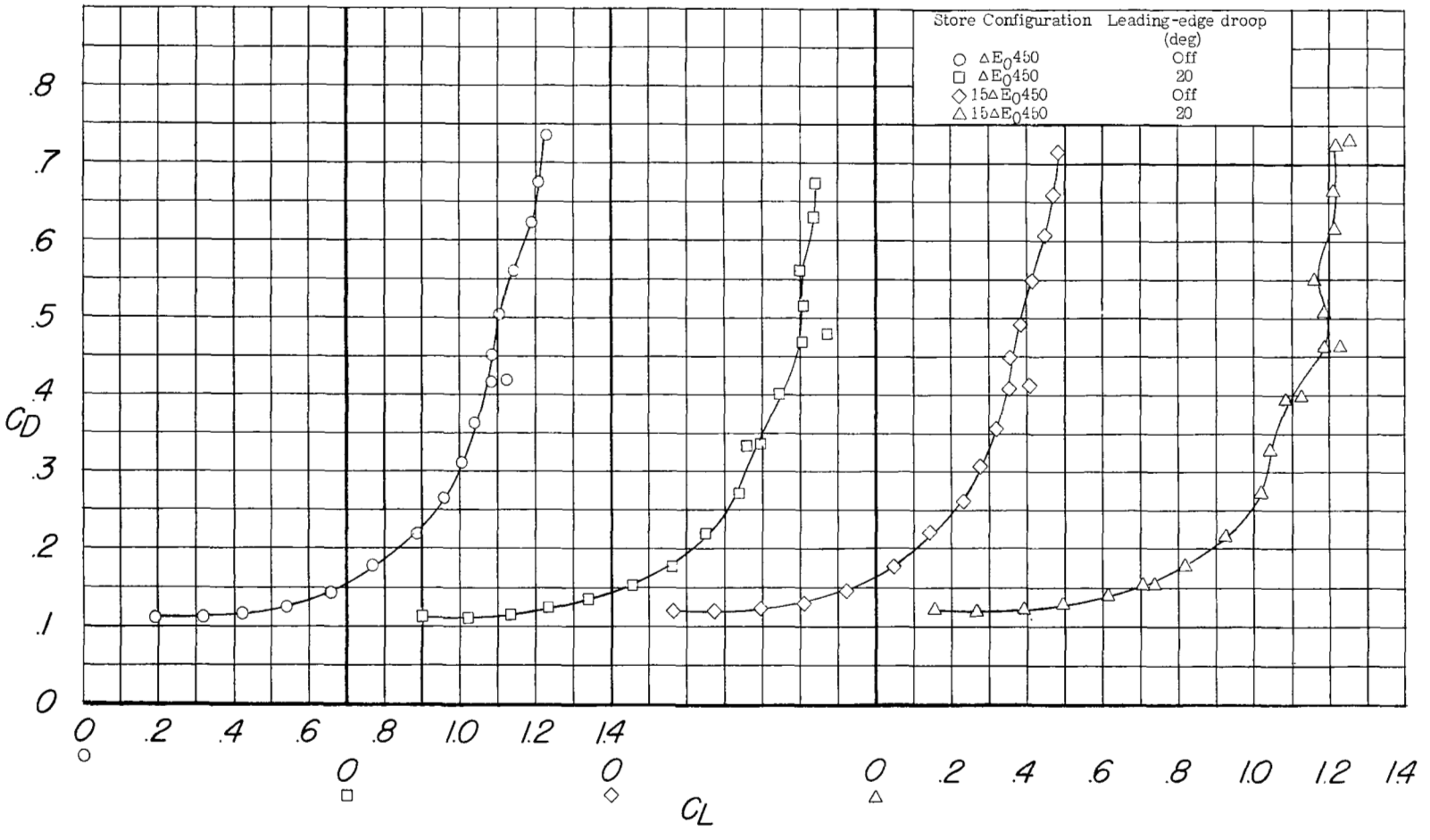

(d) C_D against C_L.

Figure 32.- Concluded.

[redacted]

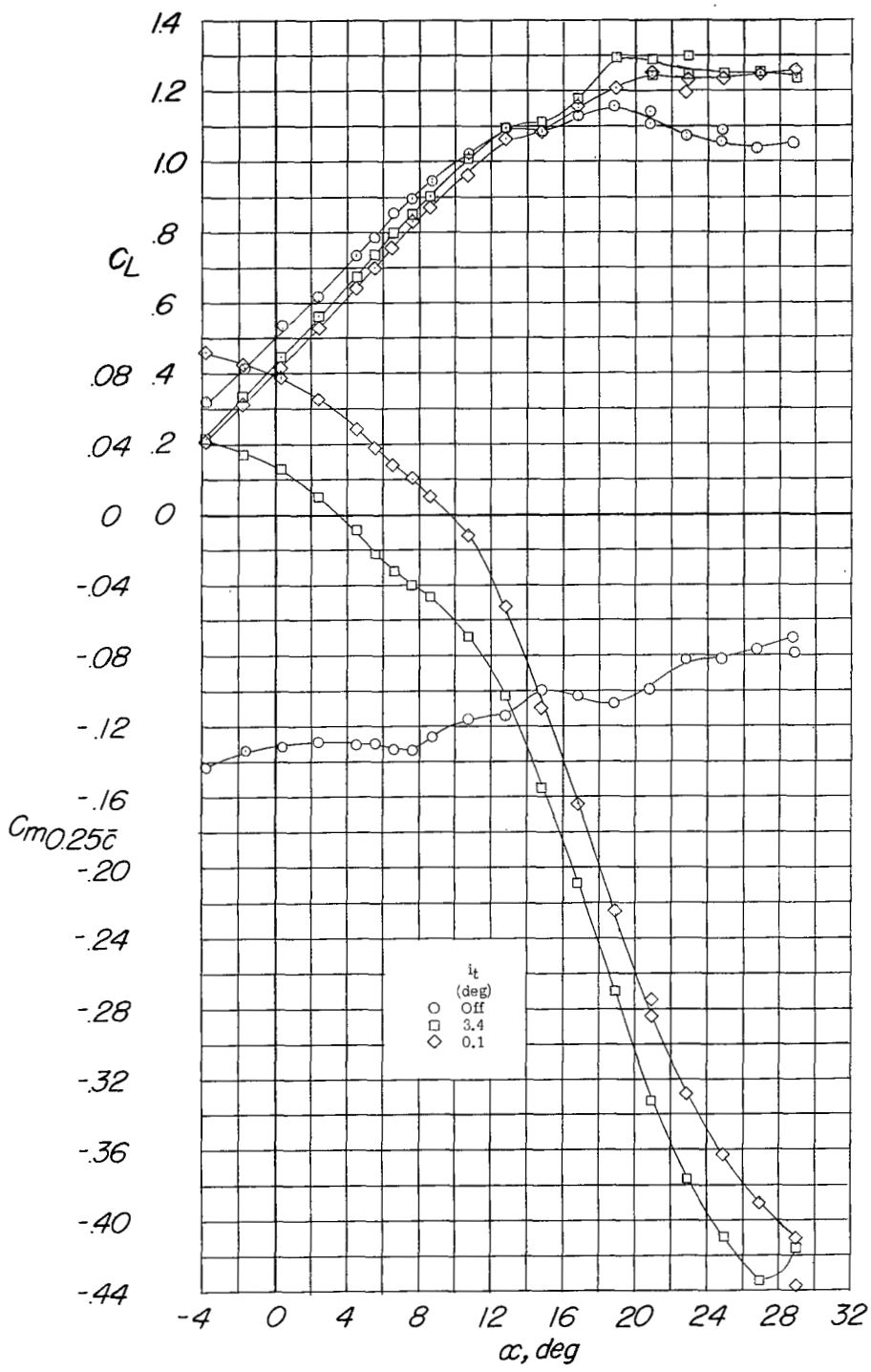

(a) C_L and C_m against α.

Figure 33.- Longitudinal characteristics of the model equipped with pylon-mounted external stores; side speed brakes deflected 40°, 60-percent-span trailing-edge flaps deflected 46°, and leading-edge flap drooped 20°. Configuration A + V + I_{SE} + (-0.123)T + 0.60F_{46} + N_{20} + $E_0$450 + $B_{0,40}$.

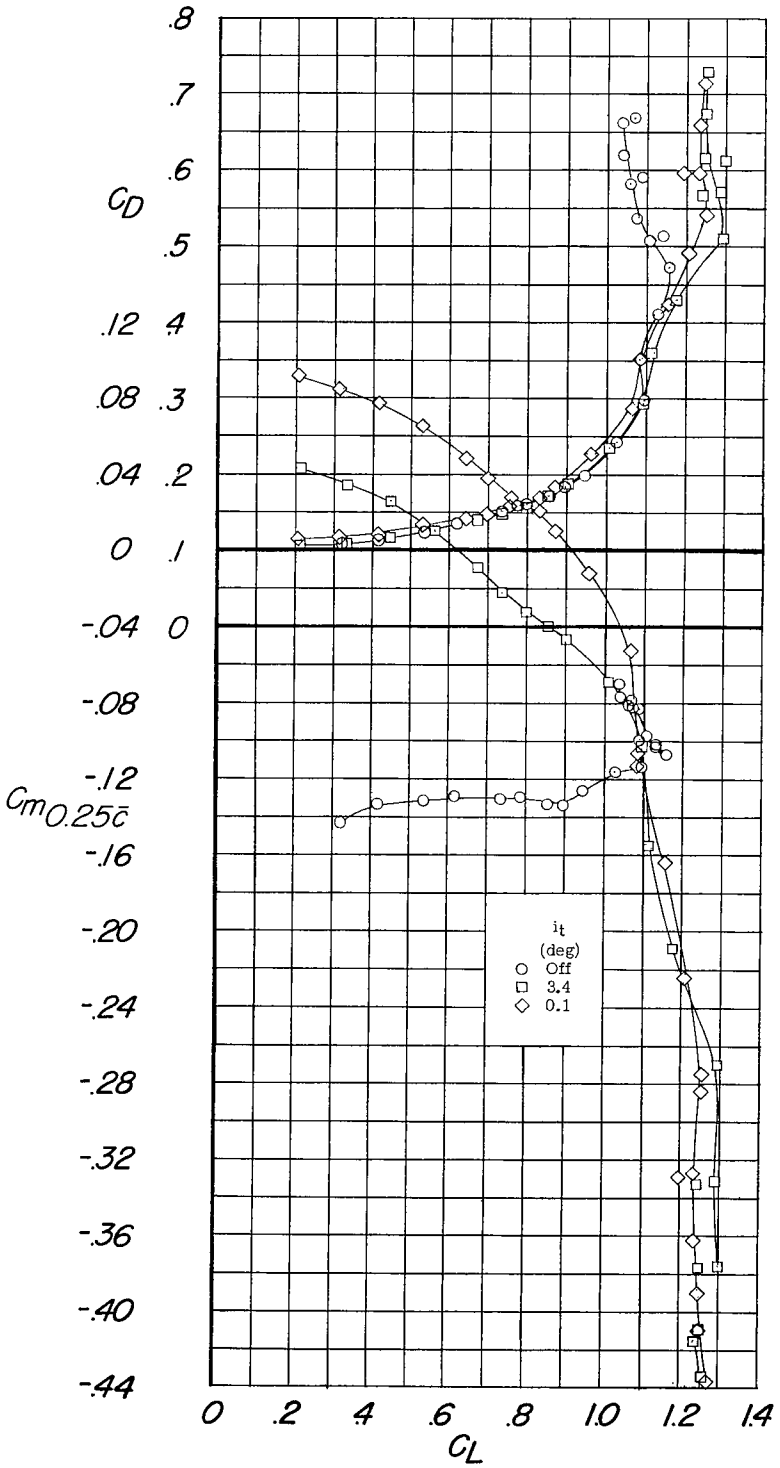

(b) C_D and C_m against C_L.

Figure 33.- Concluded.

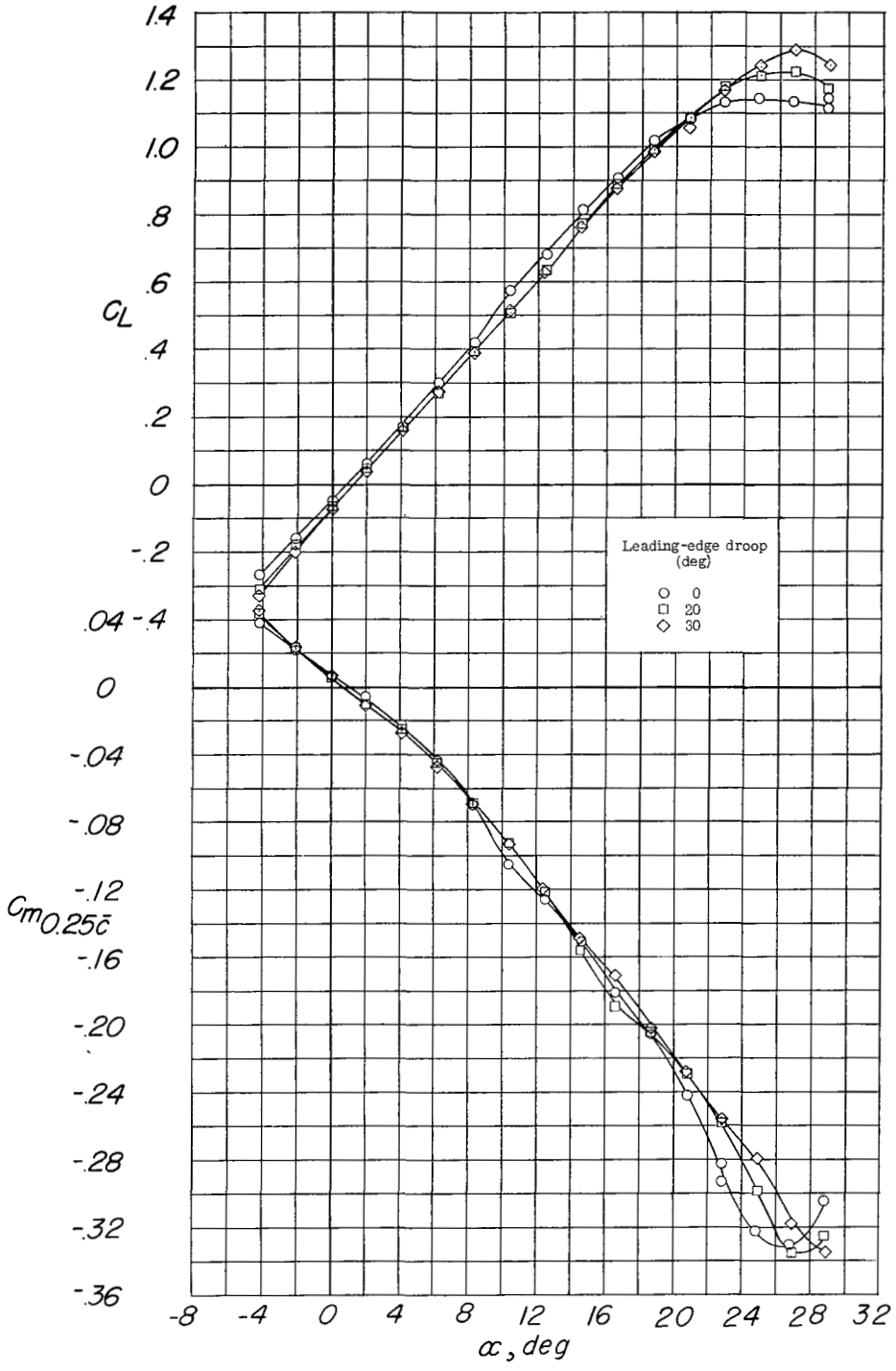

(a) C_L and C_m against α.

Figure 34.- Longitudinal stability and lateral-control characteristics of the model with the lateral-control spoiler deflected 61°. Configuration A + V + I_{SE} + (-0.123)T_0 + N + S_{61}.

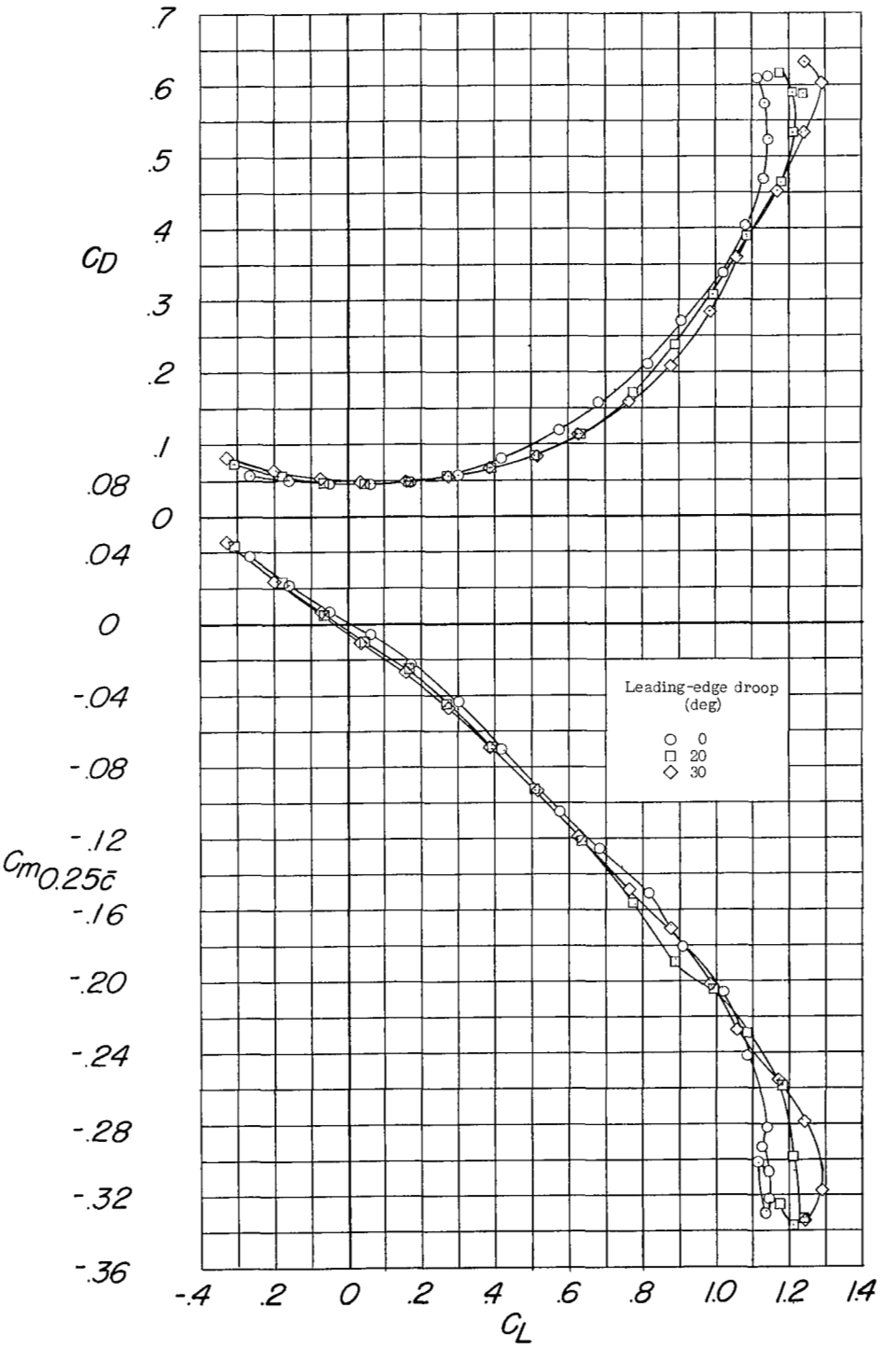

(b) C_D and C_m against C_L.

Figure 34.- Continued.

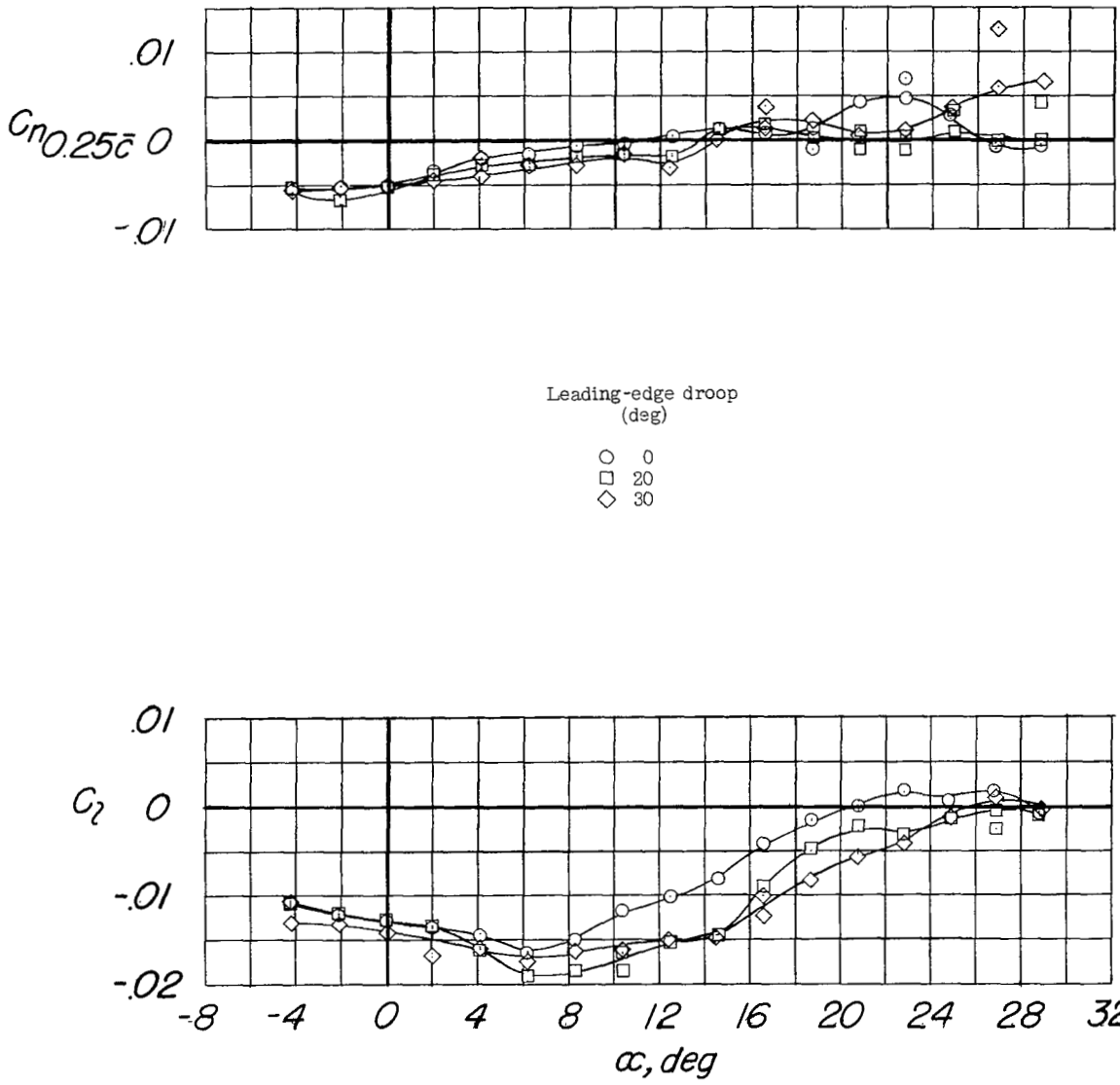

(c) C_n and C_l against α.

Figure 34.- Concluded.

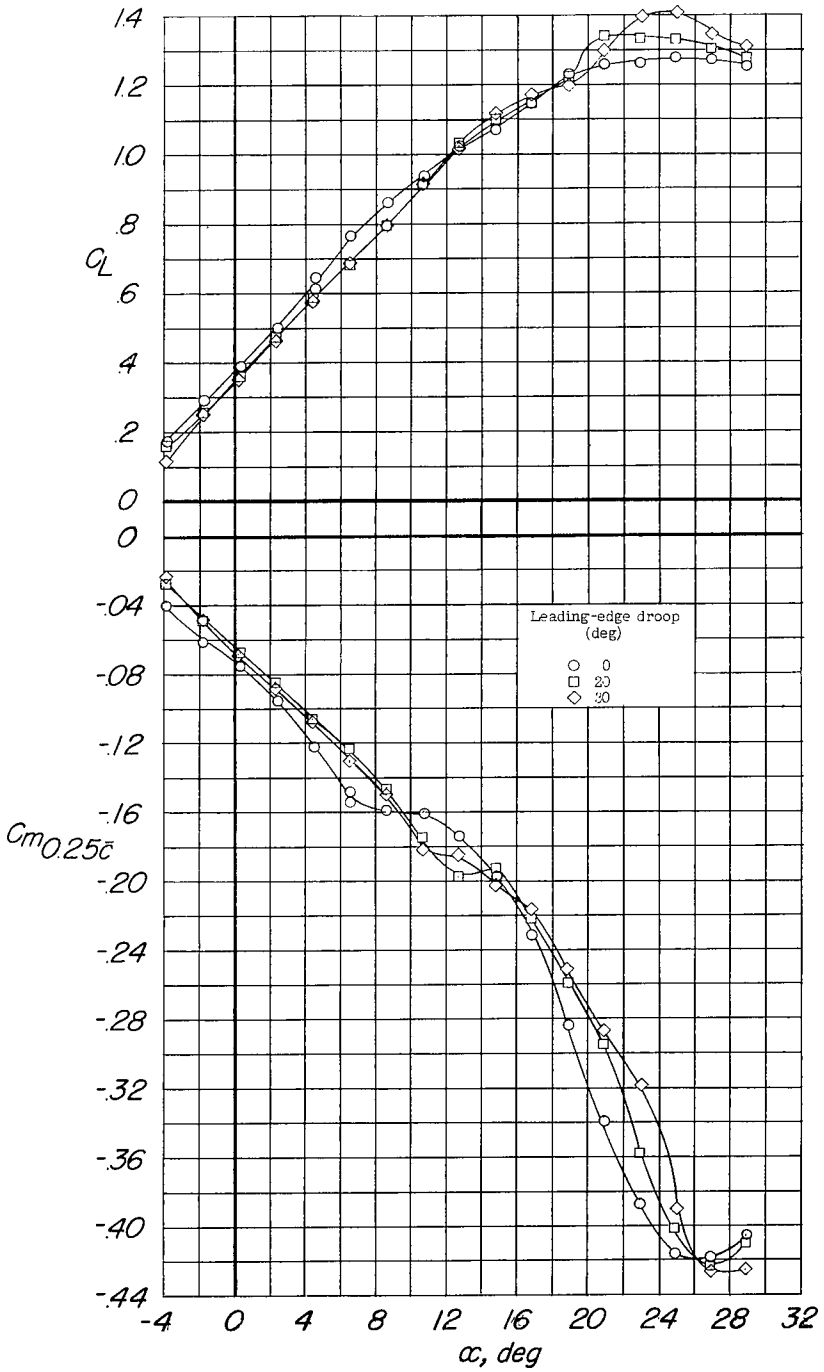

(a) C_L and C_m against α.

Figure 35.- Longitudinal stability and lateral-control characteristics of the model with the lateral-control spoiler deflected 61° and the trailing-edge flaps deflected 46°. Configuration A + V + I_{SE} + $(-0.123)T_0$ + $0.80F_{46}$ + N + S_{61}.

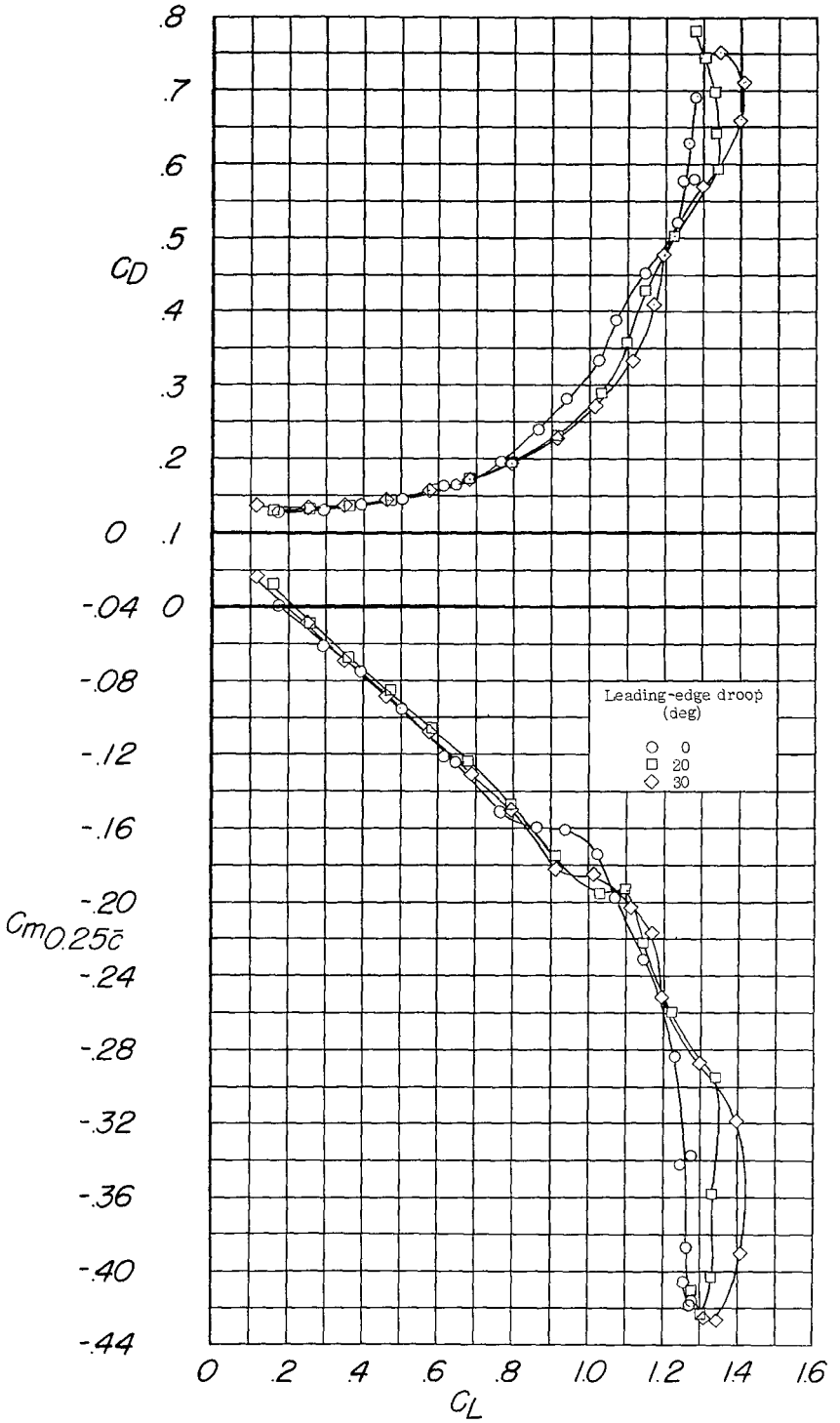

(b) C_D and C_m against C_L.

Figure 35.- Continued.

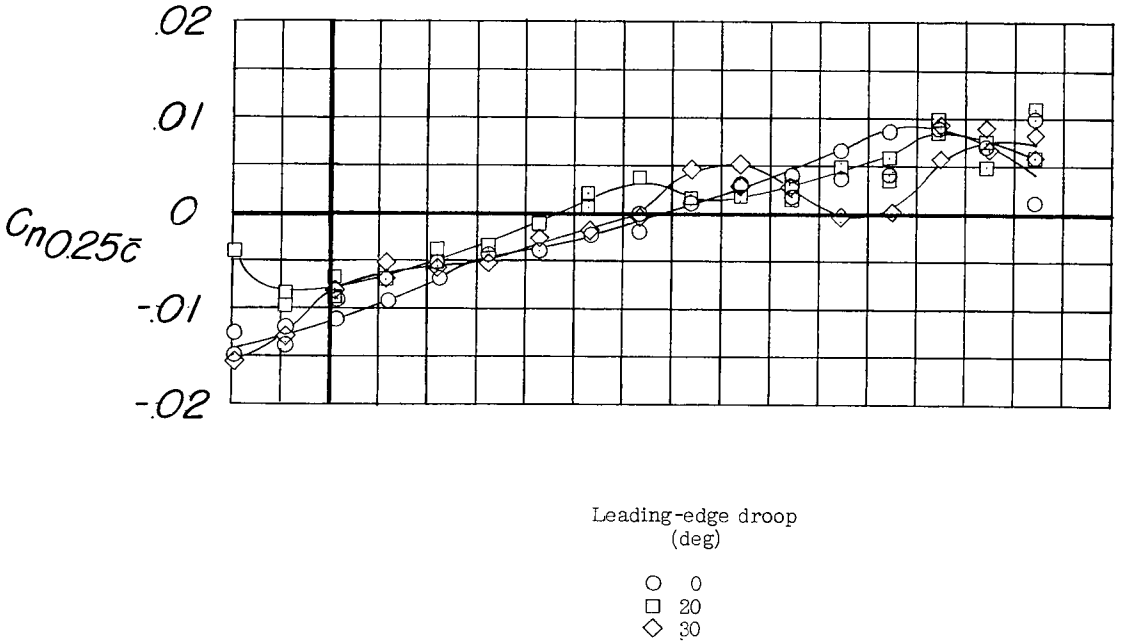

(c) C_n and C_l against α.

Figure 35.- Concluded.

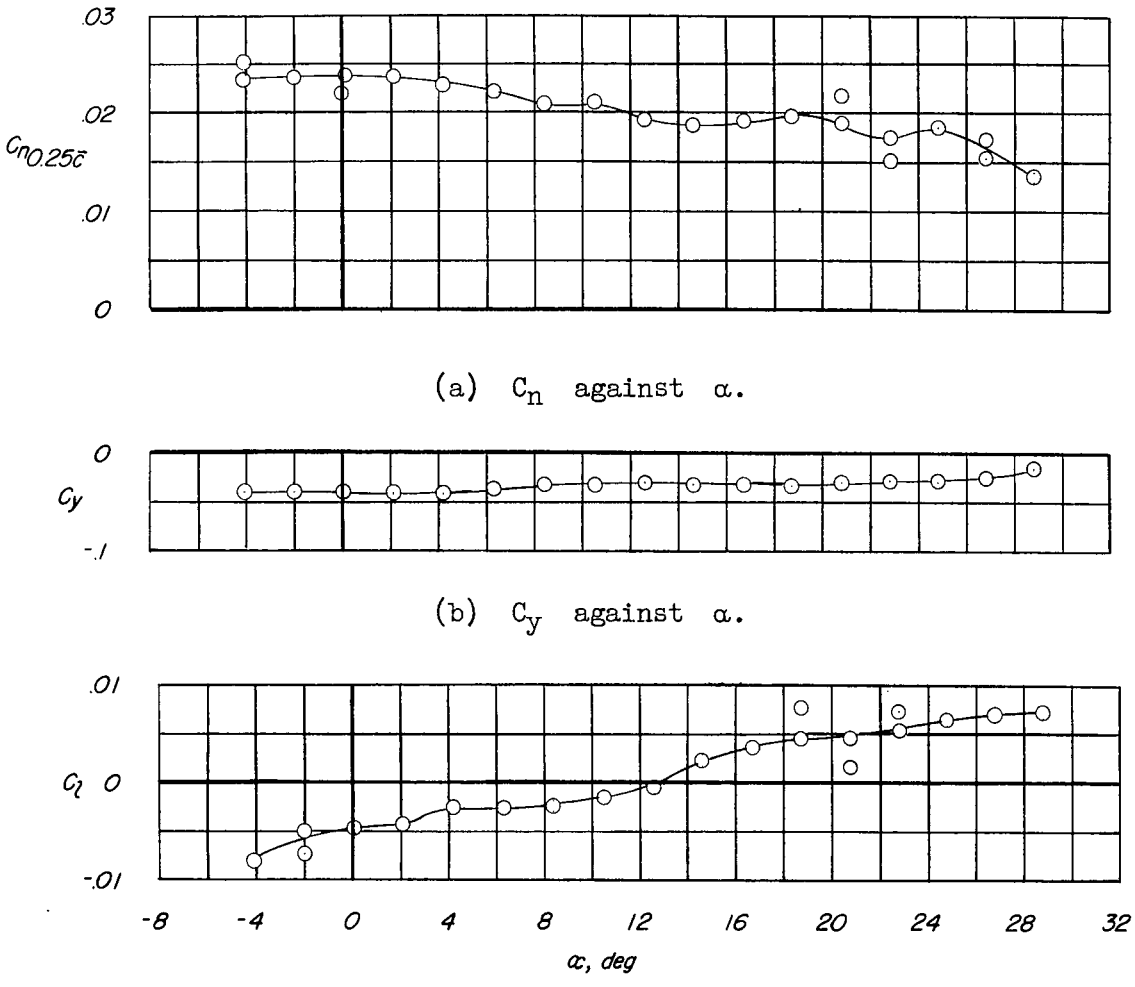

(a) C_n against α.

(b) C_y against α.

(c) C_l against α.

Figure 36.- Directional control characteristics of the model with the rudder deflected 12°. Configuration A + V + I_{SE} + (-0.123)$T_{7.0}$ + R_{12}.

[redacted]

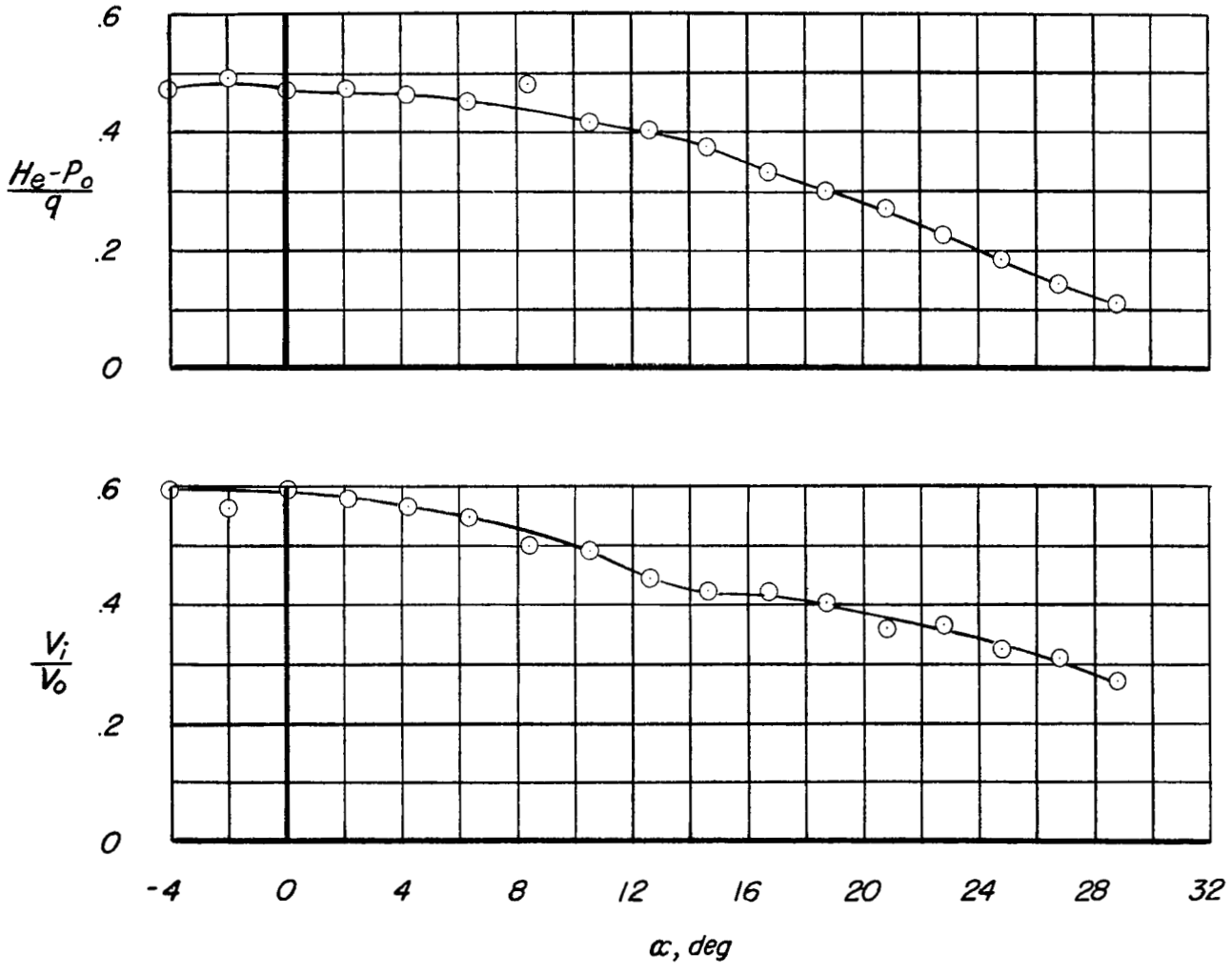

Figure 37.- Variation of pressure recovery and inlet velocity ratio with angle of attack; typical for all tests with the duct exit open. Configuration A + V + I_{SE} + $(-0.123)T_{7.0}$.

[redacted]

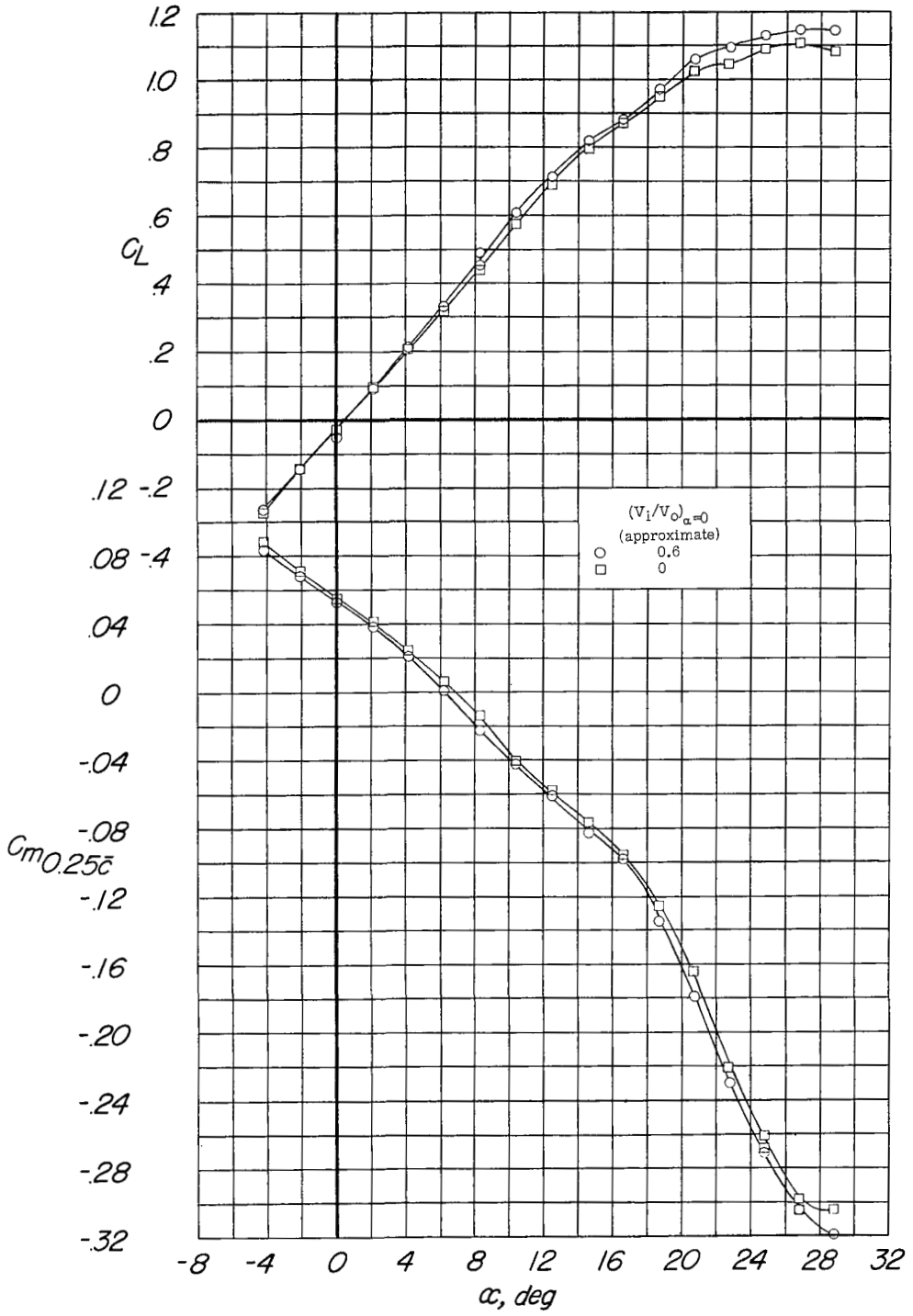

(a) C_L and C_m against α.

Figure 38.- Longitudinal stability characteristics of the model with and without duct air flow. Configuration A + V + I_{SE} + $(-0.123)T_{-3.4}$.

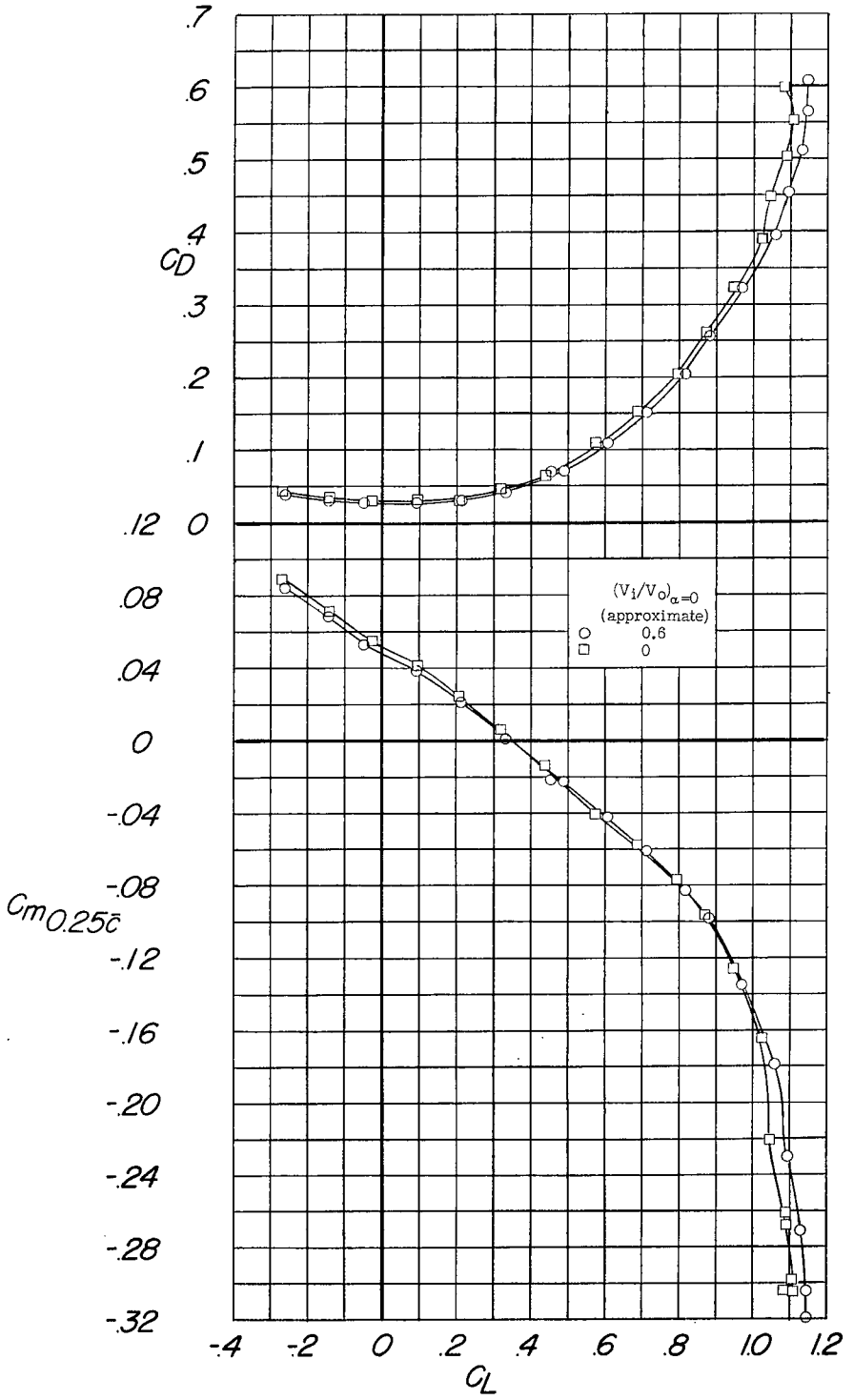

(b) C_D and C_m against C_L.

Figure 38.- Concluded.

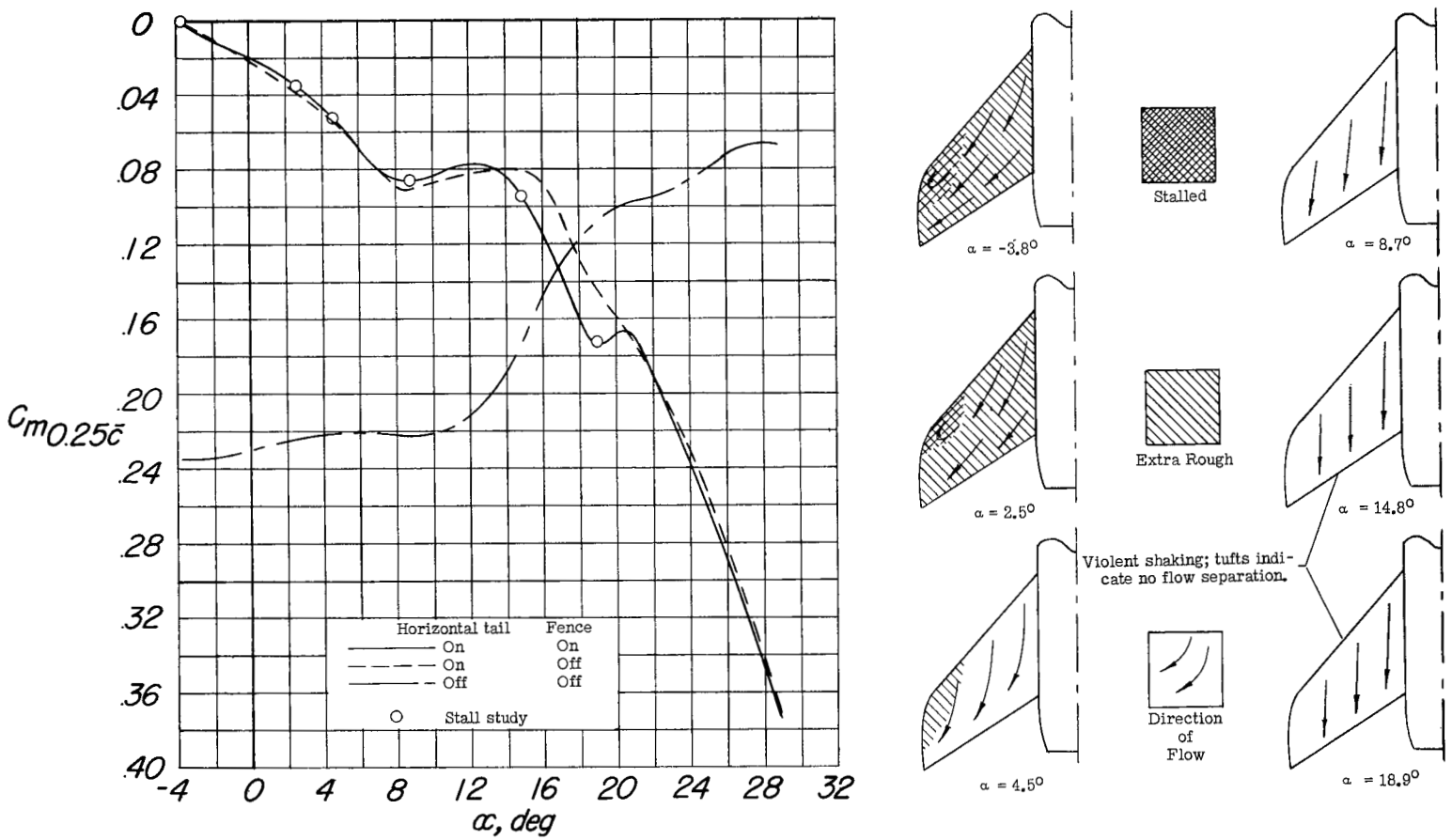

(a) C_m against α.

(b) Stall studies of the horizontal tail (lower surface).

Figure 39.- Pitching-moment characteristics of the model and stall studies of the horizontal-tail lower surface. Configuration $A + V + I_{SE} + (-0.123)T'_{-7.2} + 0.80F_{46} + N_{30} + 1W_{0.654}$.

[redacted]

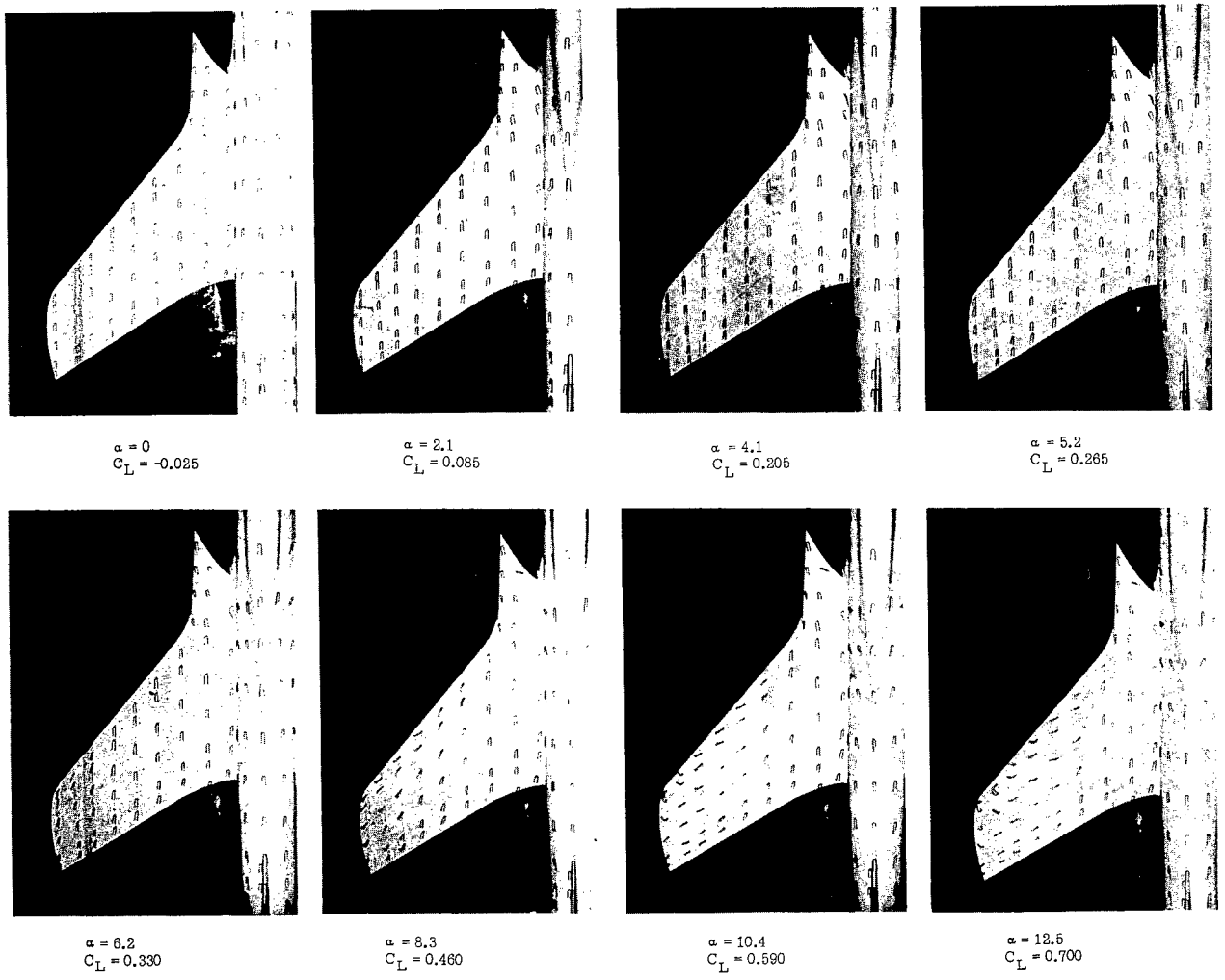

(a) $A + V + I_{SE} + (-0.123)T_{-3.5}$.

L-84898

Figure 40.- Stall studies of various model configurations.

[redacted]

[redacted]

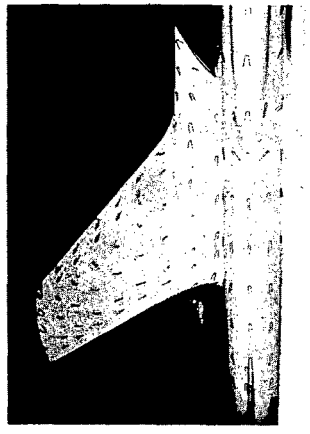

$\alpha = 14.6$
$C_L = 0.795$

$\alpha = 18.7$
$C_L = 0.960$

$\alpha = 24.8$
$C_L = 1.105$

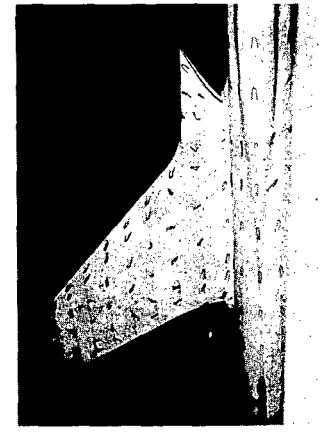

$\alpha = 26.8$
$C_L = 1.130$

$\alpha = 28.9$
$C_L = 1.155$

L-84899

(a) Concluded.

Figure 40.- Continued.

[redacted]

[redacted]

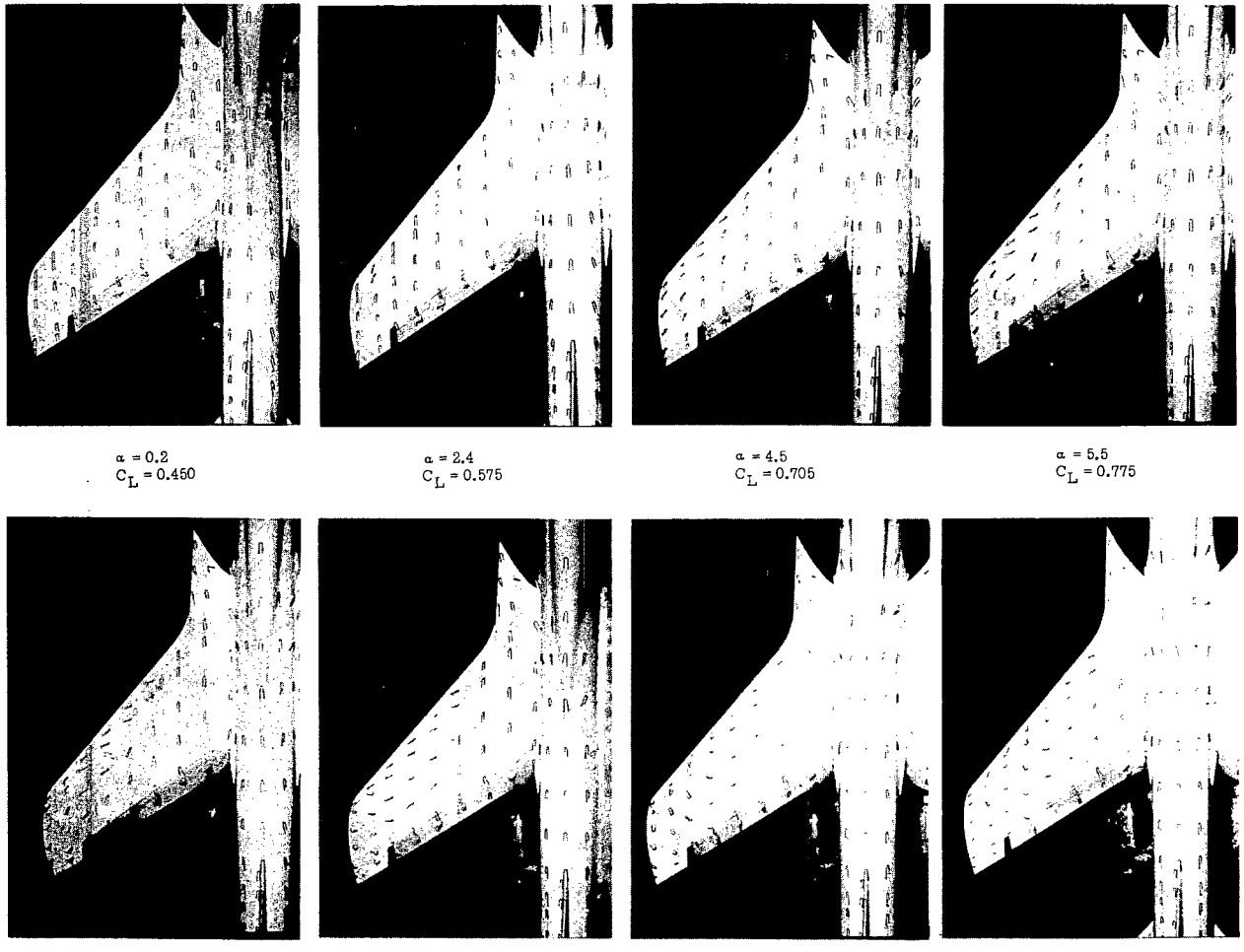

L-84900

(b) $A + V + I_{SE} + 0.80F_{46} + (-0.123)T_{-14.4}$.

Figure 40.- Continued.

[redacted]

[redacted]

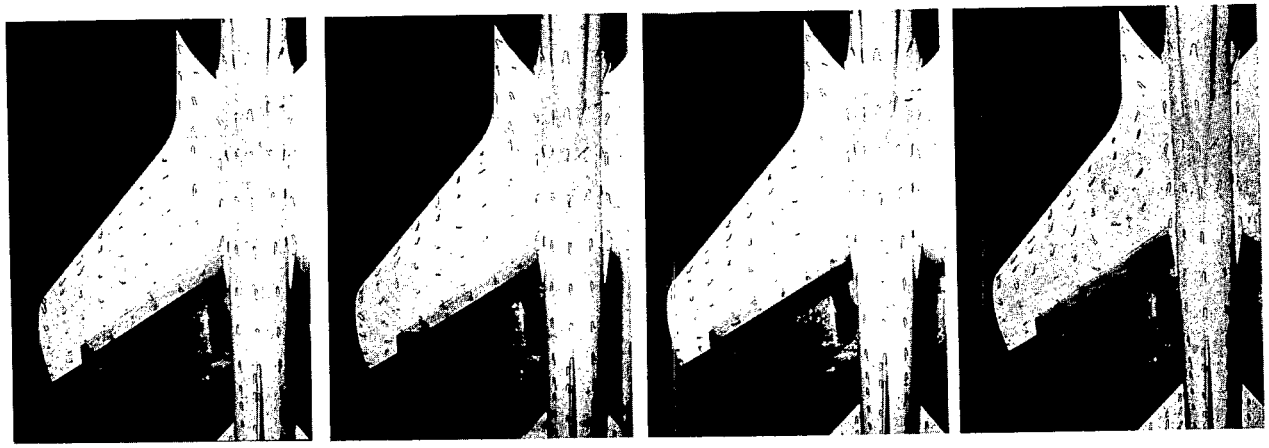

$\alpha = 14.7$
$C_L = 1.035$

$\alpha = 16.8$
$C_L = 1.095$

$\alpha = 18.8$
$C_L = 1.120$

$\alpha = 22.8$
$C_L = 1.140$

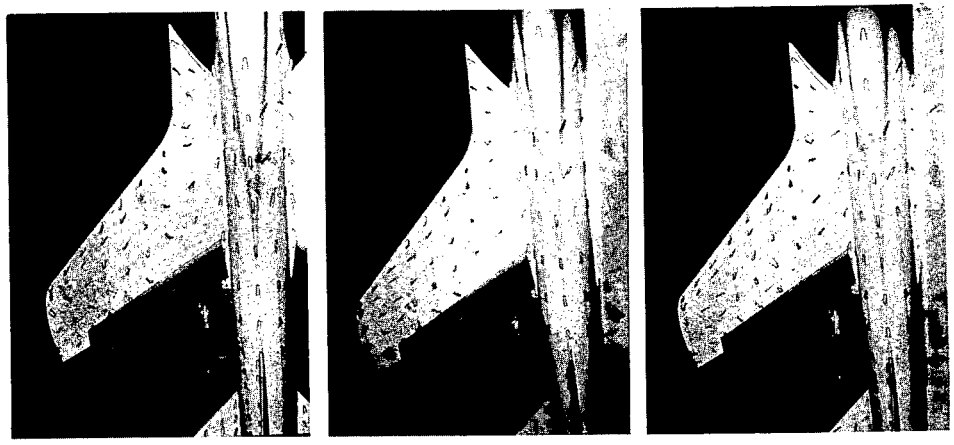

$\alpha = 24.9$
$C_L = 1.160$

$\alpha = 26.9$
$C_L = 1.185$

$\alpha = 28.9$
$C_L = 1.210$

L-84901

(b) Concluded.

Figure 40.- Continued.

[redacted]

[redacted]

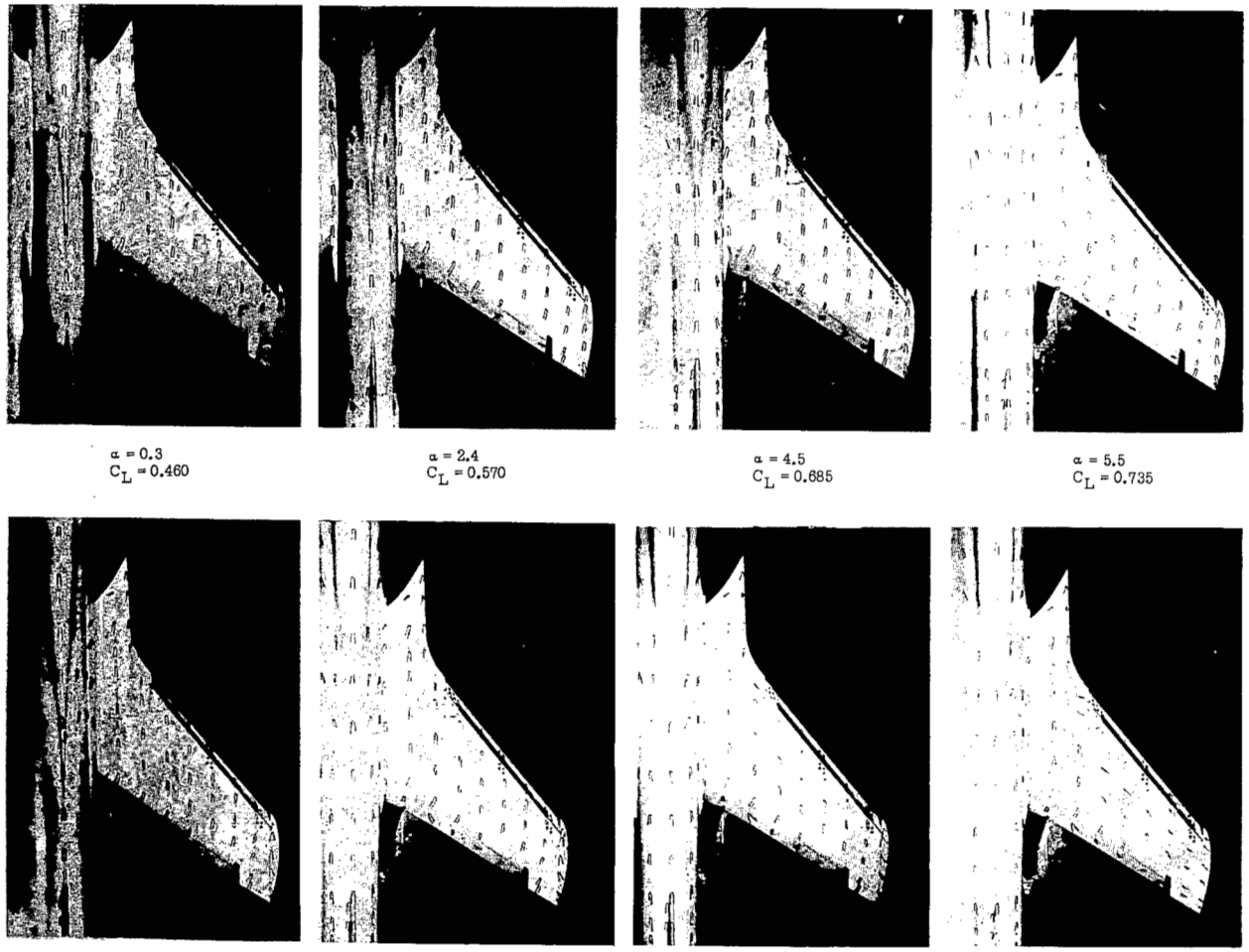

L-84902

(c) $A + V + I_{SE} + 0.80F_{46} + N_{30} + (-0.123)T_{-14.4}$.

Figure 40.- Continued.

[redacted]

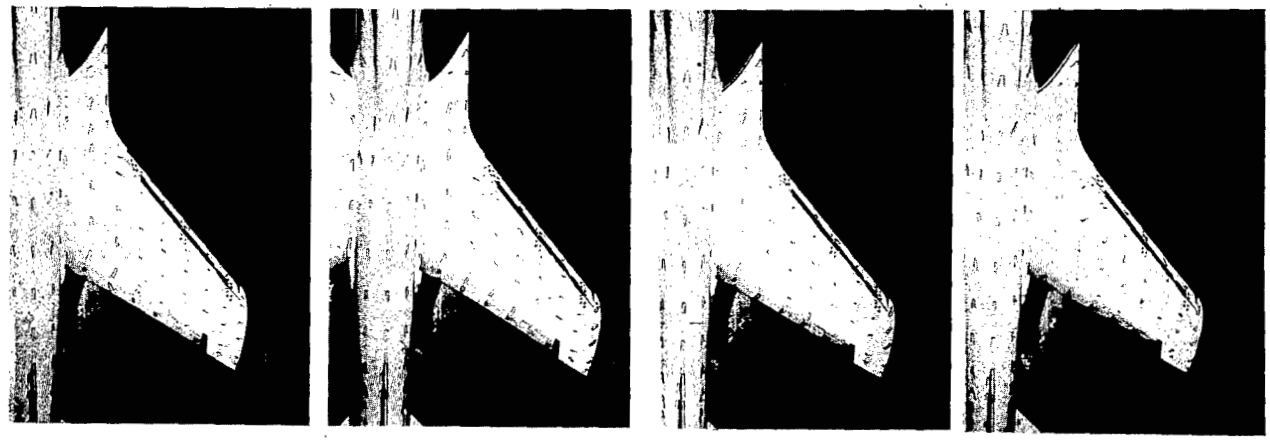

$\alpha = 14.8$
$C_L = 1.130$

$\alpha = 16.8$
$C_L = 1.165$

$\alpha = 18.8$
$C_L = 1.190$

$\alpha = 22.9$
$C_L = 1.275$

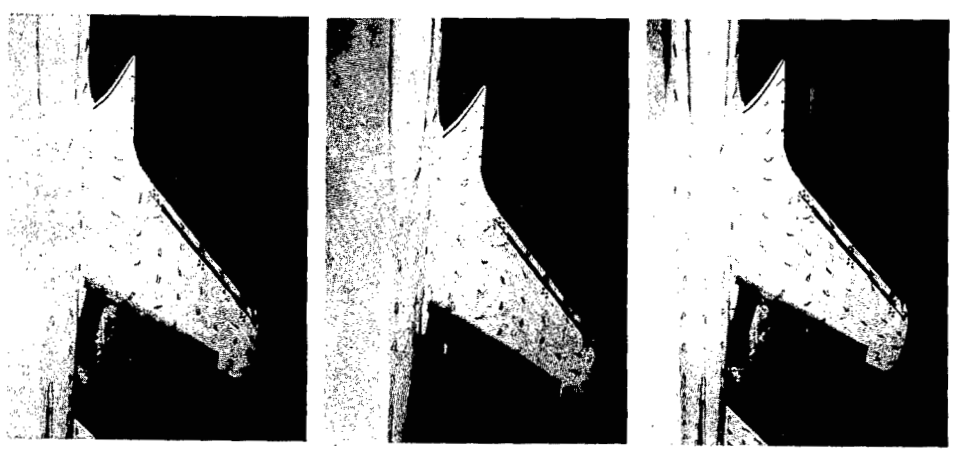

$\alpha = 24.9$
$C_L = 1.240$

$\alpha = 26.9$
$C_L = 1.240$

$\alpha = 28.9$
$C_L = 1.245$

L-84903

(c) Concluded.

Figure 40.- Concluded.

UNCLASSIFIED

[redacted]

LANGLEY RESEARCH CENTER
3 1176 00506 6130

[redacted]